INFORMATION TO USERS

This manuscript has been reproduced from the microfilm master. UMI films the text directly from the original or copy submitted. Thus, some thesis and dissertation copies are in typewriter face, while others may be from any type of computer printer.

The quality of this reproduction is dependent upon the quality of the copy submitted. Broken or indistinct print, colored or poor quality illustrations and photographs, print bleedthrough, substandard margins, and improper alignment can adversely affect reproduction.

In the unlikely event that the author did not send UMI a complete manuscript and there are missing pages, these will be noted. Also, if unauthorized copyright material had to be removed, a note will indicate the deletion.

Oversize materials (e.g., maps, drawings, charts) are reproduced by sectioning the original, beginning at the upper left-hand corner and continuing from left to right in equal sections with small overlaps.

Photographs included in the original manuscript have been reproduced xerographically in this copy. Higher quality 6" x 9" black and white photographic prints are available for any photographs or illustrations appearing in this copy for an additional charge. Contact UMI directly to order.

Bell & Howell Information and Learning
300 North Zeeb Road, Ann Arbor, MI 48106-1346 USA

UMI®
800-521-0600

PAVEMENT DEFLECTION ANALYSIS

USING

STOCHASTIC FINITE ELEMENT METHOD

By

MEHDI PARVINI, B.Sc., M.Sc.

A Thesis

Submitted to the School of Graduate Studies

in Partial Fulfillment of the Requirements

for the Degree

Doctor of Philosophy

McMaster University

PAVEMENT DEFLECTION ANALYSIS

USING

STOCHASTIC FINITE ELEMENT METHOD

To my dear wife, Parvin

DOCTOR OF PHILOSOPHY (1997) McMaster University

(Civil Engineering) Hamilton, Ontario

TITLE: Pavement Deflection Analysis Using Stochastic Finite Element Method

AUTHOR: Mehdi Parvini, B.Sc. (Tehran University)
M.Sc. (Tehran University)

SUPERVISOR: Professor D.F.E. Stolle

NUMBER OF PAGES: xv, 184

ABSTRACT

In order to assess the structural characteristics of a pavement-subgrade system, non-destructive, in-situ tests together with backcalculation procedures are widely used. Traditionally, the analytical models adopted for this process are deterministic, however, in reality, the quantities involved in the problem may be random variables. Neglecting the variable nature of the system parameters, e.g., highway material properties, may affect the reliability of the pavement response prediction. On the other hand, inverse solutions to pavement problems are often ill-conditioned and sensitive to the input parameters. Past experience has shown that the estimated values of a backcalculated parameter by different agencies may vary by several orders of magnitude, representing a high level of uncertainty in the estimated parameter. Unless the uncertainty is quantified, practitioners are forced to resort to higher safety factors, which is neither economical nor always conservative.

The present study investigates, rigorously, the behavior of a pavement-subgrade system from a stochastic point of view, and addresses the sensitivity of response variation to variations in layer properties. The results of a forward analysis are utilized to establish a relation between input and output statistical moments in order to interpret the pavement deflection data stochastically. The proposed framework in this research allows one to quantify the uncertainty level in backcalculated system parameters. It also provides a tool to infer the accuracy of the pavement performance prediction based on mechanistic models.

For the purpose of introducing the stochastic approach, the perturbation technique is applied to an idealized, two-layered, pavement-subgrade system for the case of: (a) a static solution based on Odemark definition of equivalent layer thickness; and (b) a frequency domain solution to a single degree of freedom (SDOF) system using an impedance function. The methodology is then extended to a stochastic finite element framework in order to analyze boundary-valued problems of more complex geometry and distribution of material properties. The perturbation method is a mean-based, second-moment analysis for the second-order accurate expected value, and first-order accurate cross-covariance function. For the dynamic analysis, viscoelastic response of the pavement is obtained by using the periodic-load analysis approach and Fourier synthesis.

Based on the results of the simulations, it is demonstrated that, the sensitivity of surface deflections is significantly higher to the subgrade properties than those of the surface and base layers, both in a static and a dynamic analysis. Consequently, it is concluded that, the low dominant frequency of the falling weight deflectometer (FWD) load limits the capability of this test in characterizing surface layer properties. Using the concept of coefficient matrix, it is illustrated that, the low sensitivity of deflections to surface layer properties can be interpreted as a high level of uncertainty in the estimated pavement moduli in a backcalculation exercise. It is indicated that uncertainties in backcalculated parameters often result in an unacceptable pavement performance prediction. Moreover, the physical behavior of the layers are identified by finding the contribution of each layer to the total deflection response of the system using the notation of contribution ratio.

ACKNOWLEDGEMENTS

I wish to express my deep appreciation to my research supervisor, Dr. D.F.E. Stolle, for his valuable guidance and encouragement throughout the course of this study. His excellent supervision is greatly acknowledged.

I also would like to express my sincere gratitude to the members of my supervisory committee, the late Dr. F.A. Mirza, Dr. A.C. Heidebrecht, and Dr. S. Feng, for their valuable comments and suggestions.

I gratefully acknowledge the financial support of the Ministry of Culture and Higher Education of Iran and McMaster University.

This thesis is dedicated to my wife and my parents for their understanding, patience, and sacrifices during the period of this study.

TABLE OF CONTENTS

LIST OF FIGURES

CHAPTER 3

CHAPTER 4

APPENDIX C

APPENDIX D

APPENDIX E

LIST OF TABLES

Chapter 1

INTRODUCTION AND BACKGROUND

1.1 General

Pavement characterization is important for the allocation of funds and resources to maintain and rehabilitate the deteriorating highway infrastructure. The key element in the success of any pavement management system responsible for making preventive and corrective decisions is a proper assessment of the present status and an accurate prediction of the future performance of pavement structures. Characterizing pavement properties plays a critical role in both activities. Pavement properties are also important in the structural design of overlays. In recent years, attention has turned to the use of fundamental analysis of pavement response to load in evaluation of pavement performance for design purposes. The prominent advantage of this method, usually referred to as mechanistic design procedure, is its flexibility in handling new design conditions, e.g., new construction materials, heavier axle loads, etc. However, mechanistic design necessitates

the determination of pavement layer properties. Accurate estimates of these properties are required for making realistic predictions of the remaining pavement life.

Pavement property evaluation can be achieved by means of either destructive methods, e.g., laboratory tests, or nondestructive procedures, e.g., distress surveys and in-situ response measurements. While surface distress surveys provide information which can be used to locate potential problem areas, a more detailed testing program is required to assess the overall serviceability of a pavement. There has been a constant move towards more rational methods of identifying pavement layer properties by improving the measurement devices as well as data interpretation techniques. In recent years, the most common method of pavement characterization is through nondestructive testing and backcalculation of data.

Although nondestructive tests provide quality information, the interpretation of data still remains problematic. This is due to the limitations associated with the mechanical models incorporated into the backcalculation procedures (Stolle et al. 1988), and the uniqueness and ill-conditioning of inverse solutions (Stolle and Hein 1989). The net effect of these limitations is to increase the uncertainty associated with the values of the estimated in-situ mechanical properties. Such uncertainty contributes to reducing an engineer's confidence in his/her ability to properly evaluate structural integrity of the pavement and to estimate its remaining life. This study addresses the uncertainty associated with backcalculated layer moduli, and identifies the accuracy of their estimates.

1.2 Nondestructive Tests

Nondestructive tests (NDT) have gained popularity among engineers and researchers because of their advantages in comparison to laboratory tests. Some of the advantages, which are listed by Houston et al. (1992), are: very low operational cost; short test duration; no disturbance effects; and full-scale model test. The fact that a large volume of soil is tested accounts for heterogeneity in materials, an important factor which is overlooked in small scale laboratory tests. Furthermore, for some nondestructive tests, the geometrical and stress conditions are similar to those of the real traffic loads. Owing to these desirable features, Houston and coworkers have concluded that the use of NDT is an appropriate approach to characterize pavement materials for routine pavement design.

A variety of nondestructive testing procedures have been developed which may be categorized into two main groups: seismic techniques (associated with time measurements) and surface loading techniques (associated with deflection measurements). An example of the first category is the Spectral Analysis of Surface Waves (SASW) described by Nazarian and Stokoe (1984). The main drawback of seismic methods is the difference between the test and real pavement loading conditions. Consequently, correction factors to test results are required to account for, for example, frequency dependence of elastic moduli (Lytton 1989).

Surface loading techniques, which have gained wide acceptance due to their relatively simple operation and automated data collection, are classified based on the mode of loading: (a) static or slow moving; (b) vibratory; and (c) impulsive. The earliest

deflection test methods such as Benkleman beam and California traveling deflectometer used quasi-static loads to deflect a pavement. The Dynaflect and the Road Rater are examples of vibratory loading devices. Although both devices impart steady-state dynamic (harmonic) loading, the Road Rater, which is capable of generating a wide range of loading frequencies, is preferred over the single frequency Dynaflect. Amongst the most common devices applying impulse load are the falling weight deflectometer (FWD) devices. The advantages of an FWD device is its ability to apply heavy loads, perform multi-point deflection measurement, and closely simulate the loading history associated with a moving wheel. After a thorough comparative study of different nondestructive tests, Hoffman and Thompson (1982) have recognized the FWD as the best nondestructive test for simulating pavement responses under moving wheel loads. It has gained favor among highway engineers as an empirical tool for assessing pavement integrity and performance.

An FWD generates a transient load by dropping a weight onto a spring-loaded plate resting on the pavement surface. The resulting load pulse resembles a half-sine wave. Deflection measurements can be taken at the center of the loaded area and at a number of points, referred to as offsets, outside the loaded area by means of velocity transducers (Nazarian and Bush 1989), commonly known as geophones. The details of the test are described by Sebaaly et al. (1985). A schematic of the FWD device is illustrated in Figure 1.1.

1.3 Backcalculation of Pavement Properties

While an NDT is a powerful pavement evaluation tool, its primary drawback is the absence of a comprehensive interpretation technique for collected data. The analysis of NDT data requires the estimation of layer properties from measured deflections, for which no direct analytical solution exists. The lack of a direct solution has forced the development of iterative techniques, which are based on using a mechanistic model together with estimated values for the properties, and then comparing the computed and measured responses. The comparisons are used to update the estimated properties. This general process, which is repeated until a good match is achieved, has been termed backcalculation in the technical literature. Several researchers have presented backcalculation methods for estimation of layer properties, in particular, the layer moduli.

One of the earlier backcalculation methods makes use of the closed-form solution for two layers developed by Scrivner et al. (1973) based on Burmister's layered elastic theory (Burmister 1943). Swift (1972) developed an equation, which he called "empirical", and then established a graphical method for determining the moduli of a two-layered pavement (Swift 1973). Like the Scrivner's closed-form method, both "empirical" and graphical methods give two solutions to the problem, thereby demanding expert knowledge to choose the correct answer. A multi-layered solution technique based on the least squares method has been provided by Yin Hou (1977) for the backcalculation of layer moduli. Other researchers have developed backcalculation procedures based on the equivalent layer theory introduced by Odemark (1949). Two of the equivalent layer

methods, which have been developed by Ullidtz (1987) and Lytton et al. (1979), account for nonlinear stress-strain relation in the subgrade. Numerous microcomputer methods have been developed to backcalculate layer moduli for multi-layered pavements. Based on the description by Lytton (1989), the features that all methods have in common are illustrated in Figure 1.2. Some of the more popular microcomputer backcalculation programs are MODCOMP (Irwin 1983), the "- DEF" series of programs (Bush 1980), and MODULUS (Uzan et al. 1988).

All of the above mentioned methods use a static analysis to interpret deflections, even though the deflections most often originate from a dynamic test. Many researchers have, however, discussed the importance of using a dynamic analysis and the consequence of neglecting inertia on the backcalculated results, see e.g., Mamlouk and Davies (1984), Sebaaly et al. (1985), Siddharthan et al. (1991), Zaghloul et al. (1994), and Stolle and Peiravian (1996). Dynamic backcalculation was introduced by Mamlouk (1985). He used a backcalculation program based on a discrete layer approach to dynamic analysis of pavement developed by Kausel and Peek (1982). Ong et al. (1991) used a finite element based dynamic backcalculation program called FEDPAN to backcalculate layer moduli from surface deflections. Uzan (1994) presented two dynamic backcalculation approaches in the time and frequency domains for estimating pavement material properties. A simplified two-layered approach incorporating Odemark's definition of equivalent thickness was developed by Stolle and Peiravian (1996).

Although a dynamic analysis approach is another step towards a comprehensive backcalculation algorithm, many existing approaches tend to utilize only peak deflections

to estimate properties. There are, however, other procedures which make use of the whole recorded deflection history to estimate layer properties. Among such procedures are system identification (SI) methods for finding the characteristics of pavements, as described by Glaser (1995). In these methods, the complete input and output signals are analyzed to identify the properties of the system, usually referred to as filter. An example of such methods is applied to analysis of surface wave spectra (Nazarian and Stokoe 1984). Other backcalculation techniques have also been developed which rely on the previously gathered information. The most recent methods utilize knowledge-based systems (Chou 1993) and artificial neural networks (Meier and Rix 1995). While artificial neural networks are powerful mathematical tools for curve fitting, they cannot easily accommodate the physics of the problem.

1.4 Accuracy of Backcalculated Properties

Like any other experiment, pavement characterization using a deflection measurement and a backcalculation process is susceptible to errors, the existence of which affect the accuracy/uncertainty of the estimations, i.e., layer properties. Unfortunately, a significant characteristic of most pavement inverse solutions is their sensitivity to small changes in input data. Stolle and Hein (1989) have shown that, owing to the nature of multi-layered stress analyses involving a pavement structure, the backcalculation solution is greatly influenced by the quality of the measured deflection basin. They have

demonstrated that a small variation between the actual and assumed response can lead to considerable differences between the predicted and actual moduli, meaning that errors in measured deflections may have a substantial impact on the outcome of a backcalculation exercise.

There are several sources of error which are introduced into the process of deflection measurement and backcalculation, some random and some systematic in nature. The main sources of random errors, which can be reduced by repeated measurement or calculation, are measurement errors (both force and deflection), and the spatial variation of layer materials and geometry. On the other hand, systematic errors, which can not be eliminated or reduced by repeated experiment, are mainly introduced by the assumptions made with respect to the deflection calculation model and its assumed constitutive stress-strain relation. Traditional methods use a static, linearly elastic model. Neglecting inertia and nonlinearity when interpreting data gathered by a dynamic-based testing procedure on a nonlinear system accounts for part of the overall systematic error. Some other common assumptions leading to systematic errors are uniform load distribution under the plate, perfect seating condition, and neglecting depth, stress, temperature, and moisture dependency of material properties. Another source of error, which may be random or systematic, is due to the uncertainties in estimating input values required to perform the backcalculation analysis, e.g., layer thicknesses, Poisson ratios, etc.

Many studies have addressed the effect of errors on backcalculated properties. Uzan and Lytton (1989), for example, performed an analysis of the errors involved in both the nondestructive testing data collection and the modeling of a pavement structure to

investigate the effects of the errors on the backcalculated layer moduli. Since they only used one backcalculation method in their study, the effect of systematic errors due to different backcalculation schemes was not considered. However, in another study, Lytton (1989) reported the results of different backcalculation exercises and demonstrated that scatter in estimated moduli may extend over several orders of magnitude. Chou and Lytton (1991) also indicated the discrepancy among the backcalculated moduli by comparison of the results performed by different agencies. While they attributed the differences mainly to systematic errors due to using different types of NDT devices, backcalculation methods, and input parameters, they concluded that errors significantly affect the outcome of a backcalculation exercise. Siddharthan et al. (1992) investigated the variation in deflection measurements to find the effect of such variation on the backcalculated moduli. They have shown that for a relatively uniform site, the coefficient of variation of the backcalculated surface layer modulus may reach as high as 65 percent. They also used the backcalculated moduli to evaluate the performance of pavements and noticed that the propagation of errors resulted in a wide range of uncertainty level in the pavement life prediction.

While efforts have been made to reduce the errors by employing new test devices and improving interpretation methods, the total elimination of uncertainties in input data due to errors is not conceivable. To account for such uncertainties in an analysis procedure, the only rigorous way is through a stochastic approach.

1.5 Stochastic Analysis

Statistically based techniques of data analysis have been introduced in the civil engineering practice with the objective of developing a more rational approach to the design and evaluation of constructed facilities. In the past, it has been common practice to analyze structural systems by assuming that system parameters are exactly determined. However, since such an ideal situation is rarely encountered in engineering reality, the need to address uncertainties in the design is now recognized. The stochastic analysis in the broadest sense refers to the explicit treatment of uncertainties in any quantity entering the corresponding deterministic analysis.

The complete solution of a stochastic analysis is obtained by calculating the probability density function of the response. Knowledge of this distribution function provides all the required statistical information about the random response. In practice this is not always possible in view of the complexity of the calculation and the limited information about the statistical behavior of input random variables. Thus, a stochastic analysis often means to determine a limited number of statistical properties associated with the solution. Among the most useful properties of a random solution are the statistical moments, particularly the expected value and the covariance function. Such stochastic description avoids the details of the spatial distribution but retains a measure of the uncertainty associated with the spatial variability.

Different methodologies can be adopted to quantify response uncertainty by calculating its statistical moments. Monte Carlo simulation (Thomas 1971, and Harr

1977) relies on directly simulating an experiment. In this method, a set of random numbers is generated first to represent the statistical uncertainties in the structural parameters. These random numbers are then substituted into the response equation to obtain a set of random numbers which reflect the uncertainty in the structural response, and should be statistically analyzed to produce a qualification of the uncertainty. Perturbation method (Kleiber and Hien 1992) is the most widely used technique for analyzing random systems in engineering (Ghanem and Spanos 1991). This fact is mainly due to the mathematical simplicity of the method. The perturbation scheme consists of expanding all the random quantities around their respective mean values via a Taylor series (Benjamin and Cornell 1970) to formulate a linear relationship between some characteristics of the random response and the random structural parameters. Among other methodologies are Neumann expansion (Adomian 1983), Karhunen-Loeve decomposition (Karhunen 1947 and Loeve 1948), Rosenblueth's method (Rosenblueth 1975), and hierarchy closure approximation (Bharrucha-Reid 1959).

Although different stochastic approaches may be employed in an analysis procedure, for the practical application of statistical methods to structural analysis, such techniques should be implemented into efficient and powerful computational methods. This is because uncertainties are usually spatially distributed over the region of the structure and must be modeled as random fields. Also, the structures themselves are frequently too complex to be analyzed by analytical techniques even in the deterministic case. Therefore, the need for an effective numerical tool to deal with a broad class of stochastic structural problems becomes evident. The stochastic finite element method

(SFEM) provides a computational tool to combine the complexity of large engineering systems with uncertainty models that accommodate random characteristics. While different statistical techniques may be incorporated into a finite element framework, the perturbation approach seems to be both theoretically sound and computationally feasible to combine with finite element analysis. In this approach, the system characteristics are defined in terms of not only their mean values (first-order statistical moment), as is the case for classical finite element method, but also their higher order statistical moments. In turn, the results of a stochastic finite element analysis includes the expected value of the response as well as its higher order statistical moments. Most often only statistical moments up to the second order are calculated due to the impractical computing efforts required to find higher moments (Nakagiri and Hisada 1982).

Many authors have developed and adopted the stochastic finite element method for the analysis of systems characterized by uncertainty. Among many contributors, Cornell (1975), Contreras (1980), Vanmarke and Grigoriu (1983), Hisada and Nakagiri (1985), and Shinozuka (1985) have provided significant contributions to the SFEM development. Within the geotechnical area, this method has been used for the settlement analysis of a shallow foundation (Brzakala and Pula 1992), the prediction of differential settlement (Baecher and Ingra 1981), soil-structure interaction (Dasgupta 1985), slope stability reliability analysis (Ishii and Suzuki 1987), and for complex geotechnical systems (Righetti and Harrop-Williams 1988). Also, more recently, Ghanem and Brzakala (1994) have used this method to account for geometric randomness in layered geotechnical media. No

reference has been found, however, which addresses the application of SFEM in pavement deflection analysis.

1.6 Objectives

The objectives of this study are to investigate the effect of variation in layer properties (non-homogeneity) on the stochastic response (deflection and its variation) of a pavement-subgrade system, and to quantify the anticipated level of uncertainties in the estimated system properties backcalculated from surface deflection measurements. To achieve these goals, the statistical variation in the surface deflection is calculated given random variations in layer properties. The variation in deflection due to a variation in layer property provides a measure of sensitivity of deflection relative to that property. Moreover, a random variation may be viewed as an uncertainty in the estimation of a uniform property. For this reason, when examining the effects of randomness on the deflection, often comments are made with regard to the uncertainty in the backcalculated parameters. To perform the analysis, a stochastic finite element framework based on the perturbation technique is adopted. The computer program developed for the analysis is a mean-based, second-moment algorithm for the second-order accurate expected value and first-order accurate cross-covariance. A linear, elastic idealization of the highway material properties is considered since the effect of nonlinearity is small given the relatively small increase in the existing gravity stresses, and short duration of the FWD loading.

With respect to the stochastic characterization of a problem, a layer is assumed to be defined by a statistically homogeneous random field; i.e., the mean and the variance of the random layer property (e.g., the elastic modulus) are constant throughout a layer. Furthermore, the random property is assumed to be perfectly correlated within the entire layer. Variation[1] in layer property, which may be attributed to either the inherent variability of the property, or the sampling and testing errors (including human errors), is presented by a coefficient of variation (CV). The values of the coefficients of variations in this study are often assumed to be 10%. This value is only used to demonstrate how stochastic procedures can be implemented to identify sensitivities, recognizing that variations in all parameters are neither necessarily equal nor are they equal to 10%. To emphasize the stochastic behavior of pavement systems and simplify the interpretation of the results, two-layered pavement systems are mainly considered, acknowledging the fact that real-world pavement systems usually consist of more layers. The selected values for system parameters such as layer properties are only for illustration purposes and by no means define any restriction on the applicability of the approach to other configurations. It is also important to realize that the thesis presents a framework for analyzing a class of problems in pavement engineering. Consequently, examples are given only to demonstrate the type of information that can be obtained when working within the introduced framework.

---

[1] In the text, the term "variation" is often used in a general sense and refers to the uncertainty associated with a quantity represented by a variance, coefficient of variation, or scatter in data.

This thesis is organized into five chapters. Following this chapter, which is mainly dedicated to problem identification and the scope of the study, Chapter 2 contains the analysis of deflection sensitivity to variations in layer properties within a static framework. In Chapter 3, the dynamic approach to the deflection analysis of pavement structures with random properties is discussed. The observations made in Chapters 2 and 3 are then utilized in Chapter 4 to comment on the anticipated uncertainties in the estimated pavement-subgrade properties backcalculated using measured surface deflections. Finally, Chapter 5 gives a summary and highlights some of the conclusions.

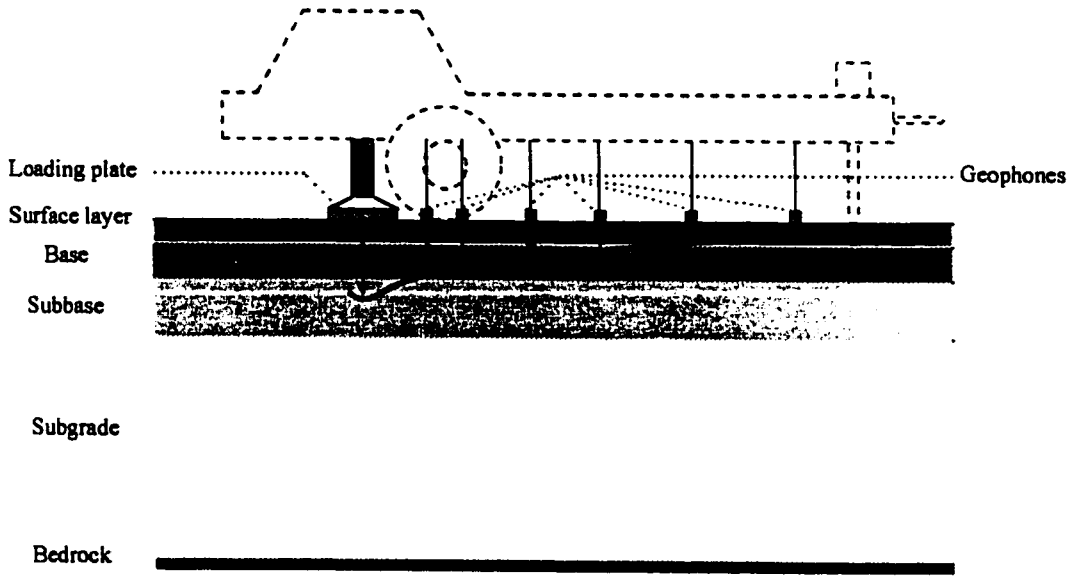

Figure 1.1 Schematic of the falling weight deflectometer (FWD) device

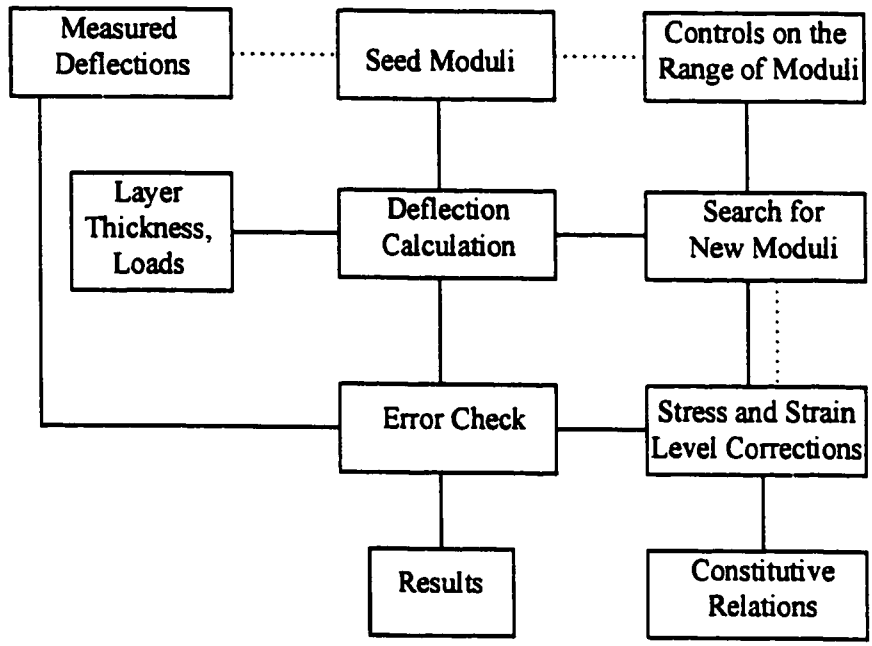

Figure 1.2 Common features of all microcomputer backcalculation methods (after Lytton 1989)

Chapter 2

STOCHASTIC ANALYSIS OF PAVEMENT STRUCTURES UNDER STATIC LOADS

2.1 Introduction

Although most of the recently developed, non-destructive, in-situ tests make use of a dynamic load in order to better simulate a moving wheel load, the static approach to pavement analysis and backcalculation of its properties is still common among practitioners. In this chapter, the inclusion of stochastic considerations in the static analysis of pavement structures is explained. The scalar equations pertaining to the stochastic analysis are derived, then matrix equations leading to a stochastic finite element framework are presented. To introduce the application of the stochastic method, a simplified solution to the pavement-subgrade interaction problem is considered first. The stochastic analysis is performed and the results are compared with those of the Monte Carlo simulations to investigate the accuracy of the perturbation method. For the stochastic finite element analysis, a two-layered pavement system is studied first in order to clearly demonstrate the behavior of a simple model from a stochastic viewpoint.

Simulations are carried out for different geometry and material property configurations of the model to predict deflections, as well as their variations when variations are assumed in material properties or geometry of the layers. Also investigated, are the effects of simultaneous variations in input random variables on the variation of the response. Toward the end of the chapter, a more realistic model consisting of three layers is considered. The results of simulations for this model are compared to those of the two-layered model and conclusions are drawn. Finally, the results of the stochastic analyses are related to the physical behavior of the systems.

2.2 Taylor's Expansion Method

The implementation of the Taylor's expansion method in the stochastic analysis and the form of the equations derived depend on the nature of the response function for the system. The stochastic equations are presented in the following sections for two main function categories; i.e., continuous, and discrete.

2.2.1 Continuous Function of a Random Variable

The Taylor's expansion of a function u(b) with respect to its variable b around b_0 is defined by

$$u(b) = u(b_0) + u'(b)\Big|_{b_0} \Delta b + \frac{u''(b)}{2!}\Big|_{b_0} \Delta b^2 + \Lambda \tag{2.1}$$

in which

$$\Delta b = b - b_0 \tag{2.2}$$

In Equation 2.1, the prime represents differentiation with respect to b, and notation "$\Big|_{b_0}$" indicates that the quantity is evaluated at b_0. One may consider u to be the displacement of a system and b one of the system properties. For a small Δb, the expansion can be truncated after a few terms which provides an approximation to u(b). Assuming that b is a random variable with b_0 being its mean value, neglecting terms higher than second order, and applying the expected value function to both sides of the truncated expansion yields (Kleiber and Hien 1992)

$$E[u(b)] = u(b_0) + \frac{u''(b)}{2!}\Big|_{b_0} \text{var}(b) \tag{2.3}$$

in which var(b) is the variance of random variable b.

To find the variance of function u(b), the first order approximation of u(b) is considered. By taking $u(b_0)$ to the left-hand side of the equation, squaring both sides, and applying the expected value function, the variance is approximated as

$$\text{var}(u(b)) = [u'(b)\big|_{b_0}]^2 \, \text{var}(b) \tag{2.4}$$

When calculating var(u(b)), the expected value of u(b) is approximated with $u(b_0)$. The definitions and properties of the expected value and variance functions (Helstrom 1984) given in Appendix A are used for the derivation of Equations 2.3 and 2.4.

For the case of a multi-variable function, $u(b_1,\ldots b_n)$, Equations 2.3 and 2.4 may be extended to provide

$$E[u] = u(b_0) + \frac{1}{2}\sum_{i=1}^{n}\sum_{j=1}^{n}(u^{'b_i,'b_i})\Big|_{b_{0_i},b_{0_j}} \text{cov}(b_i, b_j) \tag{2.5}$$

and

$$\text{var}(u) = \sum_{i=1}^{n}\sum_{j=1}^{n}(u^{'b_i})\Big|_{b_{0_i}}(u^{'b_j})\Big|_{b_{0_j}} \text{cov}(b_i, b_j) \tag{2.6}$$

in which $\text{cov}(b_i, b_j)$ is the covariance of b_i and b_j, and $u^{'b_i}$ denotes partial differentiation with respect to b_i. To simplify the notation, the dependence of a function to its variables is not shown.

2.2.2 Discrete Function of a Random Variable

When dealing with a discrete representation of a function, direct differentiation may not be possible. In such cases, to derive the equations for the expected value and variance, the following approach is taken.

Consider a matrix equation in the form of

$$\mathbf{K}(b)\mathbf{u}(b) = \mathbf{Q}(b) \tag{2.7}$$

This equation may represent the equilibrium equation of a multi-degree of freedom system where $\mathbf{K}(b)$ is the stiffness matrix, $\mathbf{Q}(b)$ is the load vector, $\mathbf{u}(b)$ is the displacement vector, and b is a system parameter such as elastic modulus. For such a system, since the stiffness, and in general, the load are assumed to be functions of the system parameter b, the displacement will also be a function of b.

Suppose b is a random variable, therefore, it may be written in terms of its mean value b_0 and a random perturbation Δb as given in Equation 2.2. Assuming Δb to be small, and replacing the second order truncated Taylor's expansion of $\mathbf{K}$, $\mathbf{u}$, and $\mathbf{Q}$ about b_0 in Equation 2.7, one gets (Kleiber and Hien 1992)

$$(\mathbf{K_0} + \mathbf{K}'\Delta b + 0.5\mathbf{K}''\Delta b^2)(\mathbf{u_0} + \mathbf{u}'\Delta b + 0.5\mathbf{u}''\Delta b^2) = \mathbf{Q_0} + \mathbf{Q}'\Delta b + 0.5\mathbf{Q}''\Delta b^2 \tag{2.8}$$

where the subscript zero denotes that the quantity is evaluated at b_0, and prime implies that a function is differentiated with respect to b and evaluated at b_0. Again, to avoid the notation from becoming too complex, the dependence of **K**, **u**, and **Q** to b is not mentioned.

Expanding the left-hand side of the equation, and collecting terms of the same order gives a set of three equations from which the values of $\mathbf{u_0}$, $\mathbf{u'}$, and $\mathbf{u''}$ are obtained as follows

$$\mathbf{u_0} = \mathbf{K_0}^{-1}\mathbf{Q_0} \tag{2.9}$$

$$\mathbf{u'} = \mathbf{K_0}^{-1}[\mathbf{Q'} - \mathbf{K'}\,\mathbf{u_0}] \tag{2.10}$$

$$\mathbf{u''} = \mathbf{K_0}^{-1}[\mathbf{Q''} - \mathbf{K''}\,\mathbf{u_0} - 2\mathbf{K'}\,\mathbf{u'}] \tag{2.11}$$

It should be mentioned that differentiation of **K** and **Q** is defined by differentiation of each of their members with respect to b.

Considering the truncated Taylor's expansion of **u**, with analogy to the procedure outlined previously, the expected value vector and the covariance matrix of displacement are given by

$$\mathbf{E[u]} = \mathbf{u_0} + 0.5\mathbf{u''}\,\mathrm{var(b)} \tag{2.12}$$

and

$$\mathbf{cov(u)} = (\mathbf{u'})\mathrm{var(b)}(\mathbf{u'})^{t} \tag{2.13}$$

in which $(\mathbf{u'})^{t}$ is the transpose of $\mathbf{u'}$. As before, when deriving Equation 2.13, the expected value of $\mathbf{u}$ is approximated by $\mathbf{u_0}$.

For the case of a set of p random variables, and a deterministic load, Equations 2.12 and 2.13 change to the following forms (Kleiber and Hien 1992)

$$\mathbf{E[u]} = \mathbf{u_0} + \sum_{i=1}^{p}\sum_{j=1}^{p}\mathbf{S_{ij}}\mathrm{cov}(b_i, b_j) \tag{2.14}$$

and

$$\mathbf{cov(u)} = \mathbf{A\ cov(b)\ A}^{t} \tag{2.15}$$

in which

$$\mathbf{S_{ij}} = (\mathbf{K_0^{-1}K'^{b_i}})(\mathbf{K_0^{-1}K'^{b_j}})\mathbf{u_0} \qquad i,j=1,\ldots p \tag{2.16}$$

and **cov(b)** is the covariance matrix of the set of random variables **b**, with $cov(b_i , b_j)$ representing a member of this matrix, and **cov(u)** being the covariance matrix of the random displacements. The superscript b_i beside a prime refers to partial differentiation with respect to b_i. **A** is an $n \times p$ matrix consisting of p column vectors defined as

$$\mathbf{a}_i = \mathbf{K}_0^{-1}\mathbf{K}'^{b_i}\mathbf{u}_0 \qquad i=1,\ldots p \tag{2.17}$$

with $\mathbf{A}^t$ being its transpose. The parameter n represents the number of degrees of freedom.

2.3 Correlation Between Random Variables

The covariance matrix of the input random variables, **cov(b)**, consists of the variances of the random variables located on the diagonal, and the covariances of each pairs of the variables as off-diagonal members. These off-diagonal covariance terms represent the correlation between each pair of random variables through the following relation

$$cov(b_i, b_j) = \rho_{ij}\sqrt{var(b_i)}\sqrt{var(b_j)} \qquad i,j=1,\ldots p \tag{2.18}$$

in which ρ_{ij} is the correlation coefficient between b_i and b_j.

Based on Equation 2.15, the diagonal terms of **cov(u)**, which define the variances of the displacements at each degree of freedom, may be written as (Kleiber and Hien 1992)

$$\mathrm{var}(u_k) = \sum_{i=1}^{p} a_{ki}^2 \mathrm{var}(b_i) + \sum_{i=1}^{p} \sum_{\substack{j=1 \\ j \neq i}}^{p} a_{ki} a_{kj} \mathrm{cov}(b_i, b_j) \qquad k=1,\ldots n \qquad (2.19)$$

in which a_{ki} is the kith member of matrix **A**.

Using Equation 2.18, Equation 2.19 may be written in terms of the correlation coefficients as

$$\mathrm{var}(u_k) = \sum_{i=1}^{p} a_{ki}^2 \mathrm{var}(b_i) + \sum_{i=1}^{p} \sum_{\substack{j=1 \\ j \neq i}}^{p} a_{ki} a_{kj} \rho_{ij} \sqrt{\mathrm{var}(b_i)} \sqrt{\mathrm{var}(b_j)} \qquad k=1,\ldots n \qquad (2.20)$$

One should note that, if variation exists only in one random variable b_i, then $\mathrm{var}(u_k)$ due to variation in b_i, which is denoted by $\mathrm{var}(u_k)|b_i$, is given by

$$\mathrm{var}(u_k)|b_i = a_{ki}^2 \mathrm{var}(b_i) \qquad k=1,\ldots n \qquad (2.21)$$

In calculating $var(u_k)$ from Equation 2.20, two extreme cases may be considered:

(i) There is a complete positive correlation between all pairs of random variables b_i and b_j. Then $\rho_{ij}=1$ for all i,j=1,...p, and Equation 2.20 becomes

$$var(u_k) = (\sum_{i=1}^{p} a_{ki} \sqrt{var(b_i)})^2 \qquad k=1,...n \qquad (2.22)$$

or by using Equation 2.21

$$var(u_k) = (\sum_{i=1}^{p} \sqrt{var(u_k)|b_i})^2 \qquad k=1,...n \qquad (2.23)$$

(ii) There is no correlation between any pair of the random variables b_i and b_j. Then $\rho_{ij}=0$ for all i,j=1,...p and $i \neq j$, and Equation 2.20 becomes

$$var(u_k) = \sum_{i=1}^{p} a_{ki}^2 var(b_i) \qquad k=1,...n \qquad (2.24)$$

or

$$\mathrm{var}(u_k) = \sum_{i=1}^{p} \mathrm{var}(u_k)\big|b_i \qquad k=1,\ldots n \qquad (2.25)$$

Equations 2.22 and 2.24 may be expressed in terms of the coefficient of variation as,

$$CV(u_k) = \sum_{i=1}^{p} d_{ki} CV(b_i) = \sum_{i=1}^{p} CV(u_k)\big|b_i \qquad k=1,\ldots n \qquad \text{for } \rho_{ij}=1 \qquad (2.26)$$

and

$$CV(u_k) = \sqrt{\sum_{i=1}^{p} [d_{ki} CV(b_i)]^2} = \sqrt{\sum_{i=1}^{p} [CV(u_k)\big|b_i]^2} \qquad k=1,\ldots n \quad \text{for } \rho_{ij}=0 \qquad (2.27)$$

in which

$$d_{ki} = a_{ki} \frac{E[b_i]}{E[u_k]} \qquad k=1,\ldots n,\ i=1,\ldots p \qquad (2.28)$$

2.4 Stochastic Approach to Simplified Pavement Analysis

To illustrate the application of the Taylor's expansion method in stochastic analysis of pavement structures, a simplified approach to the pavement deflection analysis is chosen. For a linearly elastic, semi-infinite pavement system consisting of a surface layer and a subgrade, the surface deflection at a distance r from a concentrated load P is approximated by Boussinesq-Odemark method as (Ullidtz 1987)

$$w_r = \frac{P(1+\nu)}{2\pi e_s h_e}\Omega\left(\frac{r}{h_e}\right) \tag{2.29}$$

where h_e is the equivalent thickness defined by Odemark (1949) as

$$h_e = 0.9\, h_p \sqrt[3]{\frac{e_p}{e_s}} \tag{2.30}$$

and Ω is the shape function

$$\Omega\left(\frac{r}{h_e}\right) = \frac{1}{R^3} + \frac{2(1-\nu)}{R} \tag{2.31}$$

in which

$$R = [1 + (\frac{r}{h_e})^2]^{\frac{1}{2}} \tag{2.32}$$

In the above equations, e_p and e_s are the elastic moduli of the pavement and subgrade, respectively, h_p is the pavement layer thickness, and $\nu = \nu_p = \nu_s$ is the Poisson ratio of both pavement layer and subgrade. Strictly speaking, w_r is the deflection at a depth of h_e from the pavement surface, however, if the vertical strains in the pavement are small, this deflection can be used to approximate the surface deflection. The assumption is valid only if e_p is considerably greater than e_s and the pavement is not too thick.

Now, if the subgrade elastic modulus e_s is a random variable, the surface deflection w_r will also vary randomly. Using Equations 2.3 and 2.4, then the expected value and variance of deflection w_r are obtained in terms of the mean value and variance of e_s. The same exercise can be carried out assuming e_p to be a random variable, and finding the expected value and variance of deflection in terms of the statistical moments of e_p.

For a sample problem, where P=40 kN, e_p=4000 MPa, e_s=100 MPa, h_p=0.15 m, and ν=0.45, the variation in w_r in terms of its coefficient of variation is calculated for two separate cases: (a) only e_p is allowed to vary randomly; and (b) only e_s is allowed to vary randomly. The results of the simulations are illustrated in Figure 2.1. The figure indicates

that, the variation in deflection under the load (r=0) is almost 1/3 of $CV(e_p)$, when the pavement varies, and 2/3 of $CV(e_S)$, when the subgrade varies. These values were obtained by a simple, first order error analysis (Stolle and Jung 1992), thereby confirming the results from the analysis procedure developed in this study.

2.4.1 Effect of Higher Order Terms

If random perturbations are not small, the truncated Taylor's expansion should include higher order terms to provide acceptable accuracy. To illustrate the effect of higher order terms, the Taylor's expansion of w_r with respect to e_s is truncated up to the fourth order and the expected value function is applied to both sides of the equation to give

$$E[w_r] = w_{r0} + \frac{w_r''}{2!}\text{var}(e_S) + \frac{w_r'''}{3!}M^3(e_S) + \frac{w_r''''}{4!}M^4(e_S) \qquad (2.33)$$

where $M^3(e_S)$ and $M^4(e_S)$ are the third and fourth order central moments of the random variable e_S, respectively. If the probability density function of e_S is symmetric, the third order central moment will be zero; i.e., $M^3(e_S)=0$. Furthermore, if e_S has a normal distribution, $M^4(e_S)=3\text{var}(e_S)^2$ (Taylor 1982) and Equation 2.33 becomes

$$E[w_r] = w_{r0} + \frac{w_r''}{2} var(e_s) + \frac{w_r''''}{8} var(e_s)^2 \qquad (2.34)$$

The variance of w_r is calculated as before, except that the statistical moments of e_s up to the fourth order are taken into account here, giving

$$var(w_r) = (w_r')^2 var(e_s) + [\frac{3}{4}(w_r'')^2 + w_r' \, w_r'''] var(e_s)^2 \qquad (2.35)$$

In the derivation of Equation 2.35, w_{r0} is used as an approximation for $E[w_r]$.

Calculations were completed to compare the second and fourth order perturbation method solutions. Simulations were also carried out using the Monte Carlo technique in order to evaluate the accuracy of the perturbation methods. The Monte Carlo solutions were obtained using 1000 sets of results which were calculated by varying e_s via a random number generator based on a normal distribution.

Figure 2.2 shows the results obtained from the second order perturbation, fourth order perturbation, and Monte Carlo simulation techniques. Comparing these curves indicates that, for this problem, the effect of the higher order terms in the Taylor's expansion is small for $CV(e_s)$ of 15% or less. However, the difference between the second and fourth order schemes becomes considerable for values of $CV(e_s)$ greater than 20%. This observation is in good agreement with that reported by Brzakala and Pula (1992a). By comparing the coefficients of variations from the fourth order perturbation and Monte Carlo technique, it is clear that higher

terms than fourth order are required if CV(e_s) exceeds 25%. Furthermore, it appears that truncation leads to an underestimation of the coefficient of variation of the response. In other words, the actual variation of the response is higher than that obtained by using a truncated Taylor's expansion. A similar conclusion is made by Shinozuka and Yamazaki (1988).

2.5 Stochastic Finite Element Method

To perform a stochastic finite element analysis for a quasi-static situation, the Taylor's expansion approach in the form of Equations 2.14 and 2.15 was incorporated into a finite element program. The code was validated by comparing the results of the stochastic finite element simulations with closed-form solutions for some sample problems. A FORTRAN listing of the program, along with the input and output files for a simple two-element axial problem with random material and/or geometric properties, for which the solution is given in Kleiber and Hien (1992), is presented in a separate document (Parvini, 1997).

For an SFEM procedure, the discretization of a problem is exactly the same as that of any ordinary finite element method. The difference lies in describing material and/or geometric properties in terms of stochastic variables. These values are often defined by expected values and variances rather than by deterministic values as is the case for a traditional finite element analysis. It is important to recognize that, when there are more than one random variable, the covariances of the variables, which show their correlations, must also be provided as input.

This can be done by introducing the covariance matrix of the random variables. It should be pointed out that, the derivatives of a stiffness matrix with respect to random variables are calculated on the element level, and the resulting matrices are assembled in the usual way, taking into account the compatibility and equilibrium principles. Also, in order to calculate **A** defined in Equation 2.15, the derivatives of the stiffness matrix with respect to all random variables are required. Therefore, for each random variable it is necessary to have memory at least equivalent to what is required to store the stiffness matrix.

2.6 Sample Pavement Problem

Figure 2.3 defines the geometry of a typical multi-layer pavement-subgrade system consisting of a hot mix surface layer, a granular base and a subgrade which is supported by a bedrock. Each layer is defined by its properties such as thickness, elastic modulus, and Poisson ratio. Material properties are assumed to be linearly elastic and isotropic. The default expected values of the pavement, base, and subgrade elastic moduli are selected to be e_p=4000 MPa, e_b=300 MPa and e_s=100 MPa, respectively, with Poisson ratios of ν_p=0.35 for the surface layer, ν_b=0.40 for the base, and ν_s=0.45 for the subgrade. The selected values for the pavement properties are consistent with typical resilient (elastic) moduli and Poisson ratios for hot mix asphalt reported in the literature (Huang 1993). The subgrade modulus corresponds to the values often encountered when interpreting

Ontario FWD data (Stolle 1992). The default thickness of the pavement and base layers are assumed to be 0.15 m and 0.30 m, respectively, with the depth to the bedrock H=7.35 m. A 40 kN load is considered to be applied uniformly over a circular area of radius a=0.15 m. Although the applied load of an FWD test is of an impact nature, elastostatic analysis is completed in this chapter in order to emphasize the response characteristics associated with the stochastic nature of the problem. The inertial effects of dynamic loading on the variation of response are discussed in Chapter 3.

It should be noted that, unless stated otherwise, the values of the parameters given in this section are used for all the simulations.

2.6.1 Characteristics of the Finite Element Model

In order to analyze the problem by finite element method, the medium is divided into a finite number of elements. Strictly speaking, when dealing with a stochastic analysis, the whole structure should be analyzed using a three-dimensional finite element code as the variations in layer properties are not necessarily axisymmetric. However, in order to save computational time and to avoid a three-dimensional analysis, it is assumed in this study that the effect of randomness in the horizontal plane is the same for all directions, thereby allowing analyses with an axisymmetric finite element scheme. To satisfy the boundary condition on the line of symmetry passing through the center of the loading area,

zero shear conditions are defined along this line. The domain is subdivided into 1200, 4-noded, quadrilateral, isoparametric elements with 30 rows and 40 columns, yielding 1271 nodes and 2430 net degrees of freedom. The mesh is chosen finer close to the load and coarser as one moves away from the load. The nodes along the bottom boundary are fully fixed, simulating the presence of the bedrock. In order to minimize the effect of an artificial boundary (traction free vertical boundary) on the solution in the region of interest, the domain is extended to 11.85 m away from the center line, i.e., 79 plate radii away. A schematic of the finite element model is shown in Figure 2.4. Although a less number of elements could be used to obtain accurate solutions for the static case, a fine mesh identical to the one used in dynamic analysis is chosen. The reason for using the same grid is that the author wishes to minimize the effects of discretization errors when making comparisons of solutions. It should be recognized that there are more restrictions on the maximum size of the elements in a dynamic analysis, thereby often requiring a finer mesh than is necessary for the static case.

2.7 Simulations for Two-Layered Systems

In order to clearly demonstrate the general observations associated with the stochastic analysis, the response of a two-layered pavement system consisting of a surface layer directly on top of a subgrade (h_b=0) is investigated first.

2.7.1 Predicted Surface Deflections

Figure 2.5 provides surface deflections for deterministic elastic moduli (represented by their mean values), and for a random subgrade modulus with a 20% coefficient of variation. Since deflections are most sensitive to the subgrade modulus, as indicated in Figure 2.1, only the effect of variation in the subgrade modulus on the deflections is illustrated here. A similar exercise, which took into account the variation in the pavement modulus, resulted in superimposed curves. As shown in the figure, a 20% coefficient of variation in the subgrade modulus has only a small effect on the deflection basin. Although the difference may be small, the expected value of deflection, E[u], is always greater than the deflection calculated using the mean, u_0. Recognizing that deflection is a convex function in terms of the subgrade modulus, this observation can be explained based on Jenson's Inequality (Billingsley, 1995). Because of the small differences in deflections due to variations in layer moduli, the traditional viewpoint of neglecting the effect of such variations appears to be justified. Nevertheless, small differences in deflection bowl shapes can have a large influence on the backcalculated moduli, as will be illustrated in Chapter 4.

Figure 2.5 also shows the expected values of the deflections under the pavement layer. For this relatively thin pavement, except for the points very close to the load, there is no significant difference between the deflections at the top and bottom of the pavement

layer. This justifies the assumption of zero straining of the pavement layer as was mentioned in the previously presented simplified approach.

2.7.2 Variations in Elastic Moduli

i) Typical trend for variation in deflection

Although random variations in layer moduli do not have much influence on the expected values of deflections, they do affect the statistical variations of deflections. In this study, variation is often defined in terms of a coefficient of variation. The author believes that this dimensionless quantity better represents the relative uncertainties in the parameters.

The coefficient of variation of deflection, CV(u), is plotted versus the radial offset in Figure 2.6 for two separate cases: (a) in the first case variation is only assumed in the pavement layer; and (b) in the second case it is considered only in the subgrade. For each case, results are obtained for three values of 5, 10, and 15 percent for the coefficient of variation of the elastic modulus.

It may be observed that, when the pavement modulus is allowed to vary, CV(u) under the load is the largest and decreases rapidly as one moves farther from the center line. This trend is expected since most of the straining in the pavement structure occurs

underneath the load. The distance from the load to the point where the effect of the pavement property variation on CV(u) becomes insignificant is referred to in this thesis as the pavement influence length, r_p. The ratio r_p/h_e for the configuration under study in Figure 2.6 is 1.30. An important observation from a backcalculation perspective is that a variation in the pavement modulus corresponds to a much smaller variation in deflection. In other words, small variations in surface deflections have the potential to contribute to large variations in backcalculated pavement moduli. This is consistent with the backcalculation experience where it has been found that surface moduli are difficult to predict (Lytton 1989).

The other set of curves is obtained by keeping the variation of the pavement layer modulus equal to zero and changing the coefficient of variation of the subgrade modulus, $CV(e_s)$. As shown in the figure, for a specific coefficient of variation of subgrade modulus, CV(u) increases as one moves away from the center line until a radius of approximately 0.9 m, after which CV(u) remains relatively constant at a value close to $CV(e_s)$. Again this observation is consistent with the fact that deflections farther from the load are mainly attributed to the straining of the subgrade (Uzan and Lytton 1989). Since, for the first order perturbation method, response variance changes linearly in terms of the input variance, and the effect of variation on the expected value is negligible, the increase in CV(u) is also approximately linear with respect to the increase in CV(e) for both pavement and subgrade variations.

A comparison between Figures 2.1 and 2.6 confirms that the simplified approach presented in Section 2.4 is capable of reflecting the sensitivity of the variation in deflection to variation in layer moduli. This endorses the suitability of the simplified approach for sensitivity analysis of deflection variation in quasi-static analysis of two-layered models.

ii) Effect of Bedrock Depth

The results of the previous analyses correspond to a particular pavement structure. To investigate how bedrock depths affect variations in deflections when layer moduli are allowed to vary randomly, simulations were carried out for three bedrock depths of 2.85, 4.35, and 7.35 m. For these three pavement-subgrade systems, first the expected values of deflections are considered. Figure 2.7 shows that an increase in the depth of the bedrock is equivalent to an almost uniform increase in the surface deflections. In other words, all the points at the surface are similarly affected by a change in the bedrock depth.

On the other hand, when examining Figure 2.8, which summarizes CV(u) for the three bedrock depths, one comes to the conclusion that the depth to the bedrock does not have an important effect on CV(u), whether the pavement or subgrade modulus is allowed to vary. Moreover, the pavement influence length, and consequently the ratio r_p/h_e, is independent of the bedrock depth. It must be recognized that these observations are only applicable to the quasi-static loading condition and the range of H considered here.

iii) Effect of Pavement Thickness

Three different pavement thicknesses of 0.15, 0.30, and 0.45 m were considered and simulations were carried out to find the expected value and variation of surface deflection when variations were assumed in the layer moduli. The expected values of deflections are summarized in Figure 2.9. As shown in the figure, unlike for the case of different bedrock depths, the decrease in deflection due to an increase in the pavement thickness is not uniform for all the offsets. The change in deflection for the offsets close to the center line is very significant while after a distance of about 1.2 m, there is almost no change in the deflection due to the change in the pavement thickness. It must be recognized that the offset beyond which the pavement thickness has a little influence on u depends on h_e.

Figure 2.10 indicates that for the case where the pavement modulus is allowed to vary, the thicker the pavement the higher variation in the deflection. This result is not surprising since strains within a thick pavement contribute more to the overall surface deflection than the case for a thin pavement, particularly directly under the load. Moreover, the pavement influence length increases for thicker pavements, while the ratio r_p/h_e stays constant for all three pavement thicknesses. For the case where subgrade modulus varies, on the other hand, CV(u) decreases as the result of an increase in the pavement thickness. which can be explained using the argument given for the previous

case. In summary, the results are consistent with what one would expect; i.e., as h_p increases, the importance of the pavement to the overall behavior of the system increases.

iv) Effect of Pavement Modulus

Simulations were also completed to study the effect of changing the pavement layer modulus from e_p=4000 MPa to e_p=8000 MPa on E[u] and CV(u). The results for the expected value and coefficient of variation of deflection are summarized in Figures 2.11 and 2.12, respectively. The trends observed in these figures are similar to those observed in Figures 2.9 and 2.10. The sensitivity of the deflection and its variation to the changes in the pavement modulus, however, seems to be less than that related to the changes in the pavement thickness, as will be illustrated rigorously later on when h_p is allowed to vary randomly. This is not surprising if one considers the relation of w_r to h_p and e_p in Equation 2.29. From a backcalculation perspective, the low influence of e_p on CV(u) compared to that of h_p suggests that if h_p were to be backcalculated, it would yield a more reliable quantity than backcalculated e_p.

v) Effect of Subgrade Modulus

The effect of the subgrade modulus on the expected value and variation of deflection is investigated by carrying out analyses for three different cases. For the first two cases, the mean value of the subgrade modulus is assumed to be constant and equal to e_s=100 MPa and e_s=200 MPa, respectively. For the third case, the subgrade modulus is assumed to be variable in order to more accurately simulate the real situation where subgrade moduli change with depth. The following relation is used to take into account the change in the modulus of a granular subgrade as a function of depth (Yoder and Witczak 1975)

$$M_r = 3.84\theta^{0.67} \tag{2.36}$$

where M_r is the resilient modulus of soil in terms of MPa and θ is the sum of principal stresses in terms of kPa. It should be noted that for linear problems, the resilient and elastic moduli are identical. Relating the sum of the principal stresses to the depth (for a soil with an assumed friction angle of 30 degrees and unit weight of 20 kN/m^3), the following approximate relation is obtained

$$M_r = 50\, z^{0.7} \tag{2.37}$$

in which z is the depth in meters.

To apply Equation 2.37 to the problem, the subgrade is divided into six layers of 1.2 m thick. Each layer has a uniform modulus which is calculated from Equation 2.37 based on the depth of the bottom of the layer. This results in a subgrade modulus ranging from 60 MPa at the top to 200 MPa at the bottom with an average around 140 MPa.

Simulations were carried out for the above three cases and the results are reported in Figures 2.13 and 2.14. Figure 2.13 illustrates the expected values of the surface deflections. These deflections for the case of variable subgrade modulus are higher than those for e_s=100 MPa at points close to the load. For points at larger offsets the situation is reversed. This pattern is observed because a large portion of the deflection at close points is due to strains in the upper part of the subgrade where the elastic modulus is less than 100 MPa. For large offsets, however, the straining takes place mainly deeper in the subgrade where the modulus is greater than 100 MPa. For subgrade modulus equal to 200 MPa, the expected value of deflection is almost half the value corresponding to e_s=100 MPa, especially at points located far from the load. Nevertheless, given the sensitivity of the deflection bowl shape to the manner in which the subgrade is modeled, this example clearly demonstrates why it is necessary to accurately model a subgrade when backcalculating layer properties. Unfortunately, systematic errors associated with modeling can lead to large errors in estimated pavement moduli.

By examining Figure 2.14, which provides information about CV(u), it may be concluded that the solutions are not very sensitive to the value of the subgrade modulus

when the subgrade is uniform. Even when the pressure sensitivity of e_s is taken into account, one observes that CV(u) patterns are similar to those for the cases of uniform subgrade conditions, although the magnitudes are influenced somewhat.

vi) Simultaneous Variations in Layer Moduli

Up to this point, the effects of variations in elastic moduli were considered separately for the subgrade and the pavement. In the real world, variation in modulus may exist simultaneously for all layers. For such a case, the elastic modulus of the pavement and subgrade may or may not be correlated. In this section, the effect of simultaneous variation in both layer moduli on CV(u) is investigated for two extreme cases: (a) complete correlation (ρ=1); and (b) no correlation (ρ=0), realizing that for other levels of correlations, the results will fall somewhere in between. Figure 2.15 summarizes the results of the simulations assuming a 10% coefficient of variation for the pavement and subgrade layer moduli. The results are illustrated for pavement thicknesses of 0.15, and 0.45 m. The figure shows that, for ρ=1, the accumulated CV(u) is independent of the radial distance and pavement thickness, with a constant value almost equal to 10%. On the other hand, when ρ=0, CV(u) due to variation in both moduli is close to the value of CV(u) for which only the subgrade modulus varies. A deviation from this tendency occurs for the case of thick pavement at locations close to the load. This may be explained by

considering the low effect of variation in the pavement modulus on CV(u) at far distances, but the increasing effect of the pavement on the response close to the load as thickness increases.

Simulations with other pavement-subgrade configurations give similar results confirming that, CV(u) is almost equal to $CV(e_s)$=$CV(e_p)$ when the elastic moduli of both layers are allowed to vary and ρ=1. For ρ=0, the CV(u) curve tends to be close to the one associated with the case when only the subgrade elastic modulus varies.

In the previous discussion CV(u) was directly obtained by assuming variations in both layer moduli and carrying out the simulations. However, the same results could have been obtained from the results of the simulations when layer moduli varied separately by using Equations 2.26 and 2.27 (for the case of ρ=1 and ρ=0, respectively).

2.7.3 Variations in Other Properties

In the previous section, variations in deflections due to variations in layer moduli were calculated for different pavement configurations. There are, however, other pavement properties which affect surface deflections, e.g. Poisson ratio, and layer thickness. In this section, CV(u) due to variations in layer Poisson ratios, and layer thicknesses are found.

i) Variation in Poisson ratio

Figure 2.16 shows CV(u) due to variations in Poisson ratios. When the pavement Poisson ratio varies, CV(u) has a trend similar to that when the pavement elastic modulus varies. When the subgrade Poisson ratio varies, however, CV(u) increases almost linearly with radial distance, with a value of about 10% at a distance 1.8 m away from the load. This means that, although the influence of the subgrade Poisson ratio on the surface deflection is often considered negligible (Baecher and Ingra 1981), the effect of its variation on CV(u) can be important at locations far from the load. The curves associated with simultaneous variation in both layers are also plotted for ρ=1, and ρ=0. Unlike for the case of varying elastic moduli, when ρ=1, the accumulated CV(u) is not constant. For ρ=0, the accumulated CV(u) is close to the CV(u) due to CV(ν_s) alone. This is similar to what is observed when considering variations in elastic moduli.

ii) Variation in layer thickness

The values of CV(u) when the coefficient of variation of either the pavement layer thickness or subgrade thickness is 10% are summarized in Figure 2.17. The results given in this figure are consistent with those reported in Figures 2.7 and 2.9. They confirm that for locations close to the load, the sensitivity of the deflection variation to the variation in

the pavement thickness is much higher than its sensitivity to the variation in the subgrade thickness. At larger offsets, the opposite is true. Also, a comparison of CV(u) due to variation in the pavement thickness in Figure 2.17 with that due to the same level of variation in the pavement modulus in Figure 2.6 suggests that, deflections are almost three times more sensitive to the pavement thickness than to its modulus. This observation agrees with what is reported in the literature (Stolle and Jung 1992). As before, results are also provided for the case when variations exist in both layer thicknesses. Unlike the case of variations in elastic moduli and Poisson ratios, CV(u) due to variations in both layer thicknesses (for ρ=0 and within a distance equal to r_p) is close to CV(u) when only the pavement thickness varies.

2.7.4 Simultaneous Variations in All Layers' Properties

In the real world, variations may occur simultaneously in all of the material and geometric properties of the layers. To find CV(u) in such a case, one way is to carry out the simulations by taking into account all the variations. The other way, which is suitable when CV(u) due to separate variations of the properties are available, is to combine the existing results using relations such as Equation 2.20. It should be noted that in order to apply Equation 2.20, the correlation coefficient (ρ) between each pair of the random properties must be known. When ρ equals either one or zero, Equation 2.20 is simplified

to Equations 2.26 and 2.27, respectively. To illustrate the application of these equations, the situation when there exists a 10% coefficient of variation in the elastic modulus, Poisson ratio and layer thickness of the subgrade is considered. To be more realistic, the elastic modulus and Poisson ratio are assumed to be completely correlated, while no correlation is assumed between the layer thickness and the other two material properties. Another case, where a 10% variation is assumed in all the material and geometric properties of both layers (with the above mentioned correlation pattern within each layer and no correlation between the layers) is also studied. Figure 2.18 summarizes the results. A comparison between the two curves once again emphasizes the dominating influence of the subgrade on the surface deflections. Moreover, the figure shows that an overall 10% variation in the properties of both layers results in a variation between 13 to 21% in the surface deflection. From a backcalculation viewpoint, the information provided in Figure 2.18 may suggest that the expected variations in estimated parameters are always less than those observed in measured deflections. However, when backcalculating layer moduli, random variations in other input parameters (e.g. layer thicknesses) are often neglected. Thus, variations in deflections translate only to variations in the moduli. This results in higher levels of uncertainties in the backcalculated values, especially for the pavement layer. Unfortunately, it is not possible to separate the contribution to uncertainty for each layer parameter.

2.8 Simulations for Three-Layered Systems

Pavement-subgrade systems usually have more than two layers. In order to add an additional level of complexity to the pavement problem, the three-layered model shown in Figure 2.3 is considered in this section. The characteristics of this model are identical to the one defined in Section 2.6. Simulations were carried out assuming that the coefficient of variation of the pavement, base, and subgrade moduli were equal to 10%, however, one at a time. The results are summarized in Figure 2.19. Based on this figure, CV(u) due to $CV(e_b)$ is slightly larger than CV(u) due to $CV(e_p)$, while it is much less than that due to $CV(e_s)$. Also, the curve belonging to the variation in the base layer has a similar trend as that of the pavement. This indicates that the sensitivity of the deflection variation to the variation in the base layer is the highest close to the load and becomes negligible as one moves farther away. If the stiffness of the pavement layer is increased, the value of CV(u) due to $CV(e_p)$ increases, as was observed previously for the two-layered system. However, for most of the points on the surface, this increase is accompanied with a decrease in the value of CV(u) due to $CV(e_b)$, as illustrated in Figure 2.20. This observation is consistent with the experience that surface deflections are insensitive to thin, softer layers located under a stiff layer.

Compared with the two-layered model, the curves corresponding to the variation in the pavement and subgrade are almost unchanged in pattern, except that they show a small decrease in the magnitude of CV(u) at offsets close to the center line. The

comparison is more clearly presented in Figure 2.21 where the contribution of CV(u) due to variation in each layer modulus to the accumulated CV(u) is shown. The results given in the figure are for the case where layer moduli are completely correlated in pairs (ρ=1). The figure indicates that, while CV(u) due to simultaneous variation of all layer moduli is almost the same for the two models (with an approximately constant value of 10%) its components coming from different layers are not the same. This is obvious owing to the contribution of an additional layer to CV(u) in the three-layered model. Hence, it may be concluded that, adding more layers to the pavement model, when their properties are correlated, decreases the sensitivity of CV(u) to CV(e) of each layer. This observation has a very important consequence from a backcalculation viewpoint. It suggests that trying to get more information by including more layers in a backcalculation model will increase the uncertainties associated with the estimated parameters. For a more realistic case when the layer moduli are assumed uncorrelated (ρ=0), the resulting CV(u) for the two models are shown in Figure 2.22. In such a case, overall, CV(u) for the three-layered system is slightly less than that of the two-layered model, except at larger offsets.

By changing the material properties and thicknesses of the layers, simulations were carried out on other configurations of the three-layered pavement model. Although the magnitude of the variations in the deflections were different in each case compared to the corresponding case for a two-layered system, the trends observed in the curves were similar, thereby confirming the previously reported observations with regards to the sensitivity of deflection variation to variations in layer properties.

2.9 Physical Interpretation of CV(u) due to CV(e)

For a multi-degree of freedom system with p random elastic moduli, the coefficient of variation of deflection at degree of freedom k due to variation in random modulus e_i, $CV(u_k)|e_i$, can be related to $CV(e_i)$ by

$$CV(u_k)|e_i = \left(\frac{u_k^{e_i}}{u_k}\right)CV(e_i) \tag{2.38}$$

in which $u_k^{e_i}$ is the deflection contribution of all the members with elastic modulus e_i to the total deflection at k^{th} degree of freedom, u_k. The ratio of u_k to $u_k^{e_i}$ is called contribution ratio in this thesis. Furthermore, when all the random moduli are completely correlated with the same coefficient of variation, one may get

$$CV(u_k) = CV(e) \tag{2.39}$$

The details pertaining to the derivation of Equations 2.38 and 2.39 are provided in Appendix B. Equation 2.38 may be written using a slightly different notation as

$$\frac{CV(u_k)|e_i}{CV(u_k)|e} = \left(\frac{u_k^{e_i}}{u_k^{e}}\right) \tag{2.40}$$

where **e** is a subset of the p random moduli, with the **e** in u_k^{e} and $CV(u_k)|e$ implying that deflection and its coefficient of variation at degree of freedom k are the contributions from the members with a modulus which is included in **e**, respectively.

To illustrate how Equations 2.38 to 2.40 may be utilized to interpret the results of the stochastic analysis, the two-layered system discussed in Section 2.7 is considered again. Given Equation 2.38, the information shown in Figure 2.6 with respect to the simulations where $CV(e_p)$=10% suggests that the contribution of the pavement layer deflection to the total deflection of the system is greatest close to the load, and becomes insignificant farther away. For the case where $CV(e_s)$=10%, this contribution has its highest value at points far from the load. Also, regardless of the location of the point, the subgrade deflection has always a higher influence on the total deflection when compared to that of the pavement layer. One may wonder why the ratio $u_k^{e_s}/u_k$, and consequently, $CV(u_k)|e_s/CV(e_s)$ are greater than one at far offsets. The reason may be explained by the fact that, due to the Poisson effect, the pavement layer expands farther away from the load. This is indicated in Figure 2.5, if one pays a close attention to the curve associated with the deflection under the pavement layer. The expansion of the pavement means that its effect on the total deflection is out of phase with that of the subgrade, i.e., the pavement layer has a negative contribution to the surface deflection. Therefore, the share

of the subgrade deflection becomes greater than the total deflection of the system. Since the absolute values of the deflections are used to calculate the coefficients of variations, CV(u) is always presented as a positive quantity, even if the deflection ratio is negative.

In Figure 2.15, the curve associated with simultaneous variations in both layer moduli with $\rho=1$ indicates that, the accumulated $CV(u_k)$ is equal to CV(e), which is consistent with Equation 2.39. The physical interpretation is obvious, noting that the sum of the contributions of the pavement and subgrade deflections should be equal to the total deflection.

To examine Equation 2.40, another set of simulations were carried out where the subgrade was modeled as six separate layers, each 1.20 m thick, with the same elastic modulus for all layers. Analyses were carried out when CV(e) for each layer was assumed to be 10%, one at a time. The ratio of $CV(u_k)|e_i$ for layer i to CV(u) when the entire subgrade has a 10% variation is plotted, along with the ratio of the E[u] associated with layer i to that of the subgrade. For all the layers, including the first, third, and sixth layer from the top, which are shown in Figure 2.23, a close pattern between the two sets of the curves may be noted. The difference between the patterns may be attributed to the approximations introduced when calculating CV(u) by truncating the Taylor's expansion, and using u_0 instead of E[u]. Figure 2.23 also indicates that deflections at points close to the load are more sensitive to the moduli of the upper layers, while further away, the moduli of the lower layers mainly influence the deflections. The observations made in this

figure clearly demonstrate the close relationship between the results of the stochastic analysis with the physical behavior of the system.

2.10 Concluding Remarks

The results of the simulations using an elastostatic framework indicate that, surface deflections are more sensitive to the variation in the subgrade modulus than to the variation in the pavement layer modulus. It is also noted that, the deflection sensitivity does not change significantly as a result of a change in the value of the bedrock depth and the layer modulus, given the range of the values under study. The pavement thickness, however, does have an influence on the deflection sensitivity to the variations in the layer moduli. While similar trends are observed for a three-layered pavement system, the magnitude of the deflection sensitivity to the variation in the pavement layer and subgrade modulus decreases when compared to that associated with the two-layered system.

The notation of the contribution ratio has been introduced in this chapter. It is shown that, by using this notation, one can establish a relation between the ratio of the responses and that of their corresponding variations. The contribution ratio can be effectively used to find the stiffness contribution of a group of members in the overall stiffness of the structure, as is addressed in Appendix B.

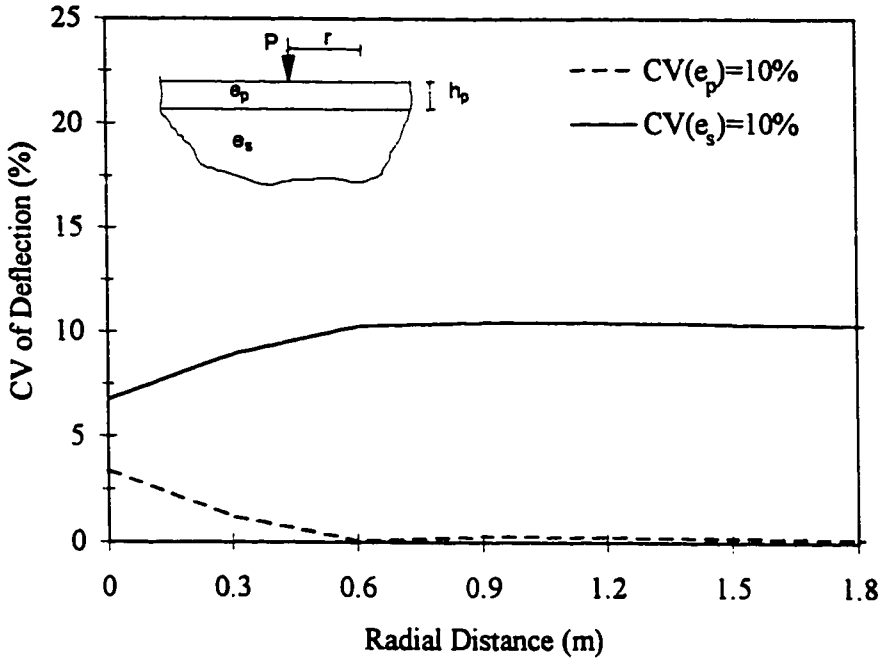

Figure 2.1 CV of deflection based on simplified approach

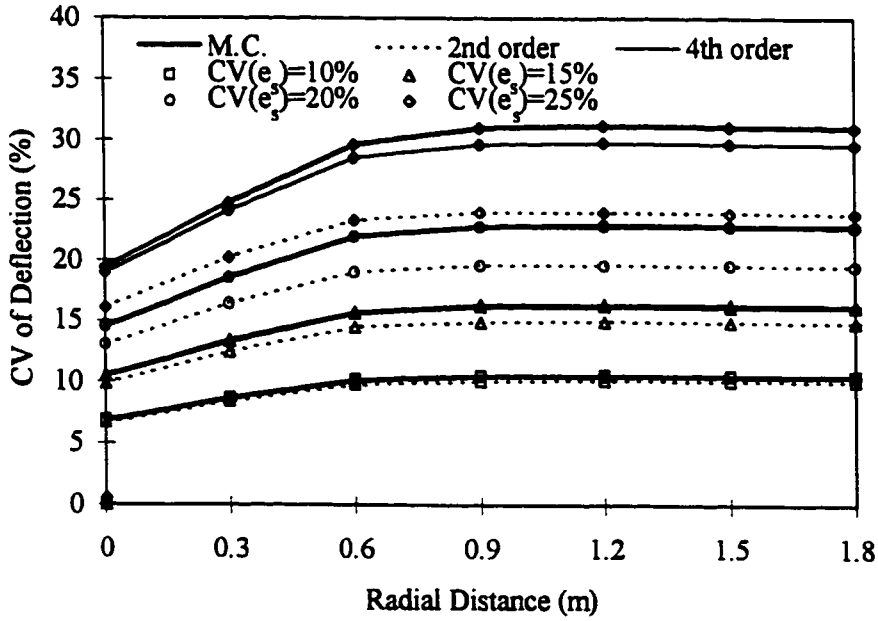

Figure 2.2 Comparison between second and fourth order perturbation technique and Monte Carlo simulation for simplified approach

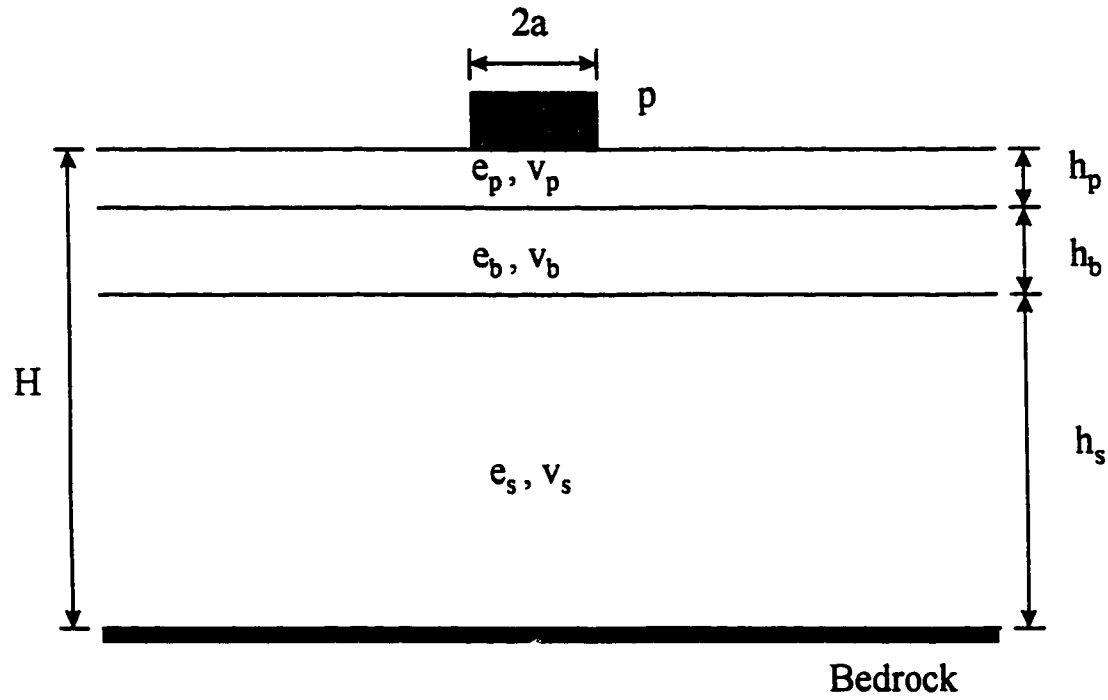

Figure 2.3 Schematic of a pavement-subgrade system

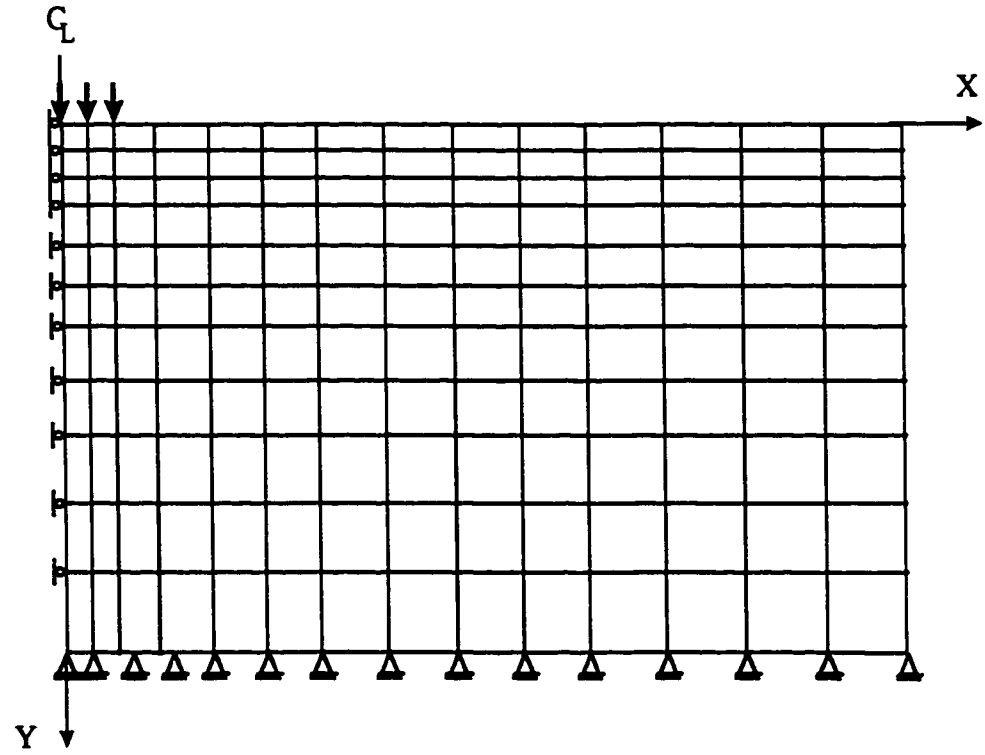

Figure 2.4 Schematic of the finite element model for a pavement-subgrade system

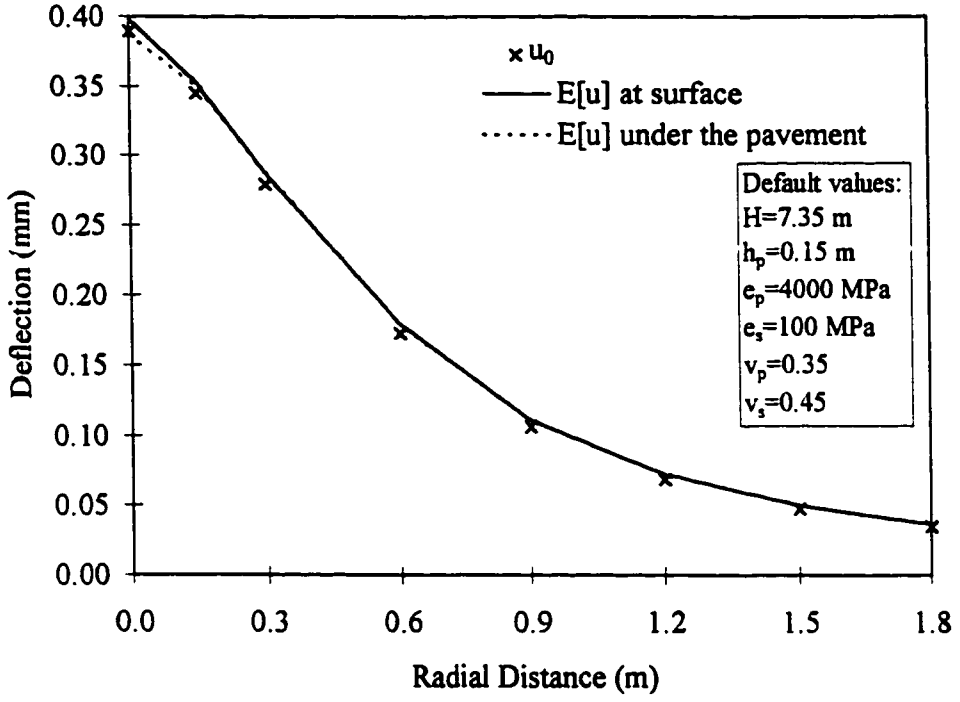

Figure 2.5 Deterministic and stochastic deflection basins (static)

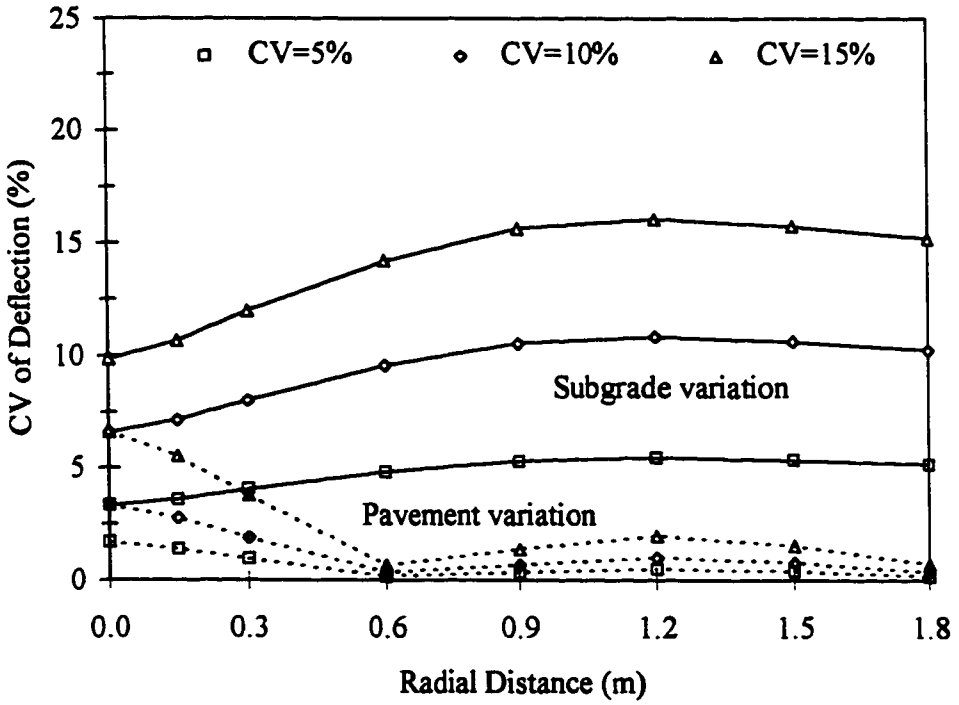

Figure 2.6 CV of deflection for different levels of random variation in elastic moduli

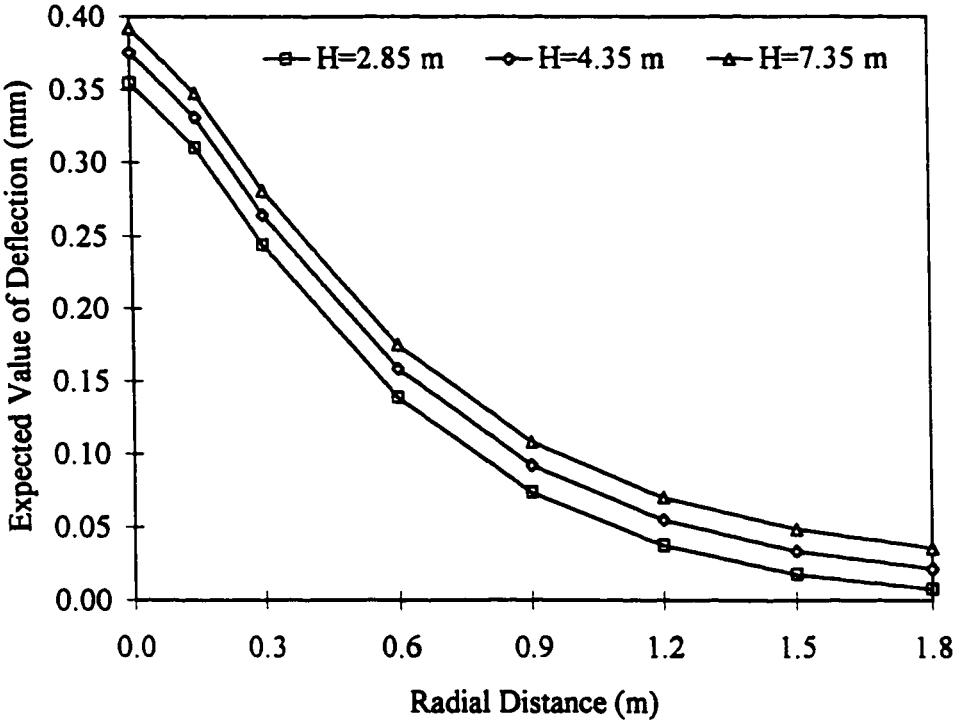

Figure 2.7 Expected value of deflection for different bedrock depths (static)

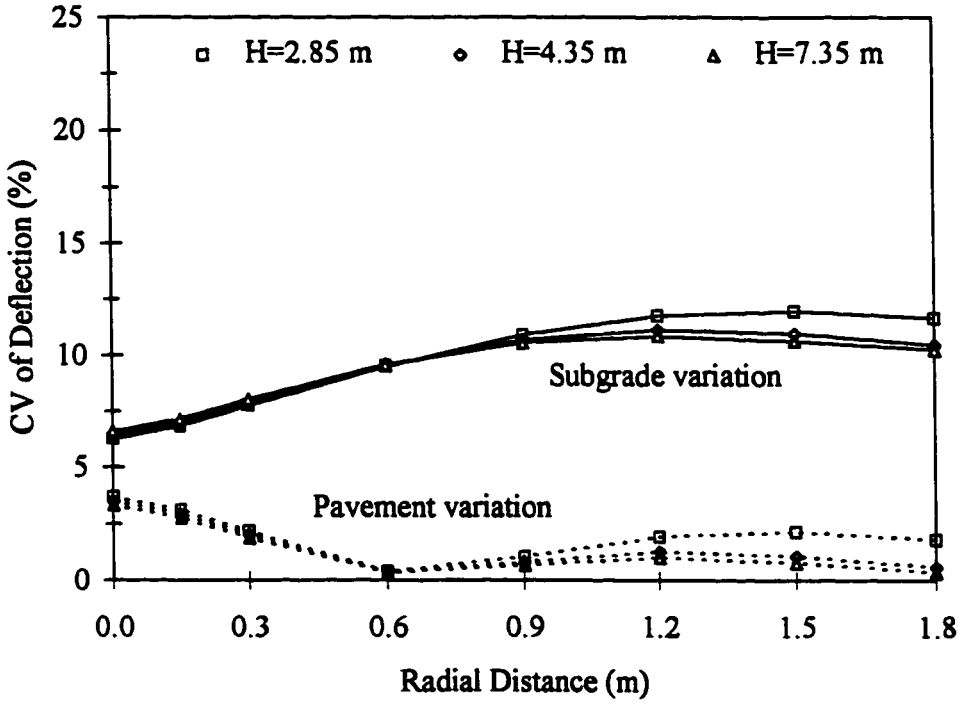

Figure 2.8 CV of deflection for different bedrock depths (static)

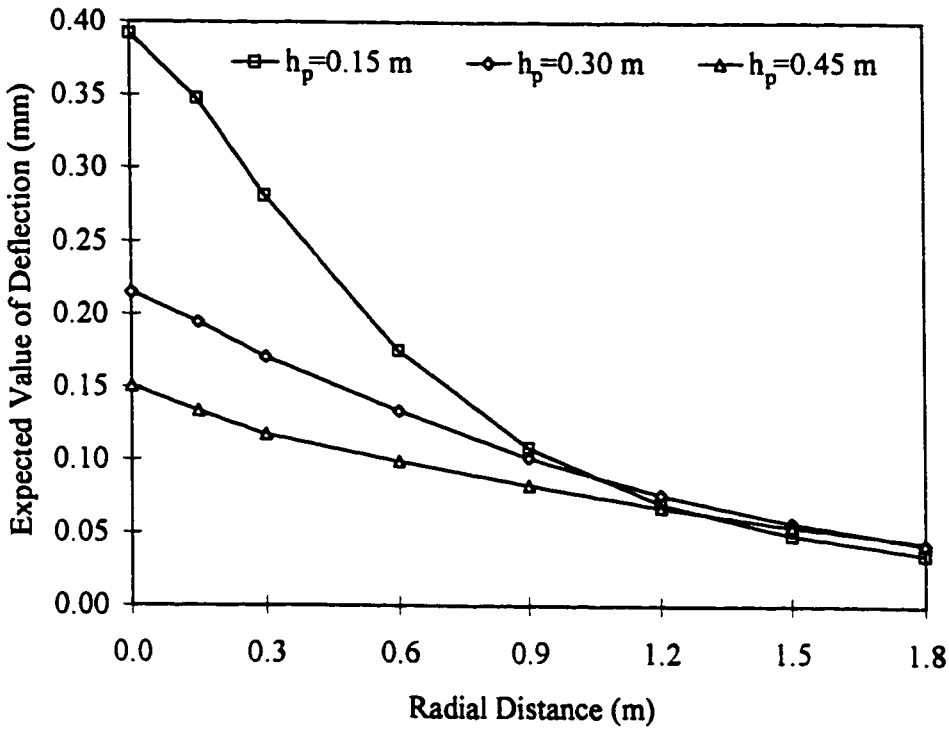

Figure 2.9 Expected value of deflection for different pavement thicknesses (static)

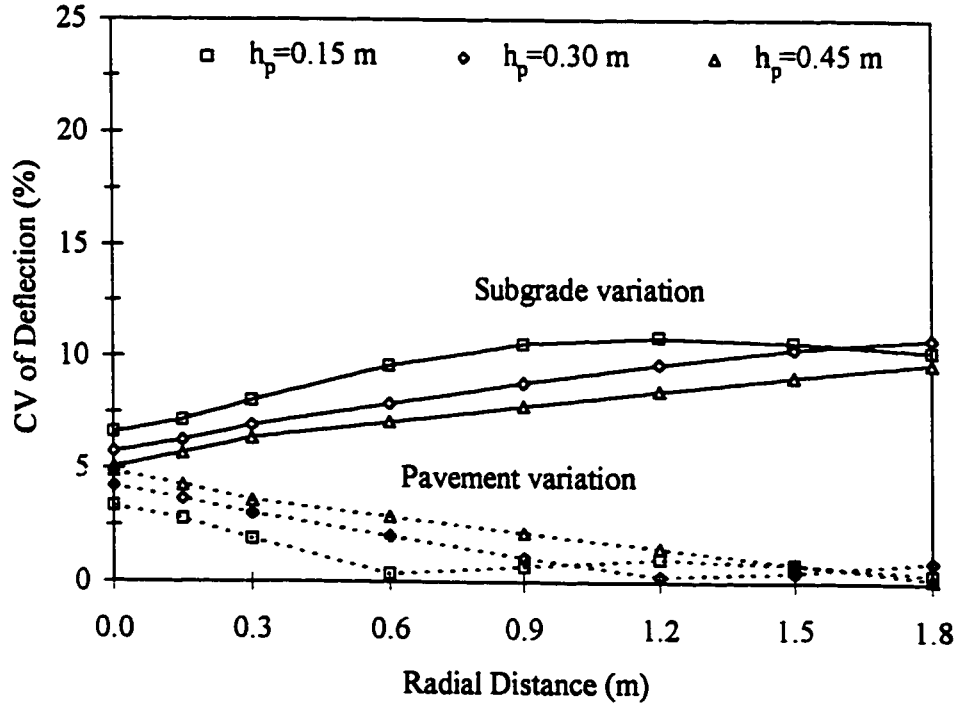

Figure 2.10 CV of deflection for different pavement thicknesses (static)

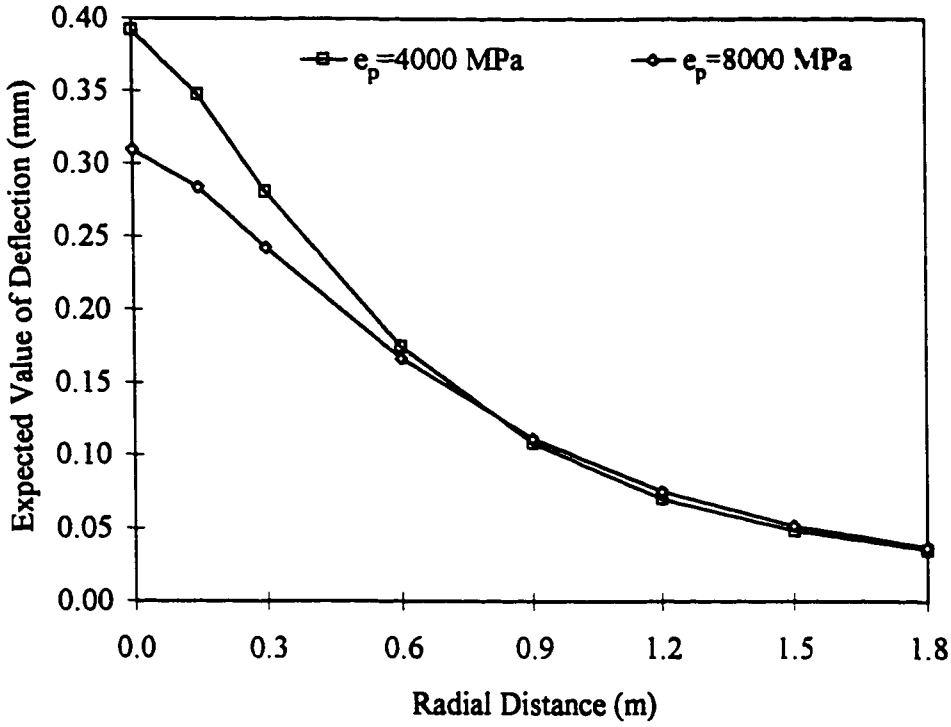

Figure 2.11 Expected value of deflection for different pavement moduli (static)

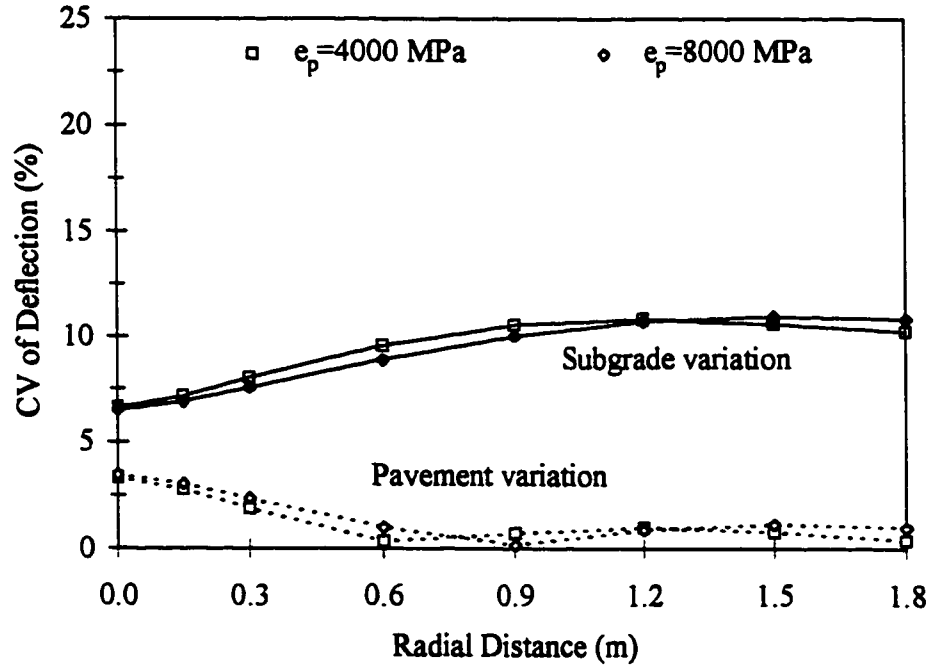

Figure 2.12 CV of deflection for different pavement moduli (static)

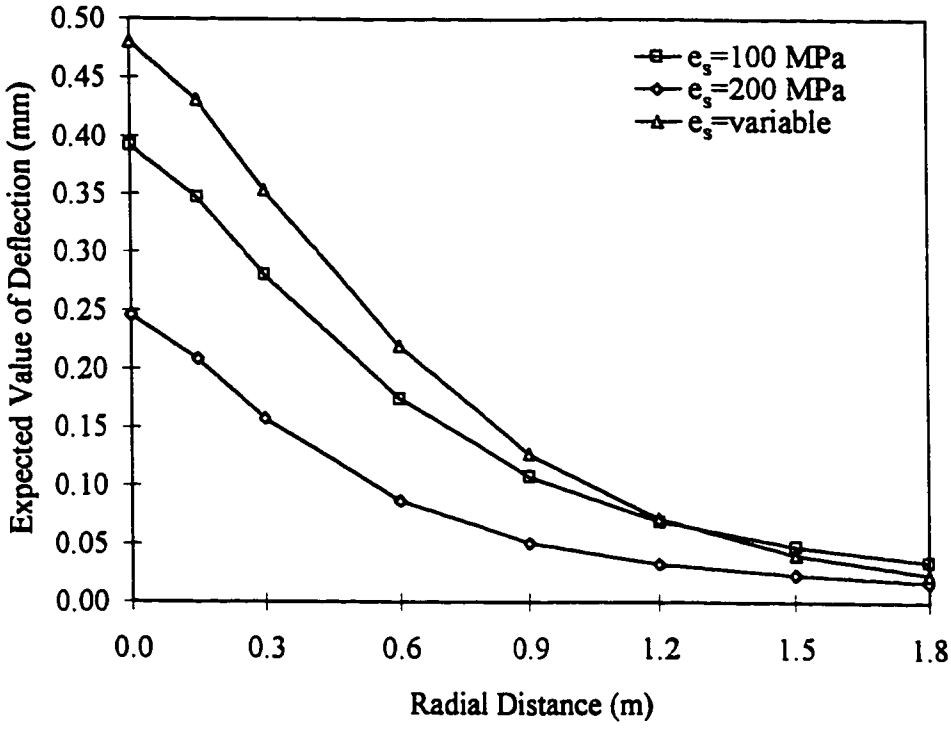

Figure 2.13 Expected value of deflection for different subgrade moduli (static)

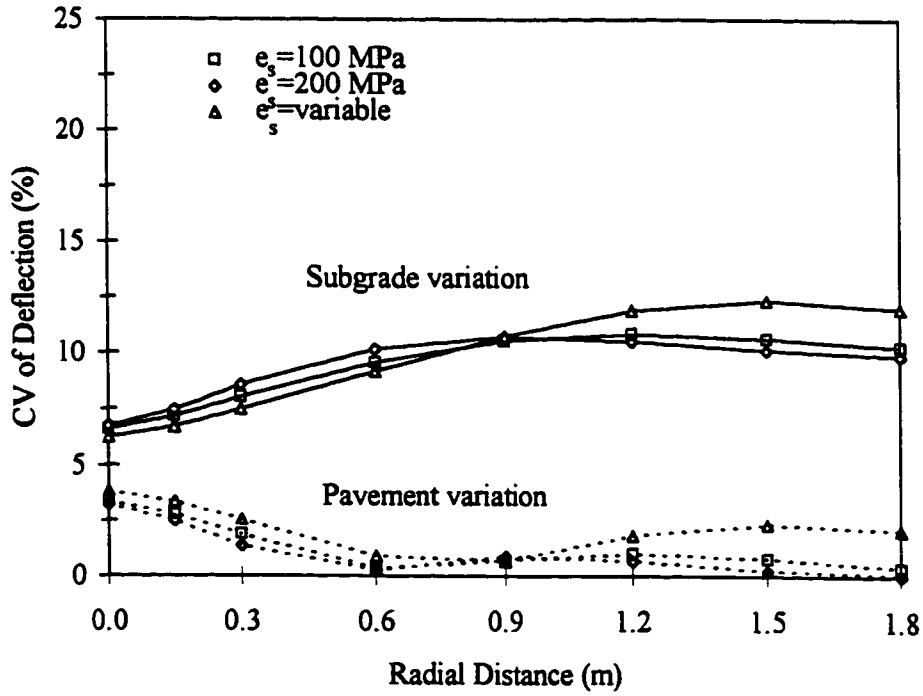

Figure 2.14 CV of deflection for different subgrade moduli (static)

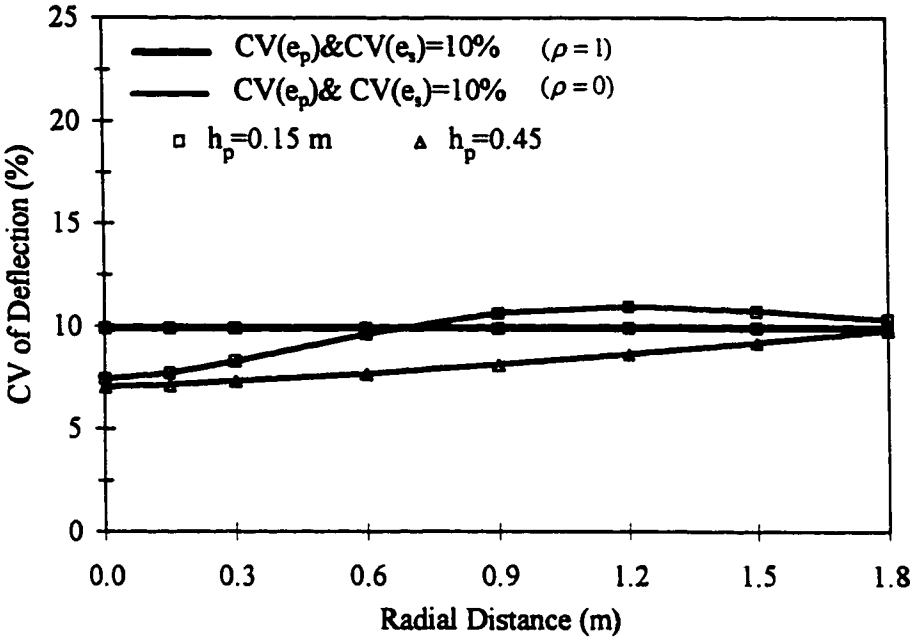

Figure 2.15 CV of deflection for simultaneous variation in pavement and subgrade moduli (static)

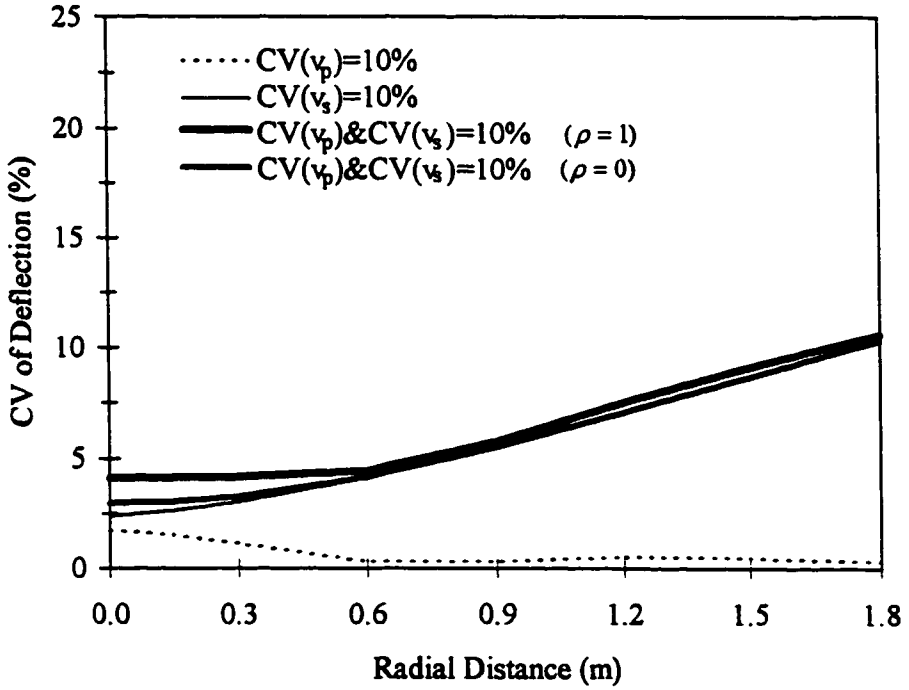

Figure 2.16 CV of deflection due to random variation in Poisson ratios

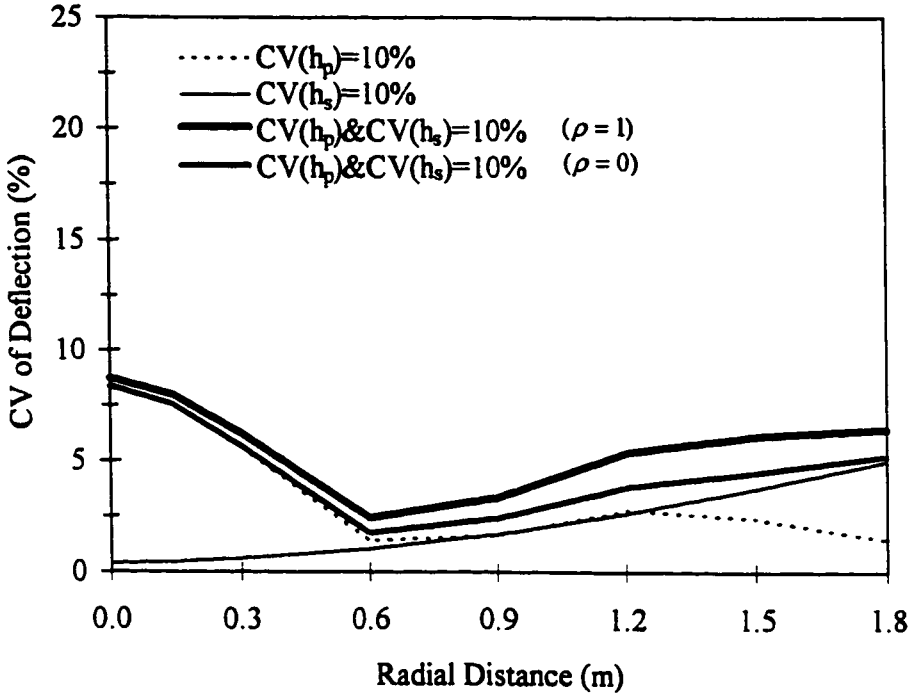

Figure 2.17 CV of deflection for random variation in layer thicknesses

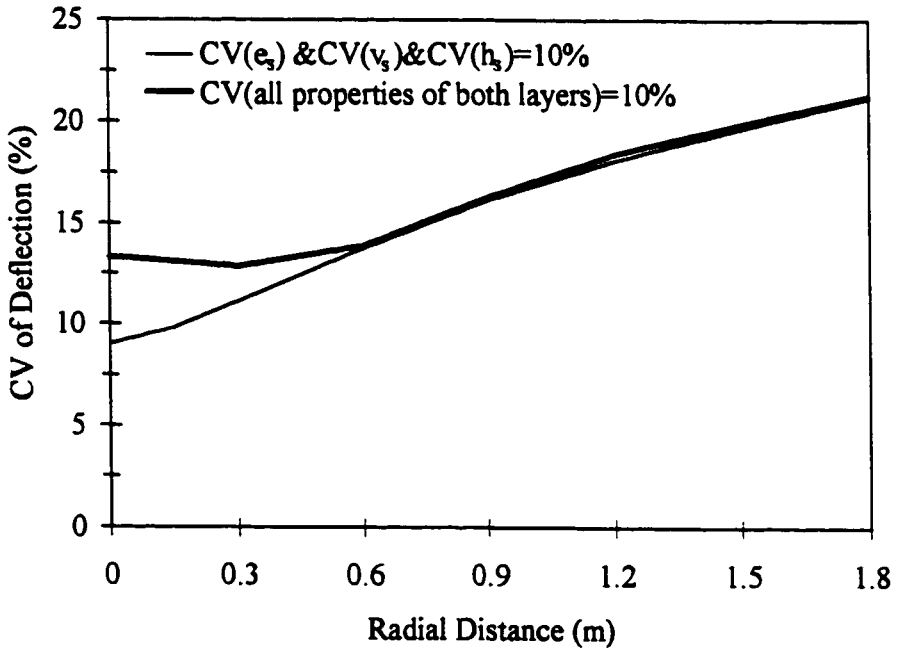

Figure 2.18 CV of deflection for simultaneous variation in all layer properties

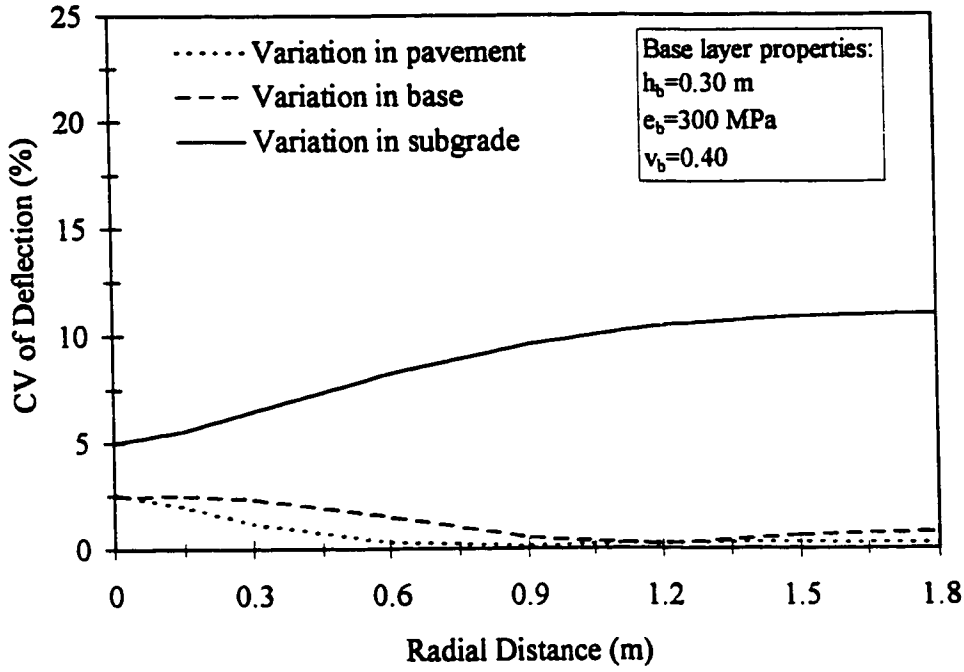

Figure 2.19 CV of deflection for a three-layered pavement model (static)

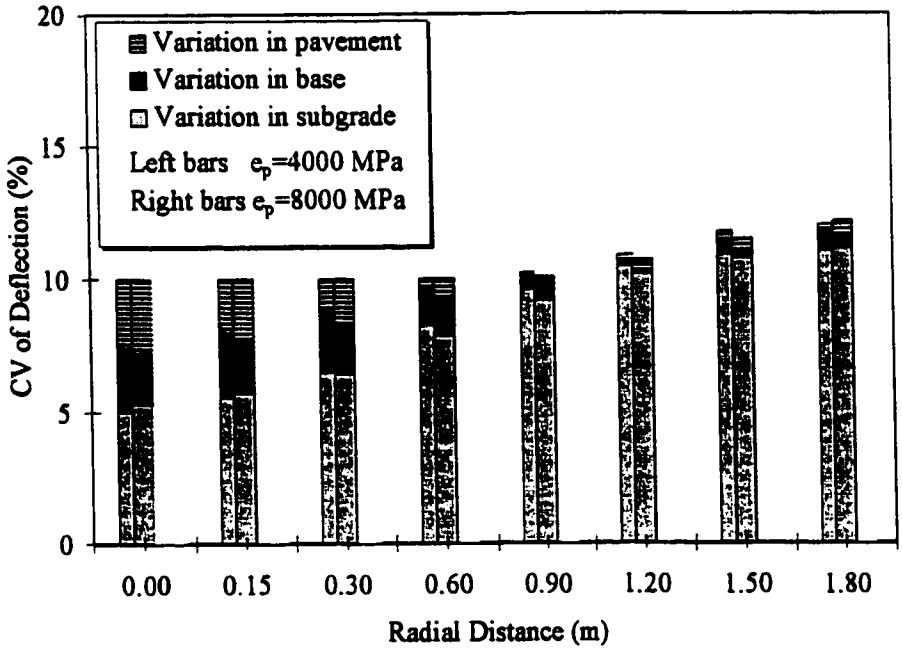

Figure 2.20 Effect of pavement stiffness on variation in deflection due to CV(e_b) for a three-layered pavement model

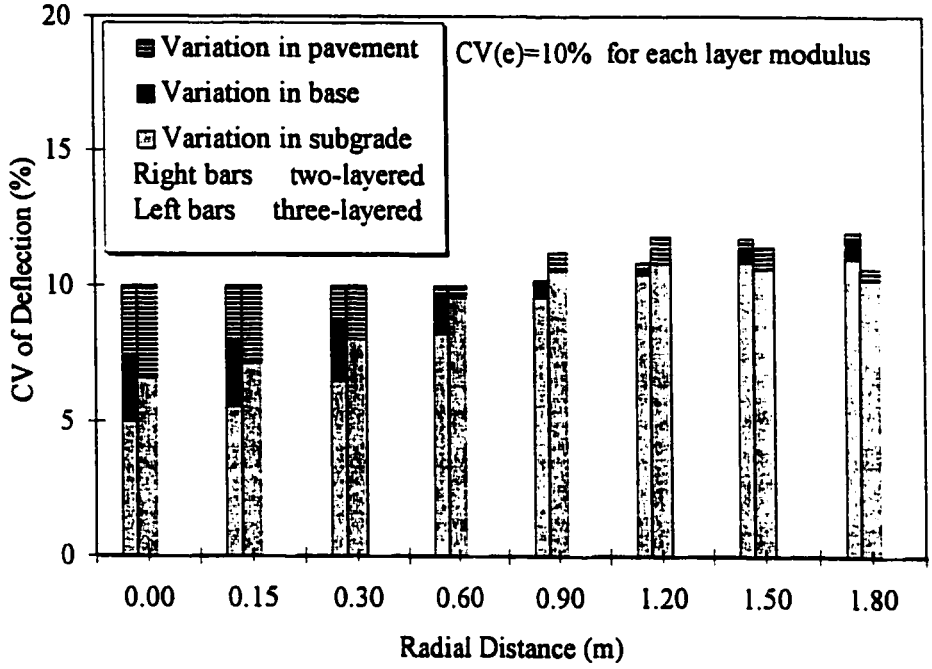

Figure 2.21 Comparison of CV of deflection for two and three-layered pavement models when layer moduli vary separately

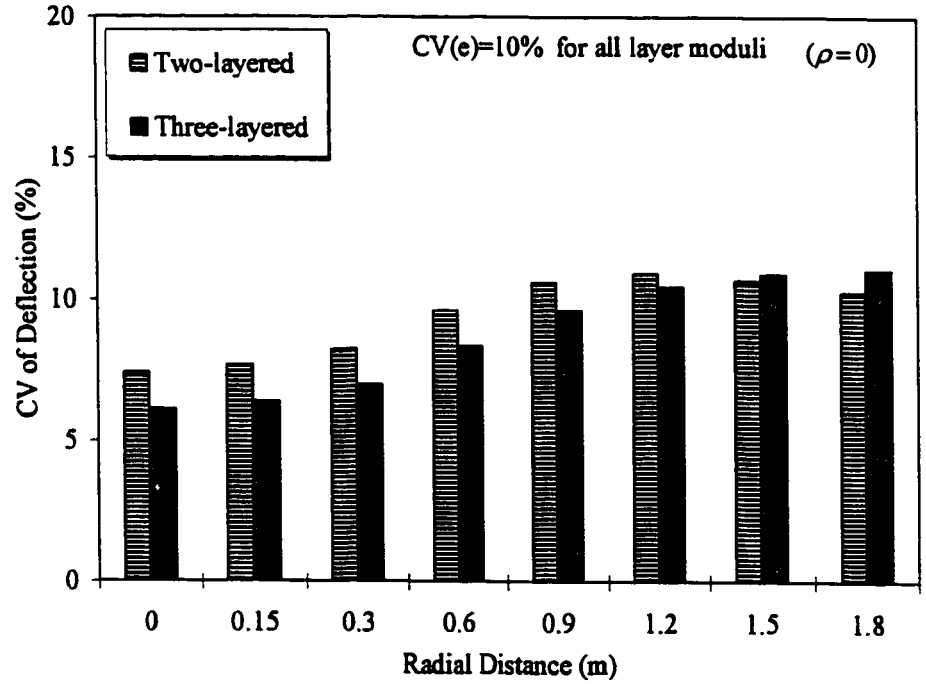

Figure 2.22 Comparison of CV of deflection for two and three-layered pavement models when layer moduli vary simultaneously

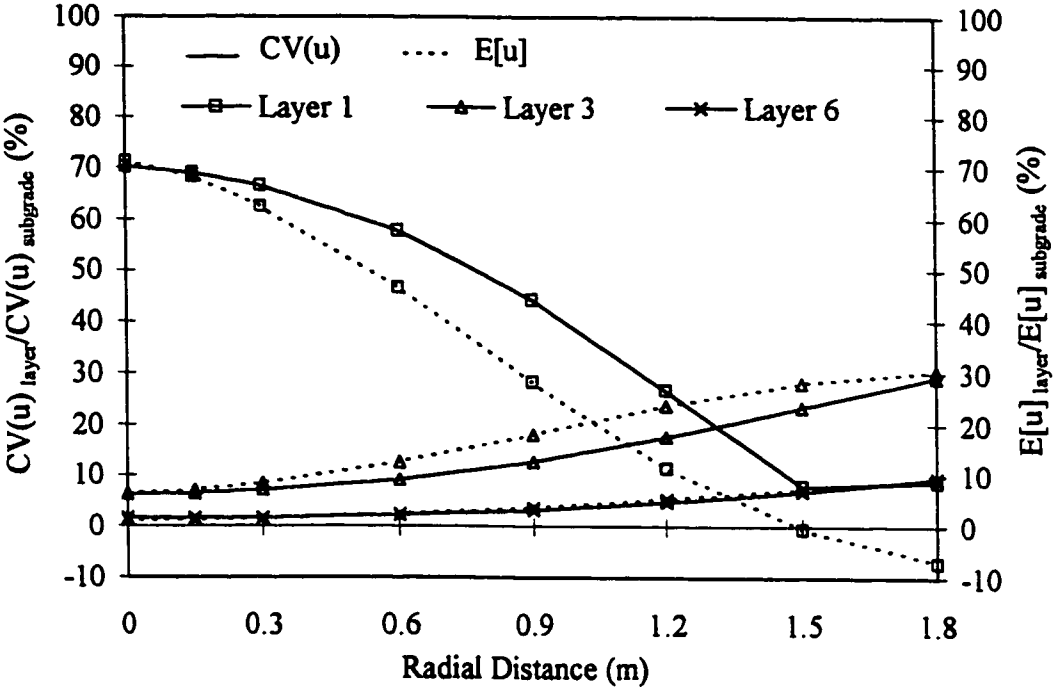

Figure 2.23 Relation between the ratio of coefficients of variations and that of the expected values of deflections

Chapter 3

STOCHASTIC ANALYSIS OF PAVEMENT STRUCTURES UNDER DYNAMIC LOADS

3.1 Introduction

In order to account for the inertial effects associated with a time-varying load applied to a pavement structure, a dynamic approach to the problem is inevitable. This includes the case when one wishes to model a pavement structure subjected to a dynamic load of a non-destructive, in-situ test, such as the FWD test. Neglecting the effects of inertia, which are generally important, introduces systematic errors (Mamlouk 1985, Ong et al. 1991, Zaghloul et al. 1994). When performing error analysis, the presence of systematic errors is particularly important since it is difficult, if not impossible, to distinguish between the uncertainty associated with random and systematic errors. To reduce the effect of systematic errors in the stochastic modeling of pavement structures under the FWD load, the dynamic analysis is employed in this chapter. First, the general formulation pertaining to the elastodynamic stochastic analysis of a single degree of freedom (SDOF) system is presented. Three dynamic schemes namely, time domain,

periodic-load analysis, and frequency domain are briefly introduced. To illustrate the application of the elastodynamic analysis of stochastic systems, a SDOF system is analyzed using the frequency domain solution. The matrix version of the periodic-load approach, which is later used in the dynamic stochastic finite element code, is then derived. Following that, multi-degree of freedom (MDOF) models of pavement systems are analyzed within a dynamic stochastic finite element framework. Simulations are completed for two-layered simplification of pavement-subgrade systems, as well as, three-layered models. Finally, the effect of loading frequency on the stochastic response of the pavement is investigated through a frequency sensitivity analysis. Wherever necessary, more detailed information is provided in the form of appendices.

3.2 General Formulation

The general form of the equation of motion for a single degree of freedom system characterized by mass m, damping c, and stiffness k is given by

$$m\ddot{u}(t) + c\dot{u}(t) + ku(t) = f(t) \tag{3.1}$$

in which f(t) is the dynamic force and u(t) is the displacement of the system. A dot over a u denotes differentiation with respect to time, t. For a system with a random property b, it

may be assumed that the mass, damping, stiffness, and the applied force are functions of the random variable. Therefore, the displacement, and consequently its derivatives with respect to time, are also functions of the random variable b. Approximating the displacement by a truncated Taylor's expansion and using the same procedure as that outlined previously, the expected value and variance of the displacement may be written (Kleiber and Hien 1992)

$$E[u(t,b)] = u(t,b) + \frac{1}{2}u(t,b)^{''} var(b) \tag{3.2}$$

$$var(u(t,b)) = (u(t,b)^{'})^2 var(b) \tag{3.3}$$

In these equations, var(b) is the variance of random variable b, the prime denotes differentiation with respect to b and all quantities are evaluated at mean value of b; i.e., at b_0. Similar equations may be derived for the first and second temporal derivatives of u in order to find the expected value and variance of the velocity and/or acceleration of the system. However, in this study, the focus is placed on the displacement of the pavement as it is the most important response in a pavement analysis.

For the cases where closed-form solutions of a problem exist, the case of a single degree of freedom system under harmonic load for example, the derivatives of the displacement with respect to b can be found directly by differentiating the displacement

function. Therefore, the expected value and variance of the displacement can be readily calculated from Equations 3.2 and 3.3, knowing the solution to the equation of motion. When there is no closed-form solution of the problem, to find the derivatives of the displacement, the equation of motion is differentiated two times with respect to random variable b, yielding

$$(m'\ddot{u} + m\ddot{u}') + (c'\dot{u} + c\dot{u}') + (k'u + ku') = f' \tag{3.4}$$

$$(m''\ddot{u} + 2m'\ddot{u}' + m\ddot{u}'') + (c''\dot{u} + 2c'\dot{u}' + c\dot{u}'') + (k''u + 2k'u' + ku'') = f'' \tag{3.5}$$

It should be noted that the arguments of the functions are not shown to avoid congestion and maintain clarity. Rearranging the terms in the above two equations results in

$$m\ddot{u}' + c\dot{u}' + ku' = F' \tag{3.6}$$

$$m\ddot{u}'' + c\dot{u}'' + ku'' = F'' \tag{3.7}$$

in which

$$F' = f' - (m'\ddot{u} + c'\dot{u} + k'u) \tag{3.8}$$

$$F'' = f'' - (m''\ddot{u} + c''\dot{u} + k''u + 2m'\ddot{u}' + 2c'\dot{u}' + 2k'u') \tag{3.9}$$

The forms of Equations 3.6 and 3.7 are identical to the equation of motion, therefore, the derivatives of the displacement with respect to b can be found using the same solution scheme used to find u in Equation 3.1, provided that the derivatives of the system properties are available. Solving Equations 3.1, 3.6, and 3.7 and replacing the resulting values in Equations 3.2 and 3.3 provides the expected value and variance of the displacement. As with deterministic analyses, there are three approaches for solving stochastic-based dynamic problems; time domain analysis, periodic-load analysis, and frequency domain analysis.

3.2.1 Time Domain Analysis

In the time domain, one of the procedures to transform the second order differential equation of motion into a simple equation is step-by-step integration. In this method, the response of the system is calculated using a time marching scheme. This is done by expressing the derivatives of the displacement at each time step in terms of the

displacement and its derivatives in the previous steps. The relations between the responses at different time steps depend on the assumptions made for a specific solution scheme. There are many step-by-step schemes available. Based on the assumption of a constant acceleration equal to the average of the values of the accelerations at the beginning and end of the time interval, the displacement at time step n, denoted by u_n, may be obtained from (Humar 1990)

$$K\ u_n = F_n \tag{3.10}$$

in which

$$K = k + \frac{2}{\Delta t}c + \frac{4}{\Delta t^2}m \tag{3.11}$$

and

$$F_n = f_n + c\left(\frac{2}{\Delta t}u_{n-1} + \dot{u}_{n-1}\right) + m\left(\frac{4}{\Delta t^2}u_{n-1} + \frac{4}{\Delta t}\dot{u}_{n-1} + \ddot{u}_{n-1}\right) \tag{3.12}$$

where f_n is the force at time step n, and Δt is the constant time increment. For a stochastic system with random variable b, the displacement at time t_n may be expressed in a general form of

$$u_n(b) = \Re_n\{m, c, k, f_n, u_{n-1}(b), \dot{u}_{n-1}(b), \ddot{u}_{n-1}(b), \ldots u_0(b), \dot{u}_0(b), \ddot{u}_0(b)\} \qquad (3.13)$$

in which $\Re_n$ is a function defined at step n. To find the expected value and variance of the displacement from Equations 3.2 and 3.3, the function should be differentiated two times with respect to b at each time step. An examination of Equation 3.13 reveals that, as the solution proceeds through time, the form of the function in terms of the random variable, and consequently the differentiation process, becomes more and more complicated. On the other hand, if approximations are applied at each time step in order to simplify the form of the function, an accumulation of systematic approximation errors could jeopardize the accuracy of the results.

Another point to consider, when carrying out stochastic analysis in the time domain, is the fact that the results of the analysis do not generally reflect the direct influence of the frequency components of the forcing function on the response of the system. This concept is important when studying the sensitivity of the stochastic response to the frequency characteristics of the dynamic load.

3.2.2 Periodic-Load Analysis

The periodic-load-analysis method is used when the forcing function is assumed to be periodic. In such a case, the force is expressed in terms of its discrete harmonic components and the solution to the problem is attained by superposition of the solutions to these harmonic components.

i) Harmonic Load

Consider once again the equation of motion for a single degree of freedom system as given in Equation 3.1. If f(t) is a harmonic load, then one may write

$$f(t) = \tilde{f}e^{iwt} \tag{3.14}$$

and the response of the system, which is also harmonic, would be (Clough and Penzien 1975)

$$u(t) = \tilde{u}e^{iwt} \tag{3.15}$$

where $\tilde{u}$ is determined from

$$\tilde{k}\tilde{u} = \tilde{f} \tag{3.16}$$

in which $\tilde{f}$ and $\tilde{u}$ are the load and displacement amplitudes, respectively, and w is the angular frequency of the harmonic load. $\tilde{k}$ is the dynamic stiffness defined as

$$\tilde{k} = k - mw^2 + icw . \tag{3.17}$$

For a system with random variable b, one may write

$$E[u(t)] = E[\tilde{u}]e^{iwt} \tag{3.18}$$

and

$$var(u(t)) = var(\tilde{u}) \tag{3.19}$$

where the expected value of $\tilde{u}$, $E[\tilde{u}]$, and its variance, $var(\tilde{u})$, are calculated from

$$E[\tilde{u}] = \tilde{u} + \frac{1}{2}\tilde{u}'' \text{var}(b) \tag{3.20}$$

$$\text{var}(\tilde{u}) = (\tilde{u}') \text{ var}(b) (\overline{\tilde{u}'}) \tag{3.21}$$

As before, the prime denotes differentiation with respect to the random variable and all quantities are evaluated at mean value of b. $\tilde{u}'$ and $\tilde{u}''$ may be found in the same way as was demonstrated for the static case from the scalar versions of Equations 2.10 and 2.11, using complex arithmetic. The reader should be aware that the complex variables must be transformed into real and imaginary components in order to perform the analysis in the real space for practical applications. Given that $\tilde{u} = x + iy$, based on the properties of the expected value and variance functions in the complex space (Miller 1974), the coefficient of variation of $\tilde{u}$ may be calculated as

$$CV(\tilde{u}) = \frac{\sqrt{\text{var}(\tilde{u})}}{|E[\tilde{u}]|} = \frac{\sqrt{\text{var}(x) + \text{var}(y)}}{\sqrt{E[x]^2 + E[y]^2}} \tag{3.22}$$

Appendix A summarizes some of the important formulae, and properties of the expected value and variance functions in the complex space.

ii) Periodic Load

For a periodic forcing function, f(t) can be expressed in terms of harmonic components. The decomposition of a periodic function into a series of harmonic components can be accomplished using a Fourier series expansion (Chapra and Canale 1988). The exponential representation of Fourier series expansion is given by

$$f(t) = f \sum_{n=-\infty}^{+\infty} c_n e^{iw_n t} \tag{3.23}$$

in which

$$c_n = \frac{1}{fT} \int_0^T f(t) e^{-iw_n t} dt \tag{3.24}$$

and $w_n = \frac{2\pi n}{T}$. The parameters f and T are the amplitude and period of the forcing function f(t), respectively.

For a linear system, the overall response is obtained by superimposing the individual responses due to each harmonic component of the forcing function; i.e., for a periodic load given by Equation 3.23 then

$$u(t) = \sum_{n=-\infty}^{+\infty} c_n u_n e^{iw_n t} \tag{3.25}$$

in which

$$u_n = \frac{f}{k - mw_n^2 + icw_n} \tag{3.26}$$

u_n is a complex-valued quantity which may be expressed in terms of its real and imaginary components as $u_n = x_n + iy_n$, and $u_{-n} = x_n - iy_n$.

Now, if there is randomness in one of the system properties, then u_n, and consequently x_n and y_n, would be random functions of that random property. For such a case, the expected value and variance of the displacement history in the exponential form is represented, using the properties of these functions in the complex space, as

$$E[u(t)] = \sum_{n=-\infty}^{+\infty} c_n E[u_n] e^{iw_n t} = \sum_{n=-\infty}^{+\infty} c_n \{E[x_n] + iE[y_n]\} e^{iw_n t} \tag{3.27}$$

$$var(u(t)) = \sum_{n=-\infty}^{+\infty} \sum_{m=-\infty}^{+\infty} cov(c_n u_n e^{iw_n t}, c_m u_m e^{iw_m t}) = \sum_{n=-\infty}^{+\infty} c_n c_m e^{iw_n t} e^{iw_m t} cov(u_n, u_m) \tag{3.28}$$

In Equations 3.27 and 3.28, the Fourier coefficients of the forcing function are assumed to be deterministic quantities.

iii) Trigonometric Representation

For practical purposes, f(t) is usually expressed in terms of trigonometric functions as follows

$$f(t) = \frac{a_0}{2} + \sum_{n=1}^{\infty} a_n \cos(w_n t) + \sum_{n=1}^{\infty} b_n \sin(w_n t) \tag{3.29}$$

in which

$$a_n = \frac{2}{T}\int_0^T f(t)\cos(w_n t)dt \qquad n=0,1,2,\ldots \tag{3.30}$$

$$b_n = \frac{2}{T}\int_0^T f(t)\sin(w_n t)dt \qquad n=0,1,2,\ldots \tag{3.31}$$

The coefficients a_n and b_n are related to c_n by $c_n = \frac{a_n - ib_n}{2}$ and $c_{-n} = \frac{a_n + ib_n}{2}$ (Chapra and Canale 1988). Replacing these values in Equation 3.25, and expressing u_n in terms of its real and imaginary components, yields

$$u(t) = \frac{a_0}{2}x_0 + \sum_{n=1}^{\infty}\left\{a_n[x_n\cos(w_n t) - y_n\sin(w_n t)] + b_n[x_n\sin(w_n t) + y_n\cos(w_n t)]\right\} \quad (3.32)$$

In deriving Equation 3.32, the definition $e^{iwt} = \cos(wt) + i\sin(wt)$ is used.

iv) Even Functions

For the case of an even function, the trigonometric representation of the forcing function by Fourier series expansion only includes cosine terms (b_n=0). Moreover, if the forcing function is approximated by the first N components of a Fourier series, Equation 3.32 becomes

$$u(t) = \frac{a_0}{2}x_0 + \sum_{n=1}^{N}\left\{a_n[x_n\cos(w_n t) - y_n\sin(w_n t)]\right\} \quad (3.33)$$

For such a case, the expected value and variance of the response in the real space are as follows

$$E[u(t)] = \frac{a_0}{2}E[x_0] + \sum_{n=1}^{N}\left\{a_n[E[x_n]\cos(w_n t) - E[y_n]\sin(w_n t)]\right\} \tag{3.34}$$

$$\begin{aligned}\mathrm{var}(u(t)) = \frac{{a_0}^2}{4}\mathrm{var}(x_0) + \sum_{j=0}^{N}\sum_{l=1}^{N} a_j a_l \{&\mathrm{cov}(x_j, x_l)\cos(w_j t)\cos(w_l t) + \mathrm{cov}(y_j, y_l)\sin(w_j t)\sin(w_l t) \\ &- \mathrm{cov}(x_j, y_l)\cos(w_j t)\sin(w_l t) - \mathrm{cov}(y_j, x_l)\sin(w_j t)\cos(w_l t)\}\end{aligned} \tag{3.35}$$

where $w_k = \frac{2\pi\ k}{T}$ for k=j, or k=l.

The coefficient of variation for any given time t is defined by

$$CV(u(t)) = \frac{\sqrt{\mathrm{var}(u(t))}}{|E[u(t)]|} \tag{3.36}$$

3.2.3 Frequency Domain Analysis

Frequency domain approach is conceptually similar to the periodic-load analysis. In this method, which is also applicable for non-periodic loads, Fourier transformation (Ramirez 1985) is utilized to transform the loading function from time to frequency domain. It should be noted that, when dealing with numerical procedures involving discrete operations, the numerical Fourier transform is identical to Fourier series approximation presented in the previous section. The frequency domain solution of Equation 3.1 may be obtained from Equation 3.16 by replacing $\tilde{f}$ with the transformed function $\hat{f}(w)$. The dynamic stiffness, often referred to as the impedance function in the frequency domain, is calculated using Equation 3.17. The statistical moments of the response can then be found using Equations 3.20 and 3.21.

In a frequency domain analysis, the expected value and variance of displacements are functions of frequencies, thereby allowing one to compare the sensitivity of the response to the variation in system properties at different frequencies.

3.3 Frequency Domain Analysis of a SDOF Pavement Model

Consider a simplified, two-layered, pavement-subgrade system subjected to a dynamic FWD impact load f(t). If the problem is represented by an idealized single degree of freedom system, then the impedance function may be defined by Equation 3.17, in which m, c, and k are the equivalent mass, damping coefficient, and stiffness of the pavement-subgrade system, respectively, and w is the angular frequency. The frequency domain solution of the displacement for such a system can be obtained from Equation 3.16, provided that the material characteristics of the SDOF system, and the Fourier transformation of the idealized FWD impact load are available. If there is randomness in either the system properties, or the applied load, then the expected value and variance of the transformed displacement may be calculated by Equations 3.20 and 3.21 in terms of the angular frequency.

i) Characteristics of the SDOF System

Assuming a linearly elastic, semi-infinite, and incompressible subgrade, the equivalent stiffness and damping coefficient of the system may be related, using curve fitting techniques, to the properties of the pavement and subgrade for low frequencies as described by Peiravian (1994); i.e.,

$$k = 0.67\pi\, e_s(0.81h_e^2 + a^2)^{1/2} \tag{3.37}$$

$$c = 0.73kh_e\sqrt{\frac{3\rho_s}{e_s}} \tag{3.38}$$

where h_e is defined by Equation 2.30, a is the radius of the circular loading area, and e_s and ρ_s are the subgrade modulus and density, respectively. The inertial effects of a pavement-subgrade system are accommodated mostly by the damping term of the SDOF approximation. The equivalent mass affects the calculation of the natural frequency of the system, but tends to have a relatively small influence on the prediction of the displacement history as the response is dominated by dissipation through radiation damping.

ii) Fourier Transformation of the FWD Impact Load

Figure 3.1 shows a typical FWD impact load history measured at the center line of a loading plate. The impulse duration is about 0.03 second with a peak pressure of about 566 kPa, which corresponds to the pressure induced by a 40 kN load uniformly distributed on a circular area with a radius of a=0.15 m. This load history may be approximated by a half-sine load, defined by the following function

$$f(t) = \begin{cases} \left(\frac{f_0}{\pi a^2}\right)\sin\frac{\pi t}{t_0} & 0 < t \le t_0 \\ 0 & t_0 < t \end{cases} \tag{3.39}$$

in which f_0=40 kN, and t_0=0.03 s. The idealized forcing function f(t) is also plotted in Figure 3.1. Review of this plot suggests that the half-sine load is a good approximation for the FWD load.

The Fourier transformed of f(t), shown in Figure 3.2, is given by

$$\hat{f}(w) = \frac{f_0 t_0 \pi \left(e^{-iwt_0} + 1\right)}{\pi a^2 (\pi^2 - (wt_0)^2)} \tag{3.40}$$

The curve representing the magnitude of the transformed function suggests that, the frequencies mostly contributing to the impact load are located in a range between zero and 300 rad/s.

iii) Results

Calculations were completed using the pavement system properties discussed in Section 2.4, together with ρ_s=2.0 Mg/m^3. For the selected properties, the values of the

equivalent stiffness and damping were found from Equations 3.37 and 3.38 as $k=93\times10^3$ kN/m, and $c=243\times10^3$ kg/s, respectively. In order to determine the sensitivity of the solution to the equivalent mass, results are obtained for three different m values. These values are in the range backcalculated by Peiravian (1994) using real FWD data. As before, analyses were performed by first allowing the subgrade modulus to vary 10%, and then the pavement modulus by 10%. The results are summarized in Figure 3.3. The figure shows that the variation in the displacement due to a variation in the modulus of each layer depends on the frequency and the equivalent mass of the system. Scrutiny of the results indicates that, overall, as w increases, CV(u) due to $CV(e_p)$ increases, while CV(u) due to $CV(e_s)$ decreases. This means that, at higher frequencies, the influence of the pavement layer on the response becomes more significant, which is not surprising if one considers that wavelengths associated with high frequencies approach the pavement thickness. The figure also shows an amplification in CV(u) when the loading frequency is close to the natural frequency of the system. For example, for the case of m=1000 kg, the coefficient of variation of the displacement is magnified at frequencies close to w=300 rad/s. The significance of these observations, from a backcalculation viewpoint for the response of a pavement-subgrade system subjected to a dynamic load which spans a range of frequencies, is addressed in Chapter 4.

3.4 Matrix Formulation of Periodic-Load Analysis

The matrix form of the equation of motion for a multi-degree of freedom system is given by

$$\mathbf{M}\ddot{\mathbf{u}}(t) + \mathbf{C}\dot{\mathbf{u}}(t) + \mathbf{K}\mathbf{u}(t) = \mathbf{f}(t) \tag{3.41}$$

in which $\mathbf{u}(t)$, and $\mathbf{f}(t)$ are the displacement and load vectors, and $\mathbf{M}$, $\mathbf{C}$, and $\mathbf{K}$ are the mass, damping, and stiffness matrices of the system, respectively. As before, a dot over $\mathbf{u}$ denotes differentiation with respect to time, t. If $\mathbf{f}(t)$ is periodic and is expressed in terms of a Fourier series expansion with N+1 components, the solution to each harmonic component of the load is given by the matrix equation

$$\tilde{\mathbf{K}}_n \tilde{\mathbf{u}}_n = \tilde{\mathbf{f}} \qquad n=0,\ldots N \tag{3.42}$$

in which $\tilde{\mathbf{f}}$ is the vector of load amplitudes, $\tilde{\mathbf{u}}_n$ is the complex-valued vector of the displacement amplitudes associated with the n^{th} component, and $\tilde{\mathbf{K}}_n$ is the dynamic stiffness matrix defined by

$$\tilde{\mathbf{K}}_n = \mathbf{K} - \mathbf{M}w_n^2 + i\mathbf{C}w_n \qquad n=0,\ldots N \tag{3.43}$$

The matrix form of the solution to each harmonic component in the case of a periodic-load analysis is similar to the matrix form of the static equilibrium equation, except that the static stiffness matrix is replaced by the complex-valued dynamic matrix.

The stochastic solution of the time-dependent displacement for a system involving randomness is obtained using the matrix versions of the previously derived scalar equations. For the case of an even periodic forcing function, if $\tilde{\mathbf{u}}_n = \mathbf{x}_n + i\mathbf{y}_n$, then the expected-value vector of the displacement is given by

$$\mathbf{E[u(t)]} = \frac{a_0}{2}\mathbf{E[x_0]} + \sum_{n=1}^{N}\left\{a_n[\mathbf{E[x_n]}\cos(w_n t) - \mathbf{E[y_n]}\sin(w_n t)]\right\} \tag{3.44}$$

in which

$$\mathbf{E[x_n]} = \mathrm{Re}\{\mathbf{E}[\tilde{\mathbf{u}}_n]\} \qquad n=0,\ldots N \tag{3.45}$$

$$\mathbf{E[y_n]} = \mathrm{Im}\{\mathbf{E}[\tilde{\mathbf{u}}_n]\} \qquad n=1,\ldots N \tag{3.46}$$

The covariance matrix of the displacement is derived from Equation 3.44, using the definition of the covariance function in real space, as

$$\mathbf{cov(u(t))} =$$

$$\frac{a_0^2}{4}\mathbf{cov}(\mathbf{x_0},\mathbf{x_0}) + \sum_{j=0}^{N}\sum_{l=1}^{N} a_j a_l \{\mathbf{cov}(\mathbf{x_j},\mathbf{x_l})\cos(w_j t)\cos(w_l t) + \mathbf{cov}(\mathbf{y_j},\mathbf{y_l})\sin(w_j t)\sin(w_l t)$$
$$- \mathbf{cov}(\mathbf{x_j},\mathbf{y_l})\cos(w_j t)\sin(w_l t) - \mathbf{cov}(\mathbf{y_j},\mathbf{x_l})\sin(w_j t)\cos(w_l t)\} \qquad (3.47)$$

in which a covariance matrix such as $\mathbf{cov}(\mathbf{x_j}.\mathbf{y_l})$ is given by

$$\mathbf{cov}(\mathbf{x_j},\mathbf{y_l}) = [\mathbf{A_x}]_j \mathbf{cov(b)} [\mathbf{A_y}]_l^t \qquad (3.48)$$

where $[\mathbf{A_x}]_j$ and $[\mathbf{A_y}]_l$ are n×p matrices consisted of p column vectors defined via

$$[\mathbf{A_x}]_j = [\mathrm{Re}(\mathbf{a_1}|j), \ldots \mathrm{Re}(\mathbf{a_p}|j)] \qquad j=0,\ldots N \qquad (3.49)$$

$$[\mathbf{A_y}]_l = [\mathrm{Im}(\mathbf{a_1}|l), \ldots \mathrm{Im}(\mathbf{a_p}|l)] \qquad l=1,\ldots N \qquad (3.50)$$

in which $\mathbf{a_i}|n$ is a vector which is associated with the n^{th} harmonic, obtained by

$$\mathbf{a_i}|n = \tilde{\mathbf{K}}_n^{-1}\tilde{\mathbf{K}}_n^{\,b_i}\tilde{\mathbf{u}}_n \qquad i=1,\ldots p, \text{ and } n=j, \text{ or } n=l \qquad (3.51)$$

As before, p corresponds to the number of random variables in the system with **cov(b)** being their covariance matrix. The similarities and differences between the dynamic and static analysis equations can be appreciated by comparing Equations 3.44 to 3.51 with 2.14 to 2.17. For a load of single frequency, the dynamic approach is virtually identical to the static one, except that real mathematical operations are replaced by the ones in the complex space. For a periodic loading containing several harmonics, additional steps involving the superposition of the components and accounting for the correlation between various harmonic components must be introduced.

3.5 Dynamic Stochastic Finite Element Method

To establish a dynamic stochastic finite element code suitable for the analysis of pavement structures, the periodic-load analysis is adopted in this study. The reason lies in the simplicity of the method as well as the potential for frequency sensitivity analysis. As was indicated previously, the discrete equation of motion for each harmonic component of a dynamic load is similar in the form to the matrix equilibrium equation. This similarity can be taken advantage of when converting a static stochastic finite element code to solve the steady state elastodynamic problems. The most important modifications include, converting the real space arithmetic to the complex space one, and substituting the static

stiffness matrix with the dynamic one. Of course, one must also account for the correlation between the various harmonic components.

The dynamic stiffness matrix, defined in Equation 3.43, includes the mass and damping matrices in addition to the static stiffness matrix. The stiffness and mass matrices are constructed by assembling the element stiffness and consistent element mass matrices, respectively, taking into account equilibrium and compatibility. Theoretically, the damping matrix, which reflects the damping properties of the materials as well as the dissipation of energy due to radiation away from the source, can be formed using the same procedure. When forming the damping matrix, this study assumes that material damping is hysteretic in nature and radiation damping can be accommodated by using special energy absorbing mechanisms at artificial boundaries. More details for the construction of the damping matrix are presented in Appendix C.

The output of the dynamic stochastic finite element program for the n^{th} harmonic includes $\mathbf{E}[\tilde{\mathbf{u}}_n]$, and a set of p vectors $\mathbf{a}_i|n$, i=1,...p. Replacing these values in Equations 3.44 to 3.50 for all harmonic components provides the expected value and covariance of the displacement.

3.6 Periodic-Load Analysis using Dynamic SFEM

Let us now consider the multi-layered representation of the pavement structure shown in Figure 2.3, again. The material and geometric properties of the system are identical to those described in Section 2.6. In addition, all the materials are assumed to have a density of 2.0 Mg/m^3, with a hysteretic damping ratio of ζ=5%, a value suggested by Richart et al. (1970) for soils. The condition at the artificial boundary located on the far vertical face of the problem is defined by transmitting boundary in the form of horizontal and vertical viscous dampers to simulate the stretch of the problem to infinity. Unless otherwise stated, this configuration is used in carrying out the simulations.

The characteristics of the finite element model, e.g., the number of nodes and elements, element type and size, and location of the artificial boundary, are exactly the same as those defined for the static case in Section 2.6.1. It should be noted, however, that solutions to dynamic problems are very sensitive to the mesh size and the location of artificial boundaries, even when transmitting boundaries are present. In order to confirm the suitability of the selected finite element model from a dynamic analysis perspective, simulations were completed on different mesh configurations in terms of the number and size of the elements, and the location of the transmitting boundary. The results of the analyses, which are summarized in Appendix D, support the suitability of the model used for carrying out this phase of the research. The details of the finite element model along with a schematic presentation of the grid are also provided in this appendix.

The uniformly distributed dynamic load, defined by Equation 3.39, is considered to be transferred to the pavement surface by means of a circular flexible plate with a radius of a=0.15 m. In order to perform a periodic-load analysis of the pavement structure subjected to an impact load, the load is expressed in terms of its harmonic components. This is achieved by employing a Fourier series expansion. The details of the process are provided in Appendix E.

3.6.1 Simulations for Two-Layered Systems

Similar to the static case, a two-layered pavement model (h_b=0) is first analyzed to concentrate on the behavior of the system from a stochastic viewpoint. Unless stated otherwise, when carrying out the simulations, a random variation is introduced to the elastic modulus of each layer, one at a time; i.e., two separate cases are usually considered: (a) in the first case, the coefficient of variation of the pavement layer modulus is assumed to be 10% with no variation in the subgrade elastic modulus; and (b) for the second case, the subgrade modulus is assumed to have a coefficient of variation equal to 10% with no variation in the pavement modulus. This is done to establish the importance of the effect of modulus variation of each layer on the uncertainty of the predicted surface displacement.

(a) Deflection

Figure 3.4 shows the deflection histories at three offsets on the pavement surface as well as the idealized FWD load history used for the analysis. As one might expect, owing to the dynamic nature of the load, there is a time lag between the peak load and the peak deflections. The increasing time lag between the load and peak deflections at increasing offset indicates that a wave is propagating through the pavement-subgrade system. The relative high rate of attenuation of a peak deflection is partially attributed to the material damping and the geometric characteristics associated with a wave propagating from a point. It should be noted that, displacements almost fully damp out before the end of the load cycle, thereby confirming the choice of the loading period.

For the interpretation of the pavement deflection measurements, the common practice is to use only peak deflections. Thus, the emphasis is placed on reporting this quantity. To investigate the effect of the variations in layer moduli on the surface deflections, the curves connecting peak deflections at each offset are plotted in Figure 3.5. A comparison of the deflection profile calculated using the mean properties (the u_0 curve) with that taking into account a random variation as high as 20% in the subgrade elastic modulus (the E[u] curve) indicates that, like the static case, the effect of random variation in the subgrade modulus on the expected value of the deflection is negligible. Similar results are obtained when a comparison is made assuming a 20% variation in the pavement elastic modulus, thereby, allowing one to conclude that the effect of variations in layer

moduli on the surface deflections is insignificant. A comparison of the peak deflection profile with the static deflection basin reveals that, for this specific problem, the static analysis underestimates the deflections coming from a dynamic load. This clearly demonstrates that systematic errors are introduced when using multi-layer elastostatic analysis to estimate layer moduli from FWD data.

(b) Variation in Deflection

i) Effect of Bedrock Depth

The effect of variations in layer moduli on the variation of peak deflection is investigated for three bedrock depths of 2.85 m, 4.35 m, and 7.35 m, keeping the pavement thickness at a constant value of 0.15 m. The expected values of peak deflections, E[u], are presented in Figure 3.6. This figure shows that changing the bedrock depth in the above range has a little effect on the peak surface deflections, especially for the points close to the load. A comparison between the curves associated with the static and dynamic analyses may imply that, owing to the higher sensitivity of the static solution to the bedrock depth, proper estimation of H is more important for the analysis under a static load condition than under an impact one.

The coefficient of variation of deflection, CV(u), was calculated for two separate cases. For the case where a random variation of modulus exists within the pavement, Figure 3.7 shows that CV(u) at larger offset is negligible. This observation is similar to that of the static analysis and suggests that most of the deflections at large offsets are due to the straining of the subgrade. Moreover, since the curves corresponding to the three different bedrock depths are almost on top of one another, the depth to the bedrock does not seem to have an important influence on this set of simulations.

When a random variation of modulus is assumed in the subgrade, it is observed in Figure 3.7 that CV(u) is much greater than that of the case where the pavement modulus varies. However, unlike the static analysis, for which the curves are almost superimposed, the patterns of curves belonging to different bedrock depths are different and show an overall reduction in CV(u) as the depth to the bedrock decreases. This is related to the frequency-dependent characteristics of the pavement-subgrade system. As the bedrock depth is reduced, the natural frequencies of the system change, thus also the relation between the frequency content of the load and the response of the system.

The fact that CV(u) due to CV(e_s) is substantially higher than CV(u) due to CV(e_p), suggests that the dynamic response of the system is dominated by the properties of the subgrade, a characteristic which is also observed for the static response. The similarity of the results may be explained by the importance of the low frequency components in the FWD impact load.

ii) Effect of Pavement Thickness

An exercise similar to that in the previous section was performed, with pavement thicknesses of 0.15, 0.30, and 0.45 m and a constant bedrock depth of 7.35 m. Figure 3.8 shows the results of the expected values, while Figure 3.9 summarizes the results regarding CV(u). A comparison between the two sets of curves belonging to the static and dynamic analyses clearly indicates that the change in the expected value due to a change in the pavement thickness is similar for both cases.

The CV(u) curves associated with varying the pavement modulus in Figure 3.9 also indicate a trend similar to that displayed for the static analysis (to prevent congestion, the results of the static analysis given in Figure 2.9 are not included in Figure 3.9). In both cases, for example, the magnitude of CV(u) increases as the result of an increase in the pavement thickness suggesting that the effect of the pavement layer on CV(u) becomes more significant as the pavement thickness increases. The increased value of CV(u) due to $CV(e_p)$ for a larger h_p explains a lower level of uncertainty in an estimated elastic modulus of a thick pavement in a backcalculation process, as is illustrated in Chapter 4. On the other hand, unlike the static case, CV(u) due to $CV(e_s)$ does not change remarkably as the pavement thickness changes. An important observation is that the changes in CV(u) associated with the variation in the pavement modulus are larger for the dynamic case, whereas those corresponding to the subgrade modulus variation are larger for the static analysis. This may partially be explained by the fact that, for the static

analysis, more of the subgrade domain contributes to the observed surface deflections, thereby there is a greater shift in CV(u) due to CV(e_s) when h_p varies.

The observations made so far may be explained by considering, for the moment, the wave propagation through a semi-infinite media. For such an idealized case, most of the energy is transmitted within a depth corresponding to approximately one wavelength of the propagating wave (Miller and Pursey 1955). Given a dominant FWD excitation frequency in the range of 0 to 200 rad/s (0 to 30 Hz) and typical shear wave velocities within subgrades, the corresponding Rayleigh and shear wavelengths exceed 4 m. These wavelengths are considerably greater than the thickness of a flexible pavement. Consequently, one would expect that the significance of the pavement properties on the variation of deflection should be small for thin flexible pavement structures, but grows as the pavement thickness increases.

iii) Effect of Pavement and Subgrade Modulus

Simulations were carried out for different values of the pavement layer and subgrade moduli. To be consistent with the static case, two values of 4000 and 8000 MPa for the pavement modulus, and values of 100 and 200 MPa for the subgrade modulus were considered. The results of the simulations associated with the selected pavement and subgrade moduli are given in Figures 3.10 and 3.11, respectively. Comparing these

figures with corresponding figures in the static case indicates a similar overall behavior with respect to the effect of the layer moduli on CV(u). The only significant difference is noticed in Figure 3.11 for the curves belonging to the subgrade variation. As discussed with respect to changing the bedrock depth, the dynamic analysis response is sensitive to the frequency content of the load relative to the natural frequencies of the system. Whether one changes e_s or H, the net result is a change in the stiffness of the system which in turn affects the natural frequencies. Consequently, the sensitivity of the response to the subgrade modulus, represented by CV(u), changes. On the other hand, a relatively constant CV(u) for different configurations of the pavement layer suggests that the pavement properties play a lesser role in the dynamic characteristics of the system.

iv) Simultaneous Variations in Layer Moduli

The assumption of separate variations in either the pavement or subgrade elastic modulus was made in the previous sets of the simulations in order to demonstrate the effect of each variation on CV(u). The case of simultaneous variations in both layers is considered in this section. As for the static case, simulations were completed assuming: (a) complete correlation (ρ =1); and (b) no correlation (ρ =0) between the layer moduli. The results are summarized in Figure 3.12 for a 10% coefficient of variation, and

pavement thicknesses of 0.15 and 0.45 m. When ρ =1, the results suggest that Equation 2.26 is applicable in the dynamic analysis. Also, the relatively smooth CV(u) curves corresponding to the thin and thick pavements resemble the static case. However, unlike that case, the value of the accumulated CV(u) changes as the pavement thickness changes. This observation may be expected based on the results shown in Figure 3.9. For ρ =0, the effect of simultaneous variations on CV(u) is close to that when only the subgrade modulus varies, whether the pavement is thin or thick. This is similar to what is observed in the static case. Again, the difference between the curves for the points close to the load, especially for the thick pavement, is attributed to the relatively high influence of the pavement variation on CV(u) in this region. It should be noted that, similar results could be obtained, if Equation 2.27 is used, indicating that the simultaneous effect of variations may be accounted for in the dynamic case by using the equations derived for the static analysis.

3.6.2 Simulations for Three-Layered Systems

To take another step towards having a more realistic pavement model, three-layered pavement systems are included in the simulations. The configuration employed in the analysis is similar to that presented in Section 2.6 for which h_b=0.30 m. As before, all

the materials are assumed to have a density of 2.0 Mg/m^3, with a hysteretic damping ratio of ζ=5%. It was previously pointed out that, for each random variable in the stochastic finite element analysis, it is necessary to have computer memory at least equivalent to what is required to store the stiffness matrix. This, along with the fact that the bandwidth of the stiffness matrix increases due to the complex arithmetic in the dynamic analysis, imply that the computer memory requirements increase substantially when compared with those associated with the conventional deterministic finite element modeling. It has been the author's experience that 32 Megabyte RAM is not sufficient to solve the problem in the dynamic mode for the case of a three-layered model with three random variables. Therefore, it is essential to use out of core storage devices.

As for the case of the two-layered model, different configurations of the three layers were considered. Based on the results of the simulations, the overall conclusion which stems from the analysis is that the behavior of the pavement layer and subgrade in terms of the deflection variation are generally similar to those observed in the two-layered case. The effect of the variation in the base layer modulus on CV(u) is found to be close to that of the pavement layer, which is not surprising if one considers the similarities between these two layers in terms of the thickness and location with respect to the subgrade. The simulations also indicate that adding an extra layer decreases the individual effect of variation in a layer modulus on CV(u). As was previously addressed in Section 2.8, the consequence of this observation from a backcalculation viewpoint is important. It implies that by adopting a more complex model in terms of the number of layers, there is a

potential to increase the uncertainty of the estimated moduli in a backcalcultion analysis. To provide an example, the results of the simulations assuming a 10% coefficient of variation for the pavement, base, and subgrade moduli, one at a time, are illustrated in Figure 3.13. One may notice that the trends observed in the results of the static and dynamic analyses are virtually identical.

3.7 Frequency Sensitivity of Deflection Variation

In the previous sections, the FWD impact load was decomposed into harmonic components each having a different associated frequency, and the pavement response and its variation were obtained by superimposing the expected values and variations of harmonic response components. Although the resulting response histories are combinations of the harmonics weighed by the Fourier coefficients, certain individual components may have a more significant effect on the overall behavior of the system than the others. This is particularly true for those harmonics associated with large participation factors.

In this section, the change in the value of CV(u), which now refers to a variation in the deflection amplitude, is investigated as a function of the loading frequency using the two-layered model. This is achieved by looking at the results of the variation in deflection amplitude for harmonic excitations with frequencies ranging from 0 to 200 rad/s, twenty

increments in all. Appendix E shows that this frequency range corresponds to the dominant frequency content of the impact load. Once again, the two separate cases, first a variation in the pavement modulus, and then a variation in the subgrade modulus are considered.

When a variation is assumed in the pavement modulus, the results indicate that the statistical variation in deflection amplitude is not sensitive to the frequency in this range. However, when the frequency range is extended to 500 rad/s, there is an indication of a slow increase in CV(u) with increasing frequency. Simulations carried out for other models having bedrock depths of 4.35 and 2.85 m gave nearly identical observations.

For the case where a variation is introduced in the subgrade modulus, the magnitude of CV(u), which is found to be confined generally to a band, is not very sensitive to the frequency. At w=60 rad/s, however, a non-uniform amplification in CV(u) is observed as shown in Figure 3.14. For the other two models with H=4.35 m and H=2.85 m, similar amplifications occur, but at frequencies equal to 90 and 140 rad/s, respectively. To confirm that the observed behavior is independent of the choice of the finite element mesh, simulations were also carried out using other finite element discretizations of the same problem. The same results were obtained.

By examining the eigenvalues of the dynamic stiffness matrix of each model, it was found that the frequency at which the behavior of the system deviates significantly, happens to be close to the second natural frequency of the system. At this frequency, the dynamic characteristic of the system changes, thereby, the sensitivity of the deflection to

the variations in the layer moduli shows a different pattern. The significance of the second natural frequency may be due to the fact that the modal direction factor in the vertical direction associated with this frequency is higher than that of the fundamental frequency. The reason why an amplification does not occur when random variation is assumed in the pavement modulus is attributed to the characteristic that pavement properties do not contribute significantly to the natural frequencies of the system (Chang et al. 1992). Although the behavior of the variation in deflection in the vicinity of the natural frequencies of the system may not be of concern for the FWD test, where a range of frequencies participate in the response, it may be important for tests performed at a single frequency.

3.8 Simulations at High Frequencies

Since it is known that measured deflections are mostly influenced by pavement layer properties at high frequencies (Heukelom and Foster 1960), the behavior of the system under a high frequency equal to w=1000 rad/s (which is not in the FWD dominant loading frequency range) is also considered in a separate analysis. In order to fulfill the recommendation given by Lysmer and Kuhlemeyer (1969) with regard to the element size when high frequencies are involved, the maximum element size of 0.15 m is used throughout the mesh. This results in a 8.85 m by 5.85 m model for 60×40=2400 elements.

The results of the analyses for the cases of variations in the pavement and subgrade moduli are summarized in Figure 3.15. The main observation is that, not only does the sensitivity of CV(u) to CV(e_p) increase significantly, but it also exceeds the values corresponding to the subgrade modulus variation. This observation may be explained by noting that characteristic wavelengths can approach the thickness of the pavement structure at high frequencies. Thus, the response depends more on the properties of the pavement, and the effect of the subgrade variation on the variation of surface deflections diminishes. Procedures such as spectral analysis of surface waves (SASW) make use of this property to characterize pavement-subgrade systems; see, e.g. Nazarian and Stokoe (1989).

Although one might suggest that tests performed at higher frequencies may be more suitable for determining the moduli of pavement layers, it must be recognized that, for frequencies where the wavelength approaches aggregate size, interpretation of tests or simulation results based on continuum mechanics may not be appropriate. Furthermore, test results would be very sensitive to minor flaws in pavement layers, and the frequency dependence of elastic moduli would become an important factor (Heukelom 1960).

3.9 Concluding Remarks

The dynamic analyses performed in this chapter were carried out using the periodic-load-analysis method in a stochastic framework. The introduction of a

frequency-based stochastic approach made it possible to easily modify a static algorithm and use it for dynamic analysis of a layered problem.

The results of the dynamic deflection sensitivity analysis show trends that are similar to those observed when performing analyses with the elastostatic model. This observation indicates that the dominant frequency of the FWD impact load is not high enough to completely capture the characteristics of the surface layer. For various pavement-subgrade configurations, it is illustrated that a change in a subgrade property has a higher influence on the surface deflection sensitivity to the variation in the subgrade modulus when compared to the case of the static load. It has also been demonstrated that by using a high frequency (1000 rad/s), the sensitivity of deflection to the variation in the pavement layer modulus increases significantly, indicating that high frequency tests are better capable of identifying pavement layer moduli.

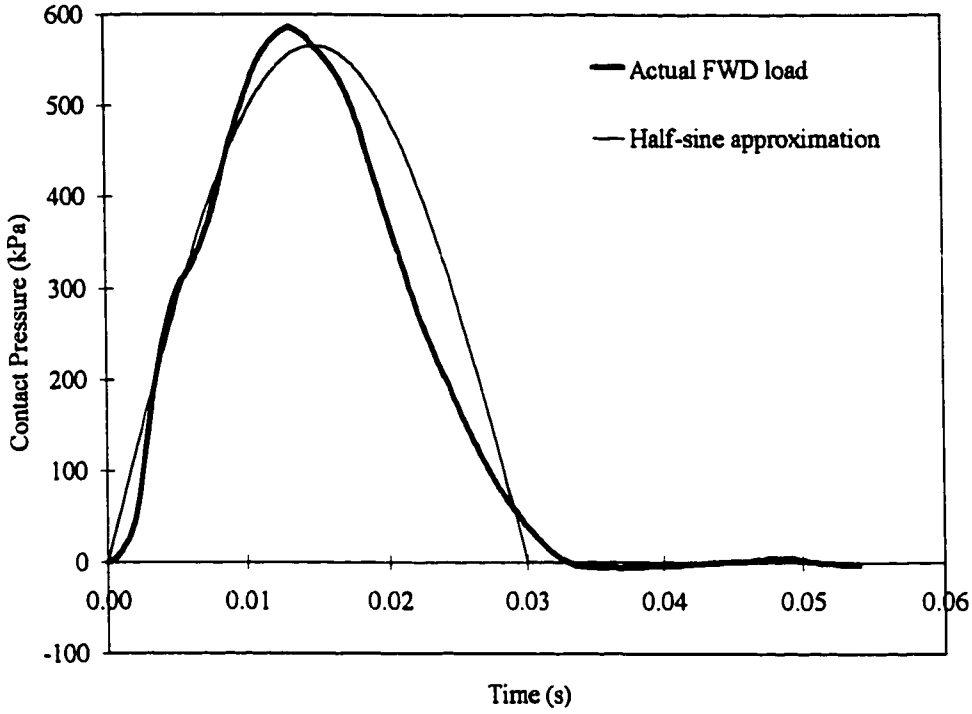

Figure 3.1 Actual and half-sine approximation of an FWD load

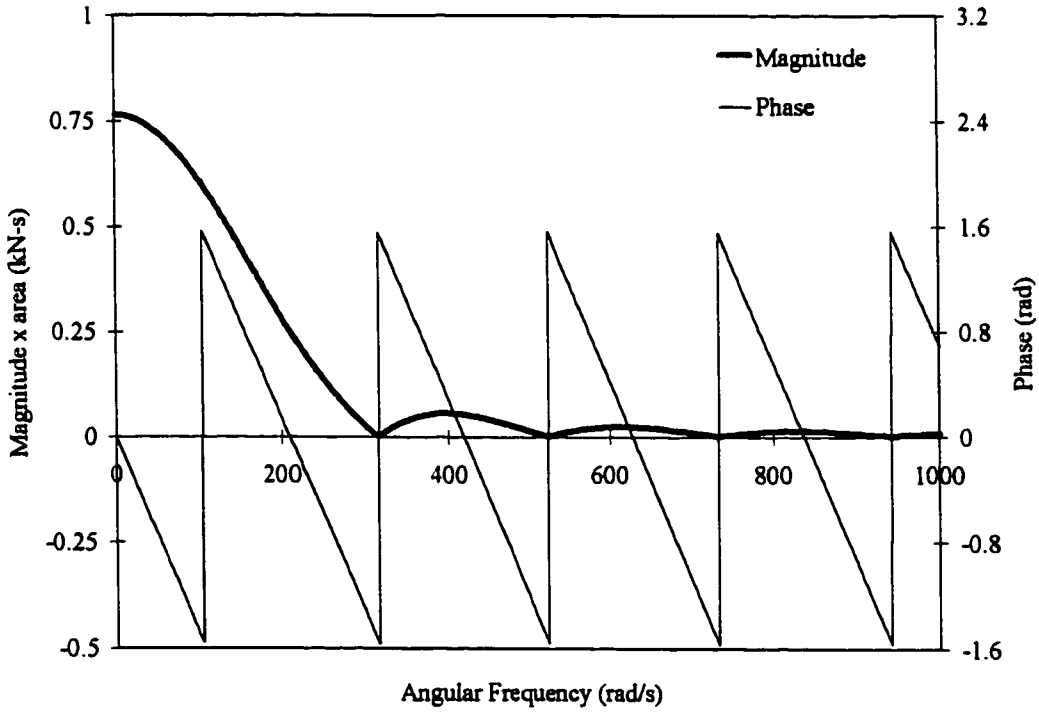

Figure 3.2 Fourier transformed representation of an FWD load

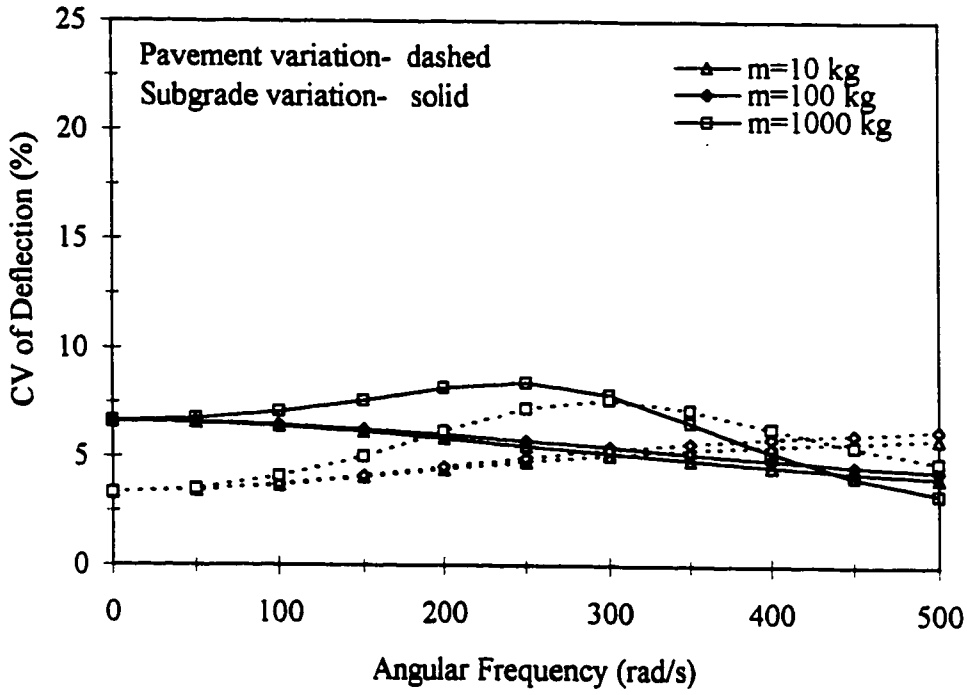

Figure 3.3 CV of deflection for SDOF idealization of pavement-subgrade system

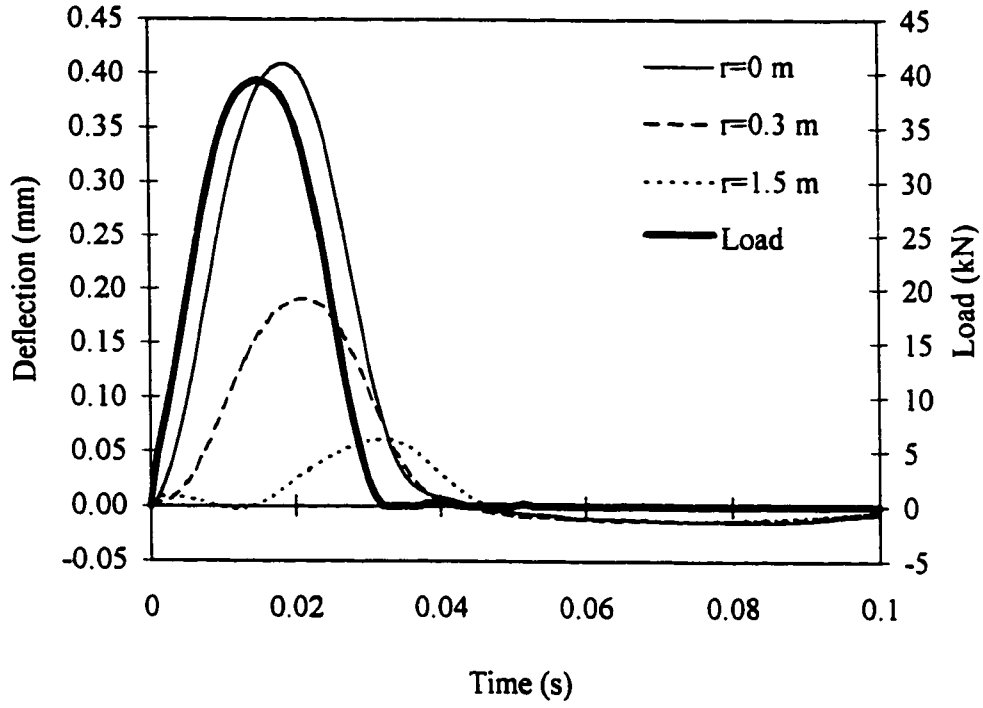

Figure 3.4 Simulated load and deflection histories in an FWD test

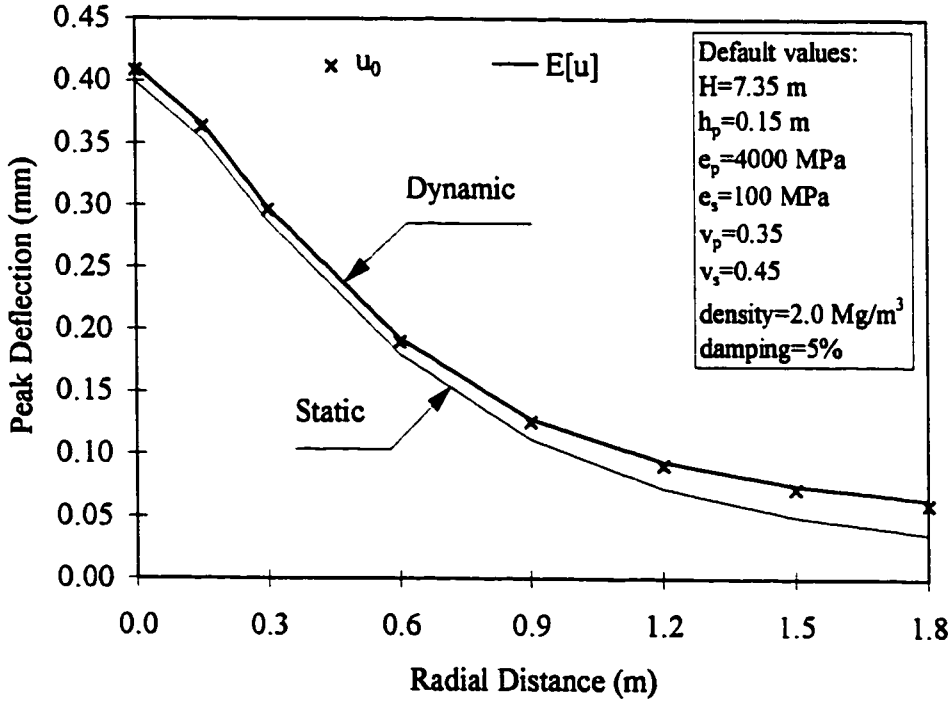

Figure 3.5 Deterministic and stochastic peak deflection profiles (dynamic)

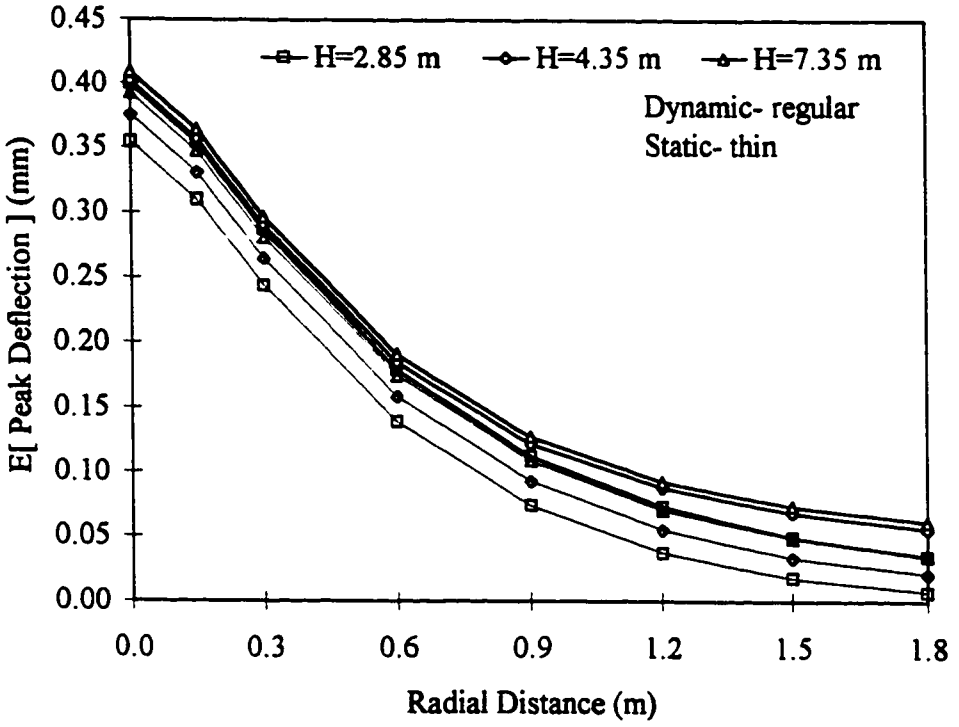

Figure 3.6 Expected value of peak deflection for different bedrock depths (dynamic)

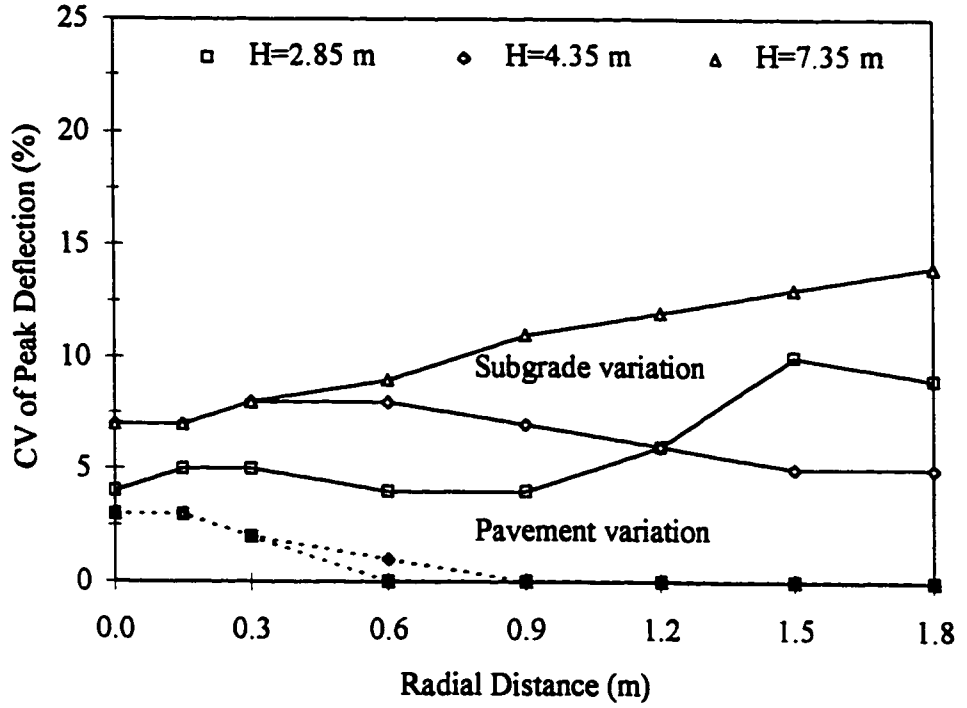

Figure 3.7 CV of peak deflection for different bedrock depths (dynamic)

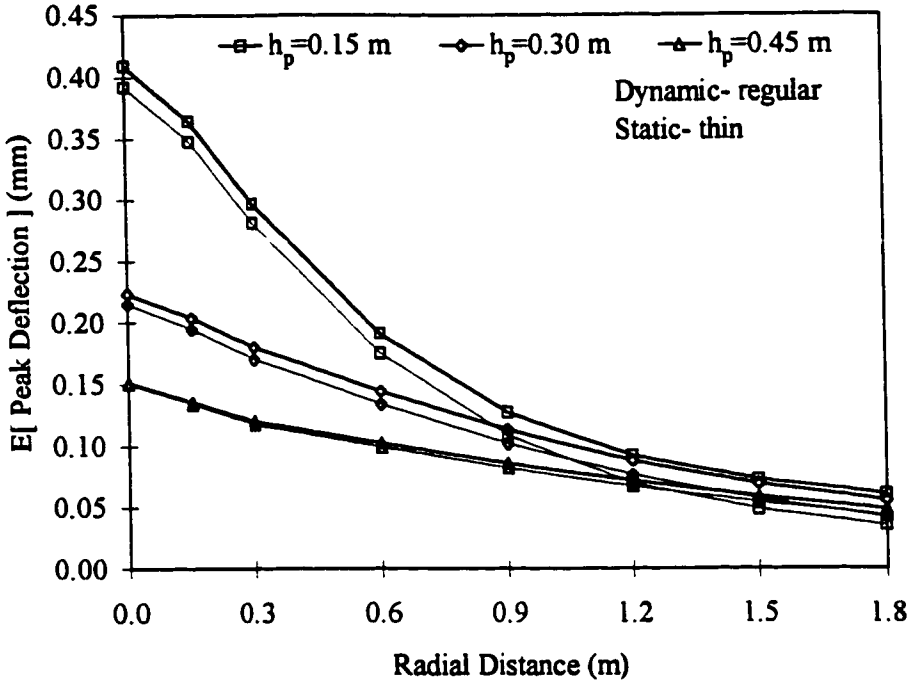

Figure 3.8 Expected value of peak deflection for different pavement thicknesses (dynamic)

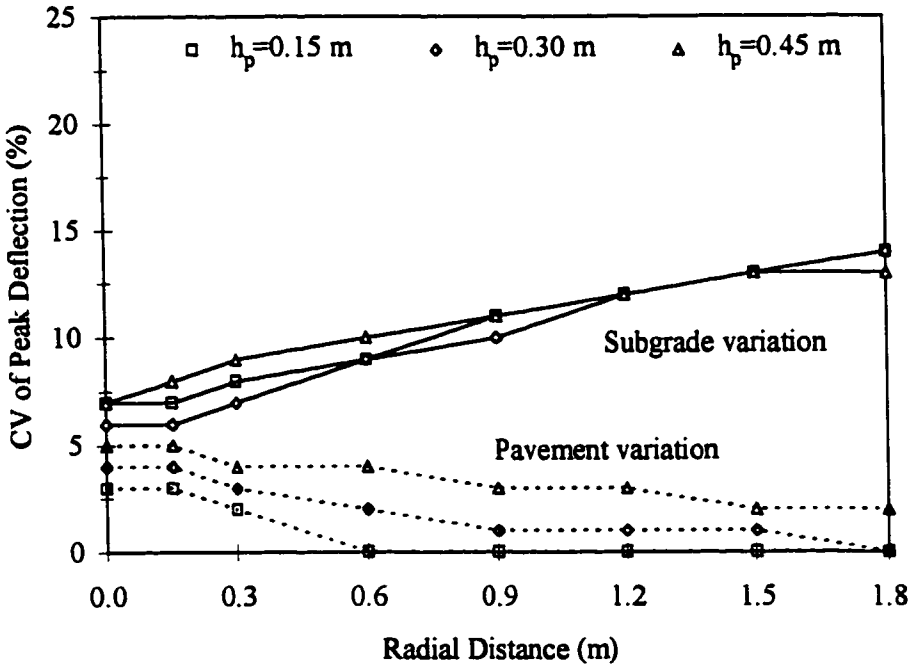

Figure 3.9 CV of peak deflection for different pavement thicknesses (dynamic)

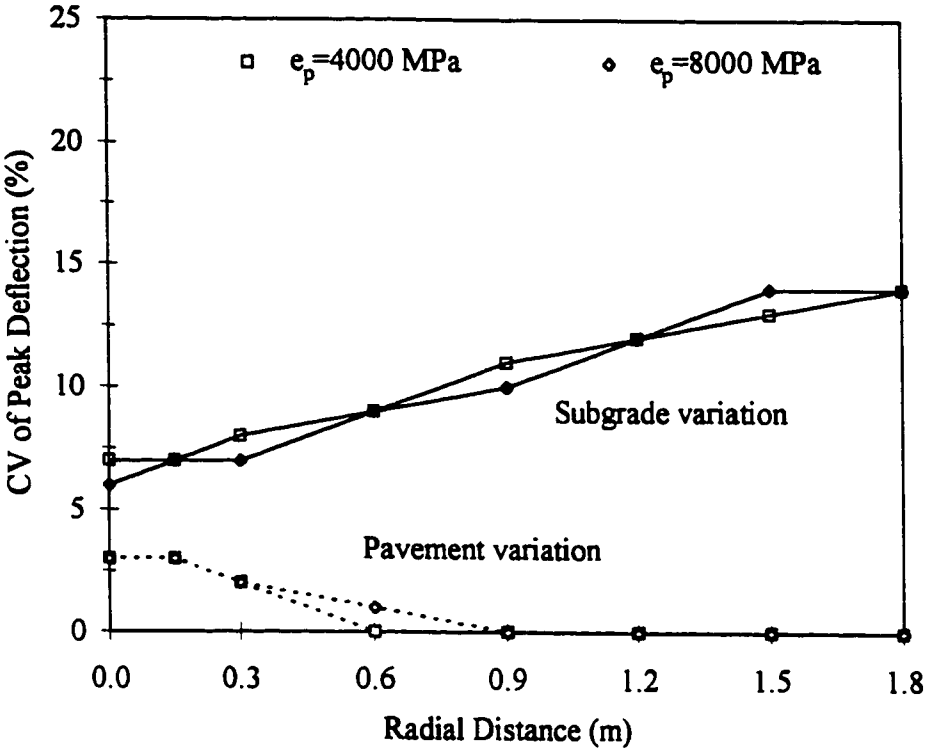

Figure 3.10 CV of peak deflection for different pavement moduli (dynamic)

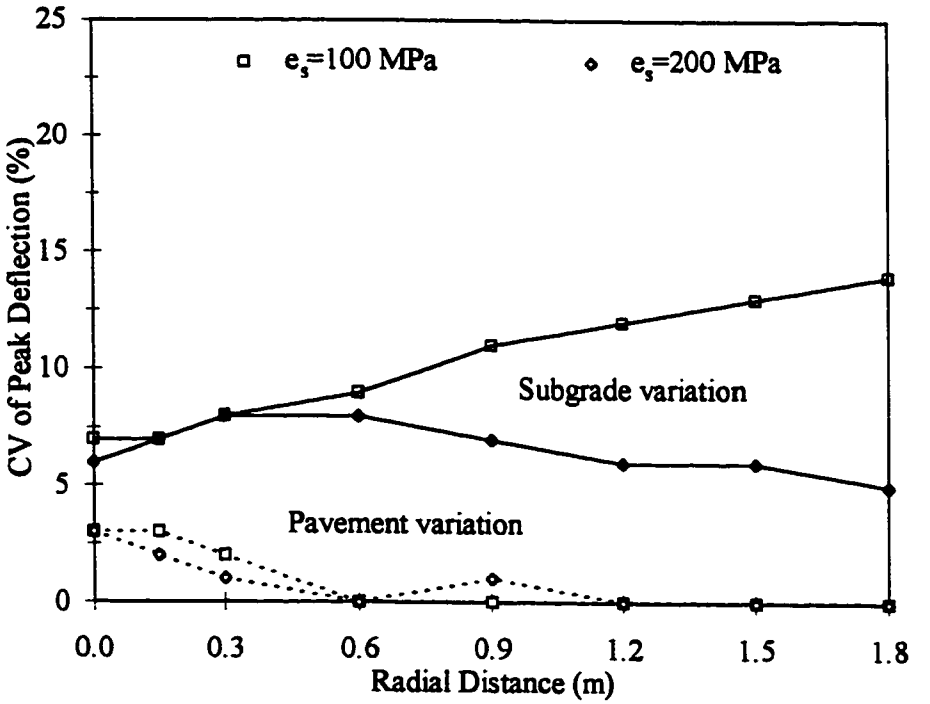

Figure 3.11 CV of peak deflection for different subgrade moduli (dynamic)

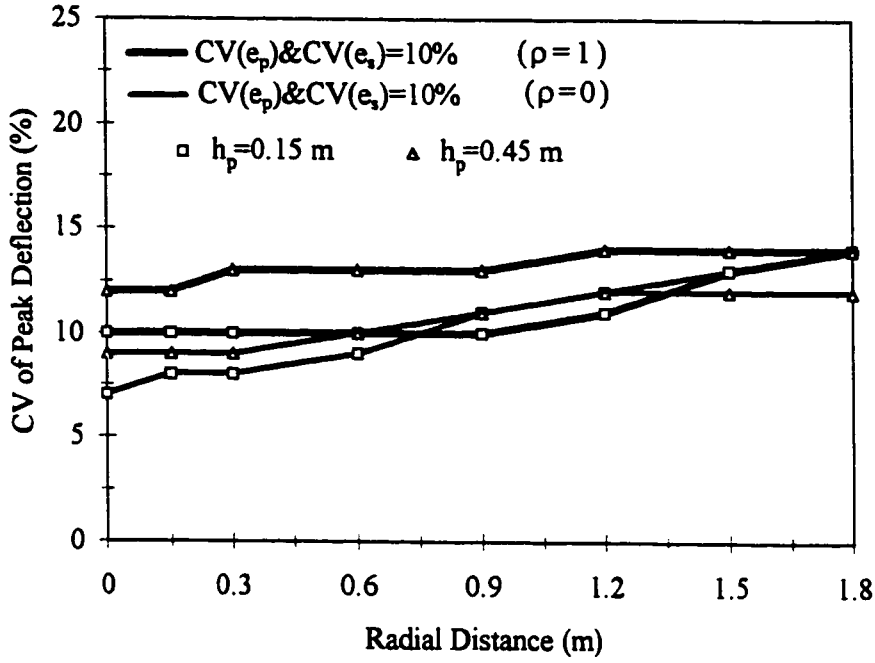

Figure 3.12 CV of peak deflection for simultaneous variation in pavement and subgrade moduli (dynamic)

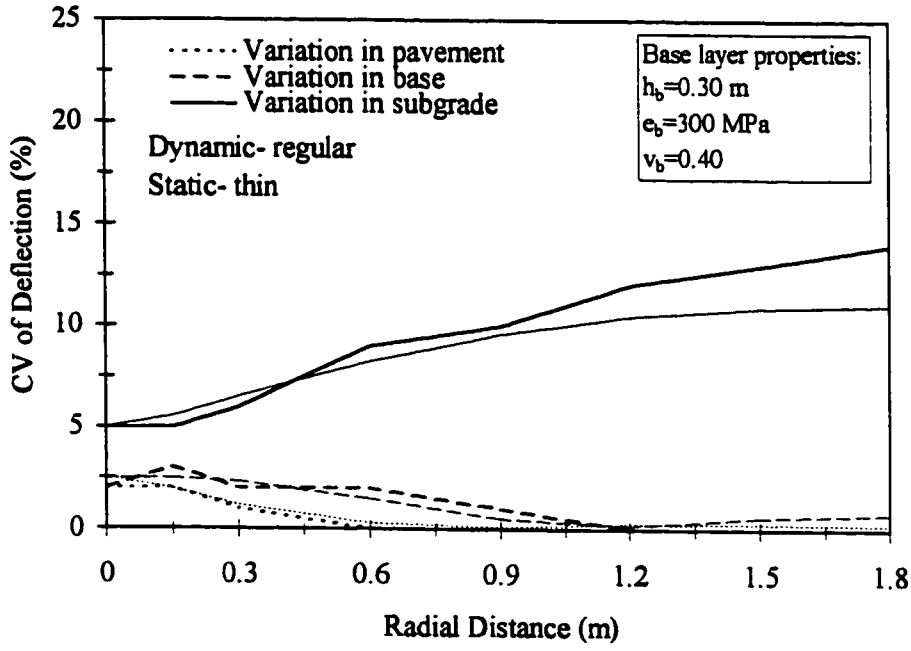

Figure 3.13 CV of deflection for a three-layered pavement model (dynamic)

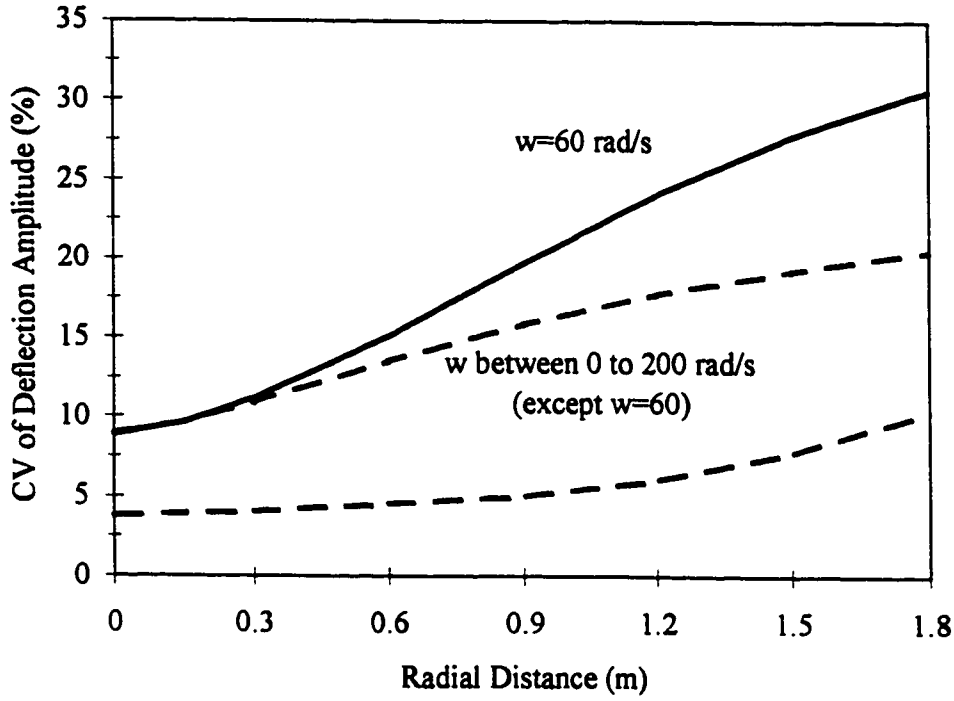

Figure 3.14 CV of deflection amplitude due to CV(e_s) for different angular frequencies

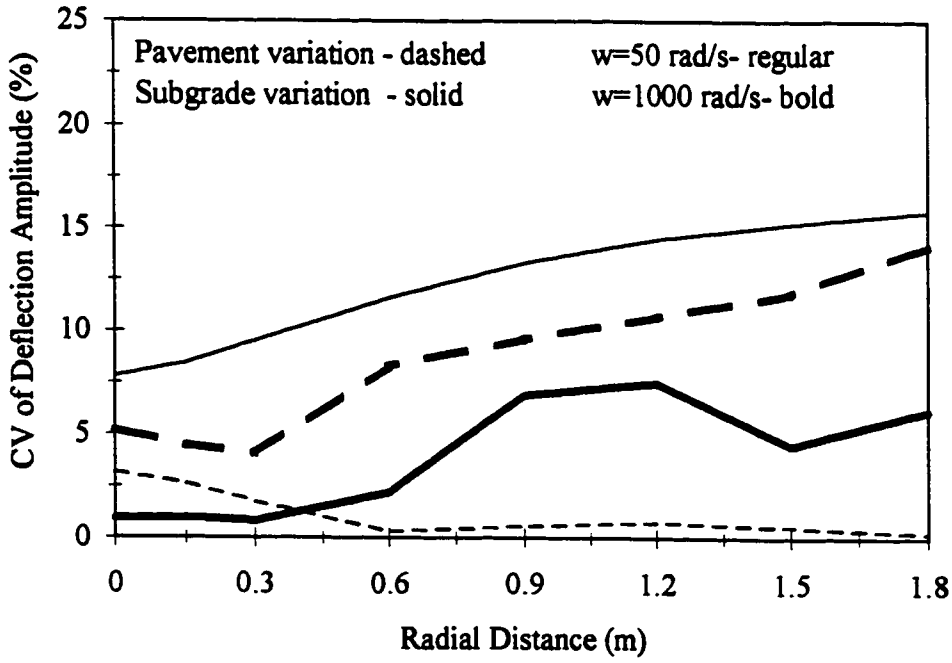

Figure 3.15 CV of deflection amplitude for low and high frequencies

Chapter 4

EFFECT OF VARIATION IN DEFLECTION ON ESTIMATED PAVEMENT PARAMETERS

4.1 Introduction

Pavement surface deflections are widely used to backcalculate pavement-subgrade system parameters, namely layer moduli. In the two previous chapters, the coefficient of variation in surface deflection at a point k, $CV(u_k)$, was calculated given the coefficient of variation in layer modulus, $CV(e_i)$, by performing a forward analysis. It was shown that the sensitivity of $CV(u_k)$ to $CV(e_i)$ depends on the layer i, which has a random variation in its properties, as well as on the location of point k on the surface. Although emphasis was placed on the random variation around a mean value, the assumed coefficients of variations of deflections and layer moduli may also be interpreted as uncertainties with respect to their actual values. Therefore, defining the relation between $CV(u_k)$ and $CV(e_i)$ in terms of the location of the layer and the location of the deflection measurement is desirable from a backcalculation point of view. This is because such a relation can provide

information on the expected level of uncertainty in backcalculated moduli, given the potential uncertainty in deflection measurements.

The information obtained from forward analyses given random properties, also provides hints with respect to the sensitivity of solutions to systematic errors. This is justified if one considers the systematic errors as a perturbation of the prediction by a model relative to the actual behavior of the system. By treating systematic errors in terms of "equivalent" random variation, it is possible to account for the observed spread of a predicted response relative to the measured one.

In this chapter, the results of a forward analysis approach are utilized to make a statement regarding the uncertainty in backcalculated moduli, whether the uncertainty stems from random or systematic errors. First, a relation between the coefficient of variation in deflection at a point on the pavement surface and the coefficient of variation in one of the layer moduli is established. Then the relation is extended to a matrix form to include the case of deflections at a set of points and all layer moduli. The relation, which is defined by a matrix referred to as variation coefficient matrix, is examined for the simplified approach presented in Chapter 2. The variation coefficient matrix is calculated thereafter based on the results of the dynamic analyses in Chapter 3. Next, the uncertainty associated with the backcalculated moduli is investigated using real FWD data. Finally, the effect of uncertainty in the estimated parameters on the predicted performance of pavement systems is discussed.

4.2 Variation in Layer Moduli due to Deflection Variation

In Appendix B, the relation between $CV(u_k)|e_i$ and $CV(e_i)$ for an elastostatic system is defined as

$$d_{ki} = \left(\frac{u_k^{e_i}}{u_k}\right) = \frac{CV(u_k)|e_i}{CV(e_i)} \tag{4.1}$$

where u_k is the total deflection at the k^{th} degree of freedom and $u_k^{e_i}$ is the deflection associated with the members with elastic modulus e_i. Equation 4.1 indicates that the ratio of $CV(u_k)|e_i$ to $CV(e_i)$ is related directly to the ratio of the deflections. This equation can be expressed from a backcalculation viewpoint as

$$CV(e_i) = \delta_{ki}\, CV(u_k)|e_i \tag{4.2}$$

in which $\delta_{ki} = 1/d_{ki}$ is referred to, in this thesis, as the contribution ratio. Equation 4.2 shows that, if the contribution ratio is known and the variation in deflection is attributed to the variation in modulus of a specific layer, then one can obtain the variation in that layer modulus. For practical purposes, contribution ratios may be obtained by finding $CV(e_i)/CV(u_k)|e_i$ via a forward analysis for different pavement configurations. The

resulting curves then may be used to comment on the value of $CV(e_i)$, which represents the uncertainty in e_i, once the variation in deflection measurements are known in the form of $CV(u_k)|e_i$.

To illustrate the procedure, the results in Figure 2.6, obtained for a two-layered system, are considered. This figure provides the values of $CV(u_k)|e_p$ and $CV(u_k)|e_s$ for selected $CV(e_p)$ and $CV(e_s)$. Referring to Equation 4.1 and using the definition of the contribution ratio, the values of δ_{kp} and δ_{ks} are obtained by calculating the ratios of the corresponding CV values. These values are represented in Figure 4.1 by bars for the configuration under study. It should be noted that, since CV(u) is almost linear in terms of CV(e), the contribution ratio may be considered independent of CV(e), therefore, all the three levels of variation in Figure 2.6 result in the same ratio.

Figure 4.1 shows that, while the contribution ratio for subgrade is almost constant and relatively small, that associated with the pavement layer is large, especially at far offsets. This means that variation in deflection would lead to much higher magnitudes of variation in the pavement layer modulus when compared to that of the subgrade. For example, a 10% variation in the surface deflection at r=0.30 m would give either 12% variation in the subgrade modulus, or 53% variation in the pavement layer modulus. For larger offsets, the difference between the two numbers increases drastically, as one might expect.

Similar exercise was performed for the remaining two-layered configurations discussed previously. The range of anticipated variation in the pavement and subgrade

moduli are plotted in Figure 4.1. As one can see, the range corresponding to the subgrade is quite narrow, whereas that for the pavement is wide. These ranges provide information about the level of uncertainty one may expect when backcalculating the pavement or subgrade modulus of a simplified two-layered system with properties similar to those used in this study.

4.3 Variation Coefficient Matrix

4.3.1 Variation Coefficient Matrix for the Simplified Approach

The simplified approach presented in Section 2.4 is considered again. Assuming that there is no correlation between the pavement and subgrade modulus (ρ =0), based on Equation 2.27

$$CV(w_r)^2 = d_{rp}^2 CV(e_p)^2 + d_{rs}^2 CV(e_s)^2 \qquad (4.3)$$

in which

$$d_{rp} = \frac{w_r{}^{'e_p} . e_p}{E[w_r]}, \text{ and } d_{rs} = \frac{w_r{}^{'e_s} . e_s}{E[w_r]} .$$

If Equation 4.3 is defined at N different r values, variations in deflections can be related to variations in layer moduli by means of a matrix, called variation coefficient matrix, as follows

$$\mathbf{CV2(w) = D\ CV2(e)} \tag{4.4}$$

where **CV2(w)** and **CV2(e)** contain the squares of $CV(w_r)$ and CV(e), respectively, and **D** is the N×2 variation coefficient matrix with elements d_{rp} and d_{rs}, $r = r_1, \ldots r_N$. Inverting Equation 4.4 yields

$$\mathbf{CV2(e) = G\ CV2(w)} \tag{4.5}$$

where $\mathbf{G} = [\mathbf{D}^t\mathbf{D}]^{-1}\mathbf{D}^t$ with $\mathbf{D}^t$ being the transpose of **D**. It should be noted that, application of Equation 4.5 without paying attention to the assumptions made to derive this equation may lead to erroneous results. This will be demonstrated subsequently.

For the configuration given in Section 2.4 and the three offsets of r=0, 0.3, and 0.9 m, Equations 4.4 and 4.5 are expressed as

$$\begin{Bmatrix} CV(w_{0.0})^2 \\ CV(w_{0.3})^2 \\ CV(w_{0.9})^2 \end{Bmatrix} = \begin{bmatrix} 0.1119 & 0.4449 \\ 0.0245 & 0.7110 \\ 0.0002 & 1.0295 \end{bmatrix} \begin{Bmatrix} CV(e_p)^2 \\ CV(e_s)^2 \end{Bmatrix} \tag{4.6}$$

and

$$\begin{Bmatrix} CV(e_p)^2 \\ CV(e_s)^2 \end{Bmatrix} = \begin{bmatrix} 9.0778 & -0.2368 & -3.7595 \\ -0.0928 & 0.4122 & 0.7267 \end{bmatrix} \begin{Bmatrix} CV(w_{0.0})^2 \\ CV(w_{0.3})^2 \\ CV(w_{0.9})^2 \end{Bmatrix} \tag{4.7}$$

A clear pattern in the elements of matrix **D** in Equation 4.6 may be recognized. Comparing the numbers in the first and second columns, one can observe that $CV(w_r)$ is much more sensitive to $CV(e_s)$ than to $CV(e_p)$. It may be tempting to seek a pattern in matrix **G**, too. However, one can not make a general comment based on any such observed pattern. Based on Equation 4.7, if a uniform deflection variation of 10% were to be assumed for all three offsets, the variation in the pavement and subgrade modulus would be 22%, and 11%, respectively. The relative predicted levels of uncertainties in the layer moduli are consistent with the results of a first-order error analysis given by Stolle and Jung (1992). On the other hand, the magnitudes of the uncertainties are much less than those reported by Lytton (1989). This can be attributed to the fact that his study implicitly includes the effects of systematic errors which are not taken into account in Equations 4.6 and 4.7. A similar exercise was carried out using other characteristics of

the two-layered model. For example, when h_p=0.45 m, the values of the coefficient of variation change to 18% and 13% for the pavement and subgrade, respectively. This indicates that a systematic error in the pavement thickness would have a direct effect on the uncertainty as expressed by the CV of the backcalculated moduli. As expected, the possible coefficient of variation of the estimated elastic modulus of a thick pavement is less than that of a thin one. However, for both thick and thin pavements, the CV of the pavement is greater than that of the subgrade. One may observe that, unless the thickness of the pavement is known accurately, considerable error in the backcalculated e_p should be expected. It is for this reason that Stolle and Jung (1992) preferred estimating the equivalent thickness h_e rather than elastic modulus e_p when analyzing FWD data.

It should be realized that, implicit in Equation 4.5, a variation in deflection is due to variations in the layer moduli; that is, $CV(w_r)$ is a combination of $CV(w_r)|e_p$ and $CV(w_r)|e_s$. This means that, in general, $CV(w_r)$ is a function of r. Although a constant value for $CV(w_r)$ was selected in the previous set of simulations, other arbitrary values which are not consistent with the pattern in $CV(w_r)$ may provide unreasonable results. In practice, where there are other sources of variations, the equation may yield negative values for $CV(e)^2$. A negative value for $CV(e)^2$ may be interpreted as an unacceptable result owing to the existence of other sources of error which are not compatible in pattern with that of the variations in the layer moduli.

4.3.2 Variation Coefficient Matrix for the Dynamic Analysis

Appendix F provides details on the construction of the variation coefficient matrix for the static and dynamic analyses. It is shown that the form of this matrix is identical for the static and dynamic cases. In the latter case, however, the variation coefficient matrix is time dependent. Since only peak surface deflections are often used in practice to interpret the data, the variation coefficient matrix is constructed based on peak deflections, which do not necessarily occur at the same time. This introduces an approximation to the variation coefficient matrix.

Based on Appendix F, by considering only the vertical degrees of freedom on the pavement surface at offsets of 0, 0.3, 0.6, 0.9, and 1.2 m for the default configuration of the two-layered problem defined in Section 3.6.1, one obtains

$$\begin{Bmatrix} CV(u_1)^2 \\ CV(u_2)^2 \\ CV(u_3)^2 \\ CV(u_4)^2 \\ CV(u_5)^2 \end{Bmatrix} = \begin{bmatrix} 0.1036 & 0.4414 \\ 0.0345 & 0.6206 \\ 0.0013 & 0.8912 \\ 0.0018 & 1.1299 \\ 0.0002 & 1.3610 \end{bmatrix} \begin{Bmatrix} CV(e_p)^2 \\ CV(e_s)^2 \end{Bmatrix} \tag{4.8}$$

Consistent with the results for the elastostatic case, the coefficients corresponding to the subgrade modulus in the second column are considerably higher than those in the first column, which are associated with the pavement layer. This observation reflects the relatively

high sensitivity of CV(u) to CV(e_s) when compared to its sensitivity to CV(e_p). Also, the decrease in the elements of the first column moving from the top to the bottom, indicates the low sensitivity of the deflection variations at large offsets to the variation of the pavement layer modulus. If one were to assume that uncertainties associated with backcalculated layer properties can be accounted for in exactly the same manner as the effect of random distribution of elastic moduli, then, from a backcalculation point of view, this equation implies that the uncertainty in the predicted modulus due to the uncertainty of measured deflections is higher for the pavement layer than for the subgrade. This observation is consistent with that reported by many researchers; e.g., Mamlouk and Davies (1984), Stolle and Hein (1989), and Siddharthan et al. (1992). One could also interpret this finding as implying that perturbations due to modeling errors would have a much greater influence on backcalculated pavement moduli than on backcalculated subgrade moduli. This important point is addressed in more detail in the following sections.

4.4 Accuracy of the Backcalculated Parameters

In the process of backcalculating moduli from measured deflections, there are a number of potential sources of errors which will eventually affect the accuracy of the backcalculated results. The observed relation between the coefficients of variations of layer moduli and those of the response may, however, be utilized to infer on the accuracy of the backcalculated moduli obtained from measured surface deflections.

Figure 4.2a summarizes the process of estimating layer properties via a non-destructive test and a backcalculation exercise. Owing to the presence of random and systematic errors at the measurement stage, there would be a scatter in the measured deflections. The scatter in the data may be characterized by a variation with respect to the mean value. This type of variation is referred to as measurement variation in this study. Given the measured deflections, the layer properties (better described as system parameters) are estimated in a backcalculation procedure.

If the backcalculated parameters, namely the elastic moduli, are employed in a forward analysis to generate the deflections, the predicted deflections would most probably be different from the measured ones. This is mainly because of the systematic errors due to modeling in the backcalculation procedure. If different techniques or input parameters are used for backcalculation procedure, then the generated deflections would indicate a scatter around the measured ones, as shown in Figure 4.2b. This scatter is referred to as backcalculation variation in this study. It should be noted that, if more than one measured deflection basins corresponding to a station are used separately to backcalculate the moduli (instead of using only the mean value of the measured deflection basins), the measurement variation will also contribute to the backcalculation variation.

Now, as illustrated in Chapters 2 and 3, variations in surface deflections can be calculated given variations in layer moduli by performing a stochastic analysis, as shown in Figure 4.2c. This type of variation is referred to as simulated variation in this study.

By comparing the measurement and backcalculation variation with the simulated variation, it is possible to draw conclusions regarding the uncertainties in the estimated

moduli. These uncertainties are a reflection of the errors, whether of random or systematic nature, involved in the process of the measurement and backcalculation, respectively. It should be noted that both simulated and backcalculation variation share modeling systematic errors in the forward analysis processes. The impact of these errors, however, may be considered negligible compared to the systematic errors in the backcalculation process. To illustrate the outlined procedure, the following case is studied.

4.5 Case Study

To demonstrate the level of uncertainty which may be expected in a backcalculation exercise, FWD test data for Section A of Highway 7N, north of Toronto is considered (Stolle 1992). For this test section, the pavement system consists of 140 mm hot mix surface layer, 150 mm type A granular base, and 400 mm sand subbase. The thick subgrade is mainly a silty clay. The FWD test results for the outside lane of Station S7 measured with a 300 mm diameter plate are considered. For this station, tests were completed for four different load levels, with four tests in each level.

In order to investigate the effect of stress-dependence characteristic of elastic moduli on the test results, the measured deflections are plotted in Figure 4.3 against the applied pressure under the plate for all the tests. It is observed that, except for one test, the data points associated with each sensor are located almost on a straight line, indicating

a linear material behavior. This shows that the errors due to neglecting the stress-dependence characteristic of elastic moduli are insignificant for the range of stress increase in an FWD test, as was assumed previously in the analysis.

4.5.1 Uncertainty in Layer Moduli due to Measurement Errors

Since measured pressures under the plate tend to be different, even in one load category, all the data are normalized to a pressure of 1071 kPa, which is almost in the middle of the measured pressure range. Table 4.1 summarizes the test data in terms of the measured pressures and deflections at seven different offsets, along with the normalized values. If no errors were involved, one would have expected the same normalized deflections at each offset for this single station. However, as shown in the table, the numbers are different, which suggests that errors do exist. These errors can be both random, e.g., measurement errors; or systematic, e.g., due to neglecting non-linearity and stress-dependence of materials (not significant in this case), seating load effects, etc. No matter what the nature of the error is, the consequence is a variation in the deflection, denoted previously as measurement variation. The measurement variation, in terms of the coefficient of variation, is calculated and plotted along with the mean values of the deflections at different offsets in Figure 4.4.

Comparing the measurement variation in Figure 4.4 with the simulated variations in Chapter 3, and noting that CV(u) curves are generally insensitive to the different

configurations of the pavement system, one may notice that the observed variation is almost equivalent to the variation in deflection, if a 3% variation were assumed in the subgrade modulus. From a backcalculation viewpoint, this suggests that the effect of the scatter in data is almost equal to a 3% variation in the subgrade modulus, given that there is no variation in the other properties. If the scatter in measured data were to be interpreted as a measure of variation in the pavement layer modulus, a much higher variation would be required to account for the observed variations in the deflections. As mentioned previously, a variation in an estimated modulus is an indication of the level of uncertainty in that quantity. It must be stressed here, since systematic errors are present, the uncertainty is expressed in terms of "equivalent" random error.

It should be emphasized that the deflection data belongs to a single station. Therefore, the scatter in the data associated with each offset excludes the variation due to the variability in material properties between stations. However, within the context of the backcalculation, this scatter may be interpreted as uncertainty in the predicted value of the estimated properties.

A similar exercise was performed by including data from an adjacent station (S8), 15 m from Station S7. The mean values and scatter in deflection did not change significantly, which could imply that there is neither a substantial variability in material properties, nor a difference in the level of measurement errors between the stations. The consequence of this observation is to expect the same level of uncertainty in the backcalculated moduli for these two stations.

4.5.2 Uncertainty in Layer Moduli due to Backcalculation Process

Given the mean values of the measured deflections, the layer moduli were backcalculated from the test data. To backcalculate layer moduli for this multilayer pavement system, the computer program MODULUS4 (Scullion and Michalak 1991) was employed. It was found, when taking into account all the layers, that the backcalculated moduli were not realistic (a very high value for the pavement layer modulus and inconsistent values for the other layers). The fact that inertial effects were neglected by using an elastostatic backcalculation model may be responsible for the poor results. To provide more realistic layer moduli and simplify the procedure at the same time, the thicknesses of the base and subbase layers were expressed in terms of their equivalent thicknesses of hot mix, using the concept of the equivalent pavement thickness (Ullidtz 1987). For the equivalent two-layered pavement system, the average modulus of the pavement layer and subgrade were found to be e_p=1724 MPa and e_s=145 MPa, respectively. At this point it should be recognized that further systematic errors were introduced by using the elastostatic data interpretation procedure and combining the layers. Given the backcalculated moduli, deflections were generated via a forward analysis procedure.

Let us assume, for now, that the mean values of the measured deflections are the true representation of the actual deflections, in the other words, neglect the scatter in the measurements. Then, if measured deflections are compared with the deflections generated based on the backcalculated moduli, as one might expect, the two profiles would not be

exactly the same. The deviation of the generated deflections from the measured ones can be attributed mainly to the systematic errors, especially in the backcalculation procedure. If we were to relax the assumption of identical measured and actual deflections, then other errors, e.g., measurement errors, would also be responsible for the difference between the measured and generated deflections.

Observing the difference between the measured and generated deflections (based on the backcalculated moduli), simulations were completed using the stochastic finite element model to identify the required variation in either the subgrade or pavement modulus which could account for the scatter of the measured deflections about a deflection profile defined by the backcalculated moduli. Figure 4.5 shows the actual measured deflections from the FWD test along with the calculated expected values of the peak deflections. The dotted lines illustrate the range of the peak deflection variation associated with a 30% variation in the subgrade elastic modulus. Assuming no systematic errors in the stochastic analysis for the moment, it can be seen that a 30% variation in the subgrade modulus could account for the distribution of the measured deflections about the expected values. From a backcalculation viewpoint, the observed scatter may then be translated to a 30% variation in the backcalculated subgrade modulus, which provides a measure of uncertainty for the estimated quantity. Since systematic errors do exist in the analysis, the anticipated level of uncertainty in the subgrade modulus is also influenced by this source of error. One must remember that for a given model all the errors associated with the backcalculation process will be reflected in the values of the backcalculated quantities.

A similar exercise was carried out for the case where variation was introduced in the surface layer modulus. For this case, as Figure 4.6 indicates, even a 30% variation in the pavement layer modulus could not account for the scatter of the measured deflections about the calculated values. Therefore, if the observed scatter were to be solely due to the variation in the pavement modulus, a much higher variation would be required to account for the scatter. From a backcalculation viewpoint, one could conclude that small variations in surface deflections would result in a large variation in the predicted pavement modulus. This would explain why in some cases estimated pavement moduli can vary by several orders of magnitude, as is reported by Lytton (1989). Figure 4.6 also confirms that, for points at large offsets, the variation in deflection is almost insensitive to the variation in pavement modulus. Implementing this fact in the backcalculation procedure is consistent with the experience where it is known that far sensors are not good candidates for backcalculating surface layer moduli (Zaghloul et al. 1994).

Strictly speaking, the 30% coefficient of variation used in the analysis of this section is not consistent with the assumption of small variation made when formulating the SFEM. For a more rigorous treatment, higher order statistical moments would be required. Nevertheless, the general observations are still applicable, only the magnitude changes a little.

It should be emphasized that, in actual fact, many different factors contribute to the scatter of measured data points about the calculated values. Nevertheless, no matter what the sources of the error are, the consequence of their presence would result in uncertainties in the backcalculated moduli. In some cases, however, systematic errors may

cancel out one another, thereby, resulting in less uncertainty than that due to the summation of their individual effects.

4.6 Uncertainty in Pavement Performance Prediction

Pavement performance prediction models are often based on the failure criterion for either fatigue cracking of the surface layer, or permanent deformation of the subgrade (Huang 1993). In both cases, the prediction model is usually expressed in the general form of (Siddharthan et al. 1992)

$$N_f = \alpha \, R^{\beta} \tag{4.9}$$

in which N_f is the number of load applications to failure, R is a representation of the pavement response under the load, e.g., displacement, strain, etc., and α and β are the constants of the equation. The specific form of this equation and the values of α and β depend on the type of the pavement response used in the equation, and the assumptions made to establish the relationship. However, in most cases, the absolute value of β varies between 2 and 6.

Applying the perturbation technique to the above equation and considering the pavement response to be the only random variable, the expected value and the coefficient

of variation of N_f in terms of the coefficient of variation of the pavement response, CV(R), are given by

$$E[N_f] = N_{f0}[1 + \frac{\beta(\beta-1)}{2} CV(R)^2] \quad (4.10)$$

$$CV(N_f) = |\beta| \; CV(R) \quad (4.11)$$

where N_{f0} is the value of N_f calculated at mean value of the response. Equations 4.10 and 4.11 suggest that, if for example β were to be equal to -4, then the expected value of N_f is greater than N_{f0} by a factor of $[1+10CV(R)^2]$. More importantly, the variation in N_f is four times the assumed variation in the response.

For the cases where R is accessible directly through measurement, e.g., displacement at a sensor in an FWD test, its variation is limited to those errors associated with the measurement process, which also includes the variability in the material properties. As was shown in the previous section, for a sample case, these variations were around 2-3% for different sensors, which (for the assumed β value of -4), translates to a variation in N_f less than 12%.

When R is not a direct outcome of a test or measurement on the pavement structure, e.g., calculated stress or strain in terms of layer properties, it is necessary to estimate these properties. When such parameters come from a backcalculation procedure,

the uncertainty in these quantities are usually much higher than those associated only with a measurement process. In the case discussed previously, it was illustrated that, the uncertainty in the backcalculated modulus could be as high as 30% for the subgrade, and even higher for the pavement. Consequently, it is anticipated that the R value calculated using these moduli would experience nearly the same level of uncertainty. This in turn could result in an unacceptable variation of 120% in N_f.

Taking into account the high sensitivity of variation in the pavement performance indices to variation in the response, along with the high level of uncertainty in the response when it is obtained in terms of the backcalculated properties, one may appreciate why it is difficult to predict pavement performance accurately. Moreover, the above discussion clearly illustrates the advantage of the performance prediction models established based on those quantities which can be measured directly in the field.

Table 4.1 FWD test data and the normalized values

	Measured Deflections (microns)						
Pressure	**Offset (m)**						
kPa	**0**	**0.30**	**0.45**	**0.60**	**0.90**	**1.20**	**1.50**
586	256	187	145	115	66	37	22
591	255	186	145	114	65	36	22
588	253	186	144	114	65	37	22
553	253	185	144	113	65	36	22
833	376	277	216	172	99	56	32
845	377	278	217	172	100	57	32
841	376	277	216	172	99	57	32
851	375	275	216	170	100	56	32
1071	471	349	273	217	126	72	41
1073	472	349	273	217	128	72	41
1077	471	349	273	217	128	72	41
1125	470	347	272	217	127	72	41
1561	687	509	401	321	189	106	61
1572	689	510	401	321	190	107	61
1561	689	509	401	321	190	106	62
1568	688	508	400	321	189	106	61
	Normalized Deflections (microns)						
1071	468	342	265	210	121	68	40
"	462	337	263	207	118	65	40
"	461	339	262	208	118	67	40
"	490	358	279	219	126	70	43
"	483	356	278	221	127	72	41
"	478	352	275	218	127	72	41
"	479	353	275	219	126	73	41
"	472	346	272	214	126	70	40
"	471	349	273	217	126	72	41
"	471	348	272	217	128	72	41
"	468	347	271	216	127	72	41
"	447	330	259	207	121	69	39
"	471	349	275	220	130	73	42
"	469	347	273	219	129	73	42
"	473	349	275	220	130	73	43
"	470	347	273	219	129	72	42

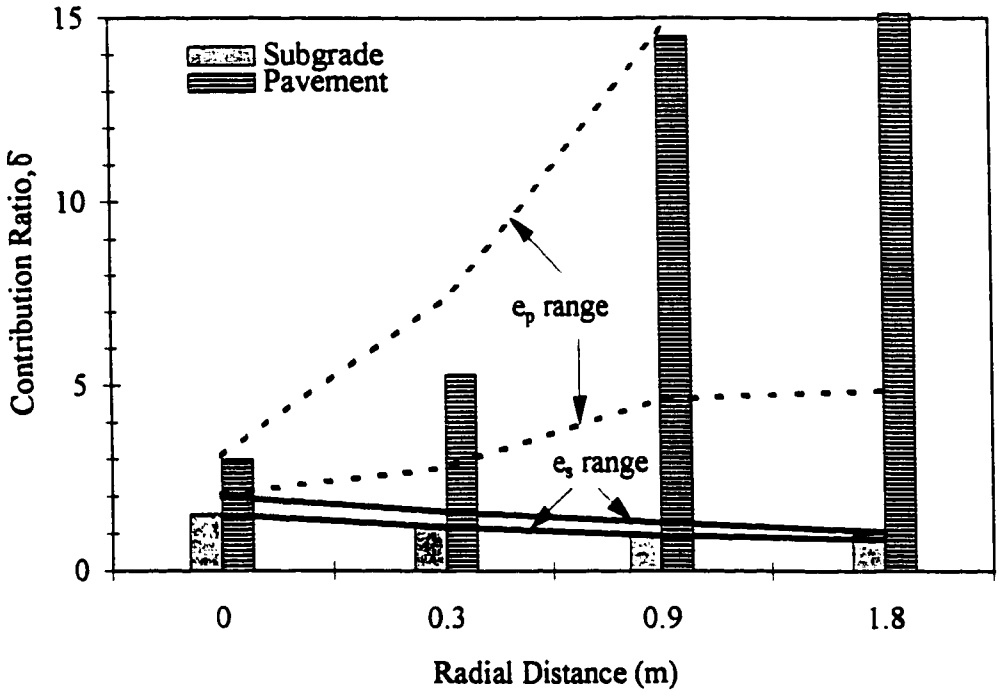

Figure 4.1 Range of contribution ratio for pavement and subgrade moduli

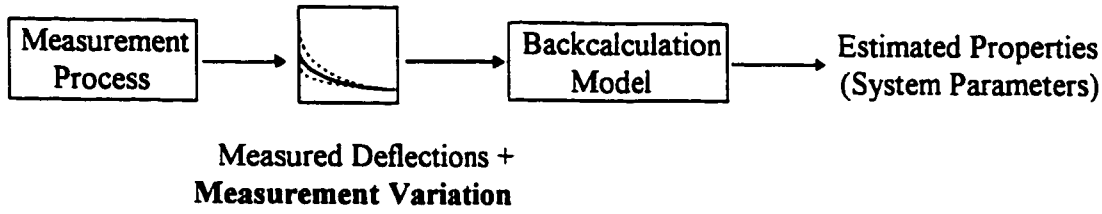

(a) Measurement and backcalculation process

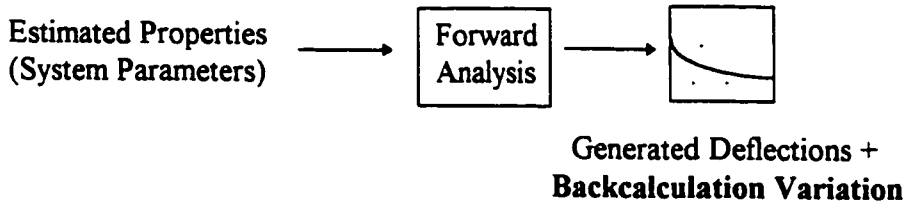

(b) Re-generation of deflections

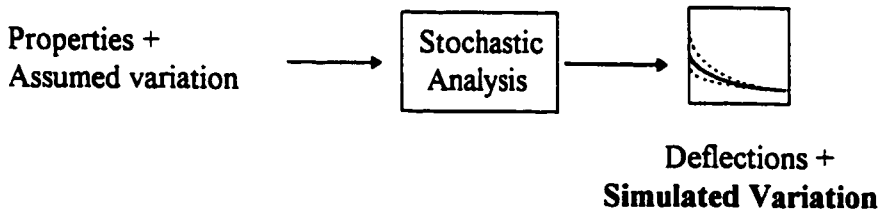

(c) Simulations assuming variations in properties

Figure 4.2 Framework for quantifying uncertainty in backcalculated properties

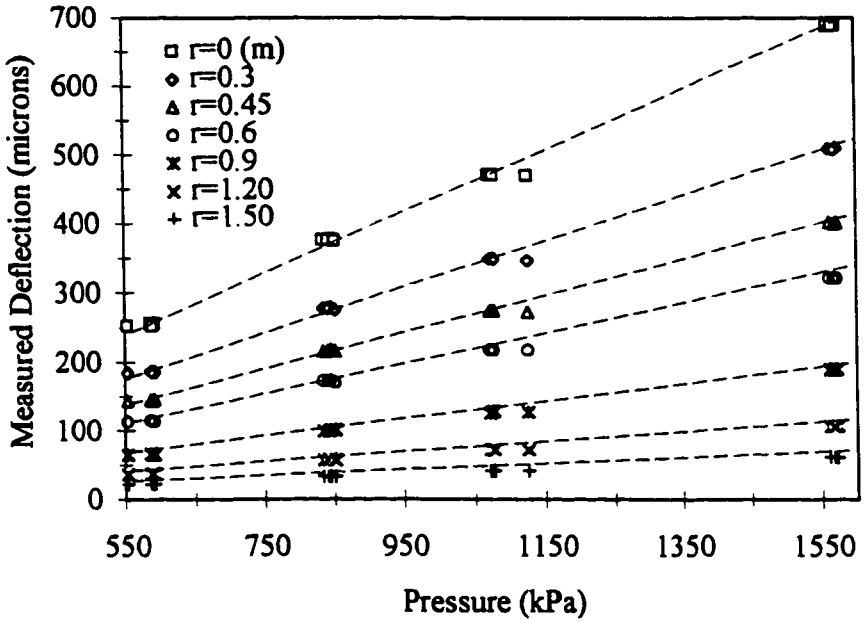

Figure 4.3 Measured deflections versus applied pressures

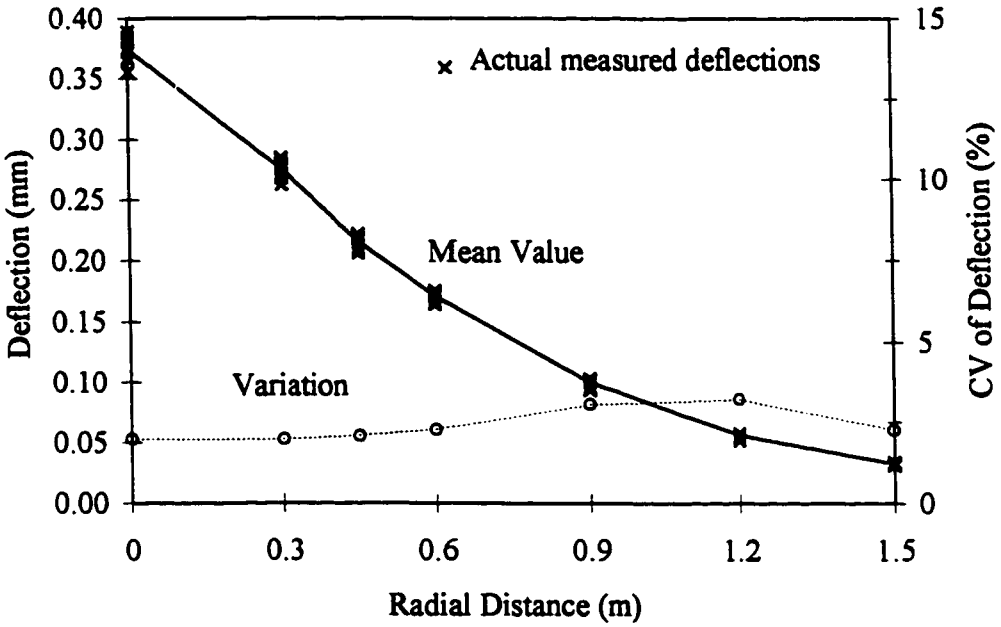

Figure 4.4 Scatter of measured deflections around mean value, and the resulting variation

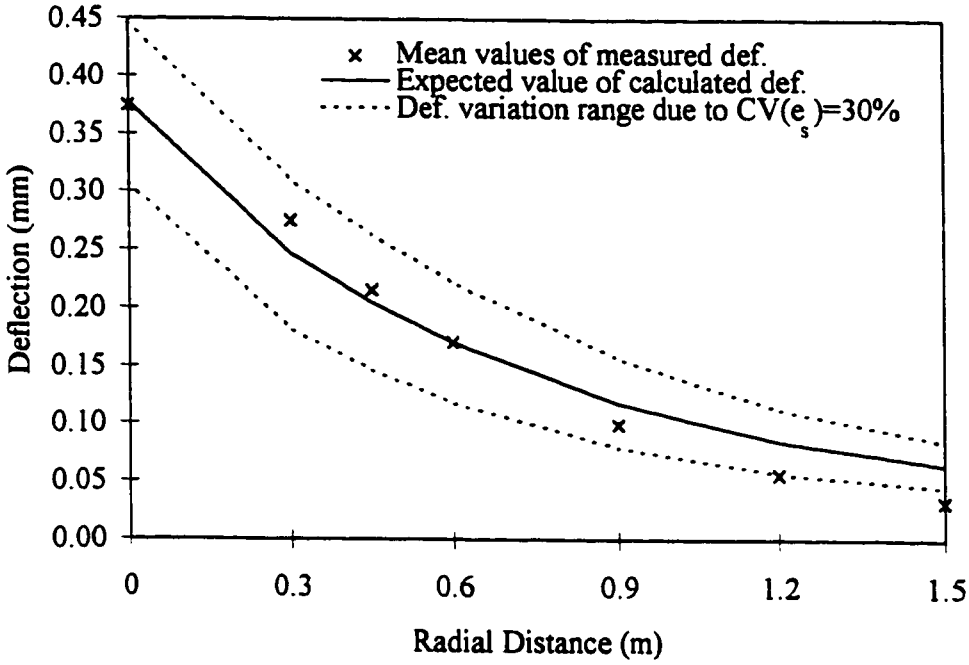

Figure 4.5 Equivalent variation in subgrade modulus which accounts for the difference between measured and calculated deflections

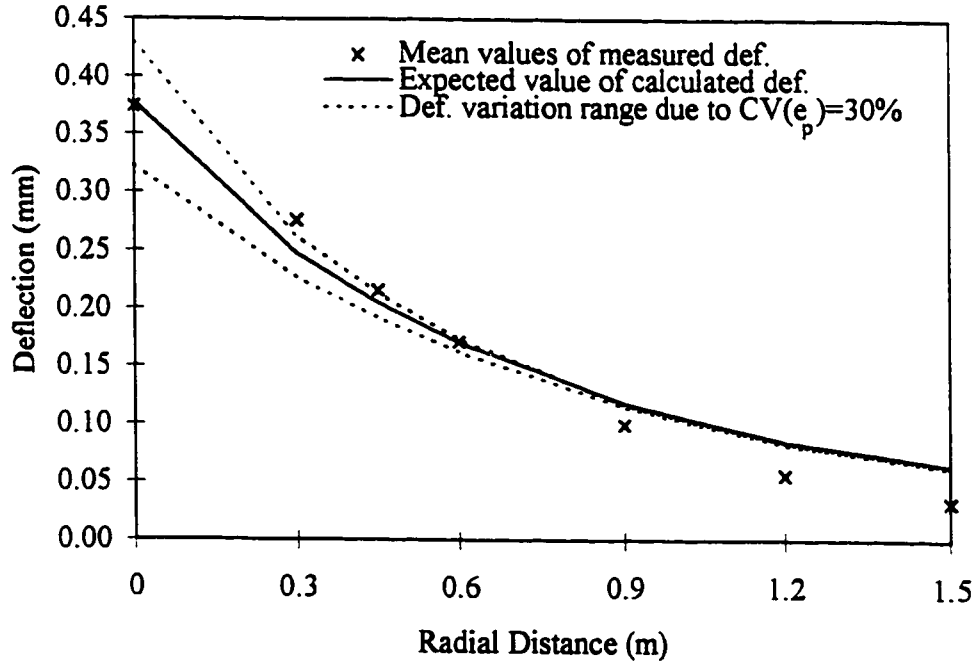

Figure 4.6 Variation in pavement modulus compared to the difference between measured and calculated deflections

Chapter 5

CONCLUSIONS AND RECOMMENDATIONS

5.1 Summary and Conclusions

To present a rigorous, systematic treatment of the effect of random variations in layer properties on the deflection response of a pavement-subgrade system, a stochastic approach to the pavement deflection analysis was developed. Random variations were assumed in layer properties and pavement surface deflections and their variations were calculated in a forward analysis for different configurations of the system and loading conditions. Owing to the perturbation nature of the approach, the variation in deflection also reflects its sensitivity to the selected layer properties, thereby, allowing one to comment on the sensitivity of the output to the input parameters. The fact that the calculation of deflection variation in a stochastic analysis provides information which is similar to that obtained when performing a sensitivity analysis by solving many different configurations of the problem, demonstrates one of the advantages of the stochastic approach over traditional sensitivity analyses.

Based on the forward analyses, the following observations and conclusions are made:

1- The expected value of deflection, E[u], is always greater than the deflection calculated using the mean. Nevertheless, the difference is small even for relatively large variations in layer moduli. Although random variations in layer moduli may have a negligible effect on the expected value of the deflection, they are significant when calculating the variation of deflection.

2- For a two-layered model and a quasi-static load condition, the variation in deflection due to variation in the pavement modulus is less than that due to variation in the subgrade modulus. This indicates that, overall, surface deflections are more sensitive to the subgrade modulus than to the surface layer modulus. The results also indicate that the influence of the pavement layer on the surface deflection is limited to the vicinity of the load, a distance referred to in this thesis as pavement influence distance. The ratio of the pavement influence distance to the equivalent pavement thickness is about 1.3 for the pavement-subgrade systems analyzed in this study.

3- The observed sensitivity of the deflection to layer moduli is not influenced significantly by the values of the pavement and subgrade modulus, nor by the bedrock depth. However, the pavement thickness does affect the level of the sensitivity. The thicker the pavement, the more sensitive is the deflection to the pavement modulus.

4- A simplified pavement deflection analysis within a stochastic framework provides results similar to those from the SFEM indicating that, the model is capable of

reflecting the sensitivity of deflection to layer moduli for simple pavement configurations under static loads.

5- A comparison between the results of the perturbation analysis with those of the Monte Carlo simulations for the simplified approach reveals that, assuming a normal distribution in modulus, truncation leads to an underestimation of the coefficient of variation of the response. In other words, the actual variation of the response is higher than that obtained by using a truncated Taylor's expansion.

6- Dynamic analyses using an idealized FWD impact load yield trends and magnitudes for the deflection variation similar to those of the static load condition. This indicates that, in general, the variation in deflection is not very sensitive to the frequency in the range usually encountered in an FWD test. Moreover, the response is primarily dominated by the stiffness of the subgrade. In other words, the frequency content of the FWD impact load is such that, like for the case of a static load, the characteristics of the pavement layer do not contribute much to the surface deflections. However, for high frequencies outside the range of an FWD load, the sensitivity of deflection to the variation in the pavement modulus may exceed that of the subgrade modulus.

7- For a single frequency loading close to one of the natural frequencies of the system, the variation in deflection due to random variation in the subgrade modulus amplifies.

8- The trends in the results associated with a more realistic, three-layered model are similar to those of the two-layered model for the pavement layer and the subgrade. The trend in the deflection variation due to the variation in the base layer modulus resembles that associated with the pavement layer. The important fact is that, the

magnitude of the deflection variation due to the variation in the pavement layer and subgrade modulus decreases when compared to the values obtained using the two-layered model, thereby indicating that the sensitivity of the deflection to the properties of the layers decreases when additional layers are included in an analysis.

9- Surface deflections are more sensitive to the pavement layer thickness than to its elastic modulus and Poisson ratio.

10- It is possible to derive a relationship between the results of the stochastic analysis with the physical behavior of the system by relating the ratio of variation in the layers to the ratio of their corresponding deflections. Using this relation, one can identify the contribution of each layer to the total surface deflection via a stochastic analysis of the pavement-subgrade system.

The results of the forward analysis were utilized to establish a relation between random variations in surface deflections and layer moduli. By inverting the relation and interpreting the variation as a level of uncertainty (or perturbation) in deflections and layer moduli, the effect of uncertainties in measured deflections on the estimated properties was addressed. This approach provides a framework for quantifying the uncertainty level in a backcalculated parameter, whether the source of error is random or systematic.

From a backcalculation perspective, the following conclusions are made:

1- For a thin pavement under a low frequency loading, the uncertainty in the backcalculated pavement layer modulus is much higher than that of the subgrade.

2- The uncertainty level in a backcalculated layer modulus, and therefore the accuracy of the estimation, may not change significantly due to the dynamic characteristic of the FWD test. Consequently, a dynamic interpretation of the FWD data may not provide more accurate estimates of the pavement layer properties than a static one.

3- Trying to get more information by including more layers in a backcalculation model has the potential to increase the uncertainties associated with the estimated moduli.

4- The significantly lower level of uncertainty in the pavement layer modulus anticipated by the simplified approach, compared to the uncertainty levels observed in practice indicates that, the selection of the backcalculation model and its input values have a greater impact on the accuracy of the results than the impact of the assumed random variation in the layer modulus.

5- Uncertainties in estimated properties due to errors associated with measurement and backcalculation processes propagate to pavement performance models causing inaccurate, and often unacceptable, performance predictions.

It is important to realize that the above mentioned observations and conclusions are limited to the governing assumptions and the configurations of the problems that were studied.

5.2 Recommendations for Future study

In this study, assumptions are made to simplify the presentation of the proposed approach and to emphasize on the overall stochastic behavior of pavement systems. Relaxing these assumptions will improve the selected pavement model by reducing the systematic errors arising from the modeling procedure. In addition it will provide a more realistic approximation of the actual problem. Some of the improvements that may be achieved in the model and the overall research work are as follows:

1- Taking into account non-linear and stress-dependent properties of highway materials and examining their effects on the stochastic response of pavement-subgrade systems.

2- Adopting a three-dimensional finite element model in order to allow one to consider more complex pavement system geometries.

3- Using a higher order truncation of the Taylor's expansion in the stochastic finite element formulation to extend the application of the method to the cases of large variations.

4- Applying the stochastic framework to interpret the results of the other nondestructive tests, especially those operating at high frequencies, and studying the sensitivity of the response to material properties for these other test conditions.

5- Investigating the stochastic behavior of systems at frequencies close to their natural frequencies, and the consequence of observed amplification in the response variation on the accuracy of the backcalculated parameters.

APPENDIX A

STATISTICAL FORMULAS

Real Space

If x is a real, continuous random variable with $p(x)$ being its probability density function, then (Helstrom 1984)

$E[x] = \int_{-\infty}^{+\infty} x\, p(x)\, dx$	expected value of x
$E[c] = c$	c constant
$E[cx] = cE[x]$	
$E[\sum_{i=1}^{N} x_i] = \sum_{i=1}^{N} E[x_i]$	x_i random variable
$E[f(x)] = \int_{-\infty}^{+\infty} f(x)\, p(x)\, dx$	$f(x)$ a function of x
$E[\Delta x] = 0$	$\Delta x = x - E[x]$

$\text{var}(x) = E[(x - E[x])^2] = E[\Delta x^2]$ variance of x

$\text{var}(c) = 0$ c constant

$\text{var}(cx) = c^2 \text{ var}(x)$

$\text{var}(f(x)) = E[(f(x) - E[f(x)])^2]$

$\text{cov}(x_i, x_j) = E[(x_i - E[x_i])(x_j - E[x_j])]$ x_i and x_j random variables

$\text{cov}(x, x) = \text{var}(x)$

$CV(x) = \dfrac{\sqrt{\text{var}(x)}}{|E[x]|}$ coefficient of variation of x

Complex Space

If z_j is a complex random variable given by $z_j = x_j + iy_j$, with its complex conjugate defined as $\bar{z}_j = x_j - iy_j$, then (Miller 1974)

$E[z_j] = E[x_j] + iE[y_j]$

$E[cz_j] = cE[z_j]$ c complex constant

$$E[\sum_{j=1}^{N} z_j] = \sum_{j=1}^{N} E[z_j]$$

$$\text{var}(z_j) = E[(z_j - E[z_j])\overline{(z_j - E[z_j])}] = \text{var}(x_j) + \text{var}(y_j)$$

$\text{var}(cz_j) = c\bar{c}\ \text{var}(z_j)$ c complex constant with $\bar{c}$ its complex conjugate

$$\text{cov}(z_j, z_k) = E[(z_j - E[z_j])(z_k - E[z_k])]$$
$$= \text{cov}(x_j, x_k) - \text{cov}(y_j, y_k) + i[\text{cov}(x_j, y_k) + \text{cov}(y_j, x_k)]$$

$$\sum_{j=1}^{N}\sum_{k=1}^{M} \text{cov}(z_j, \bar{z}_k) = \text{var}(\sum_{j=1}^{N} z_j)$$

$$CV(z_j) = \frac{\sqrt{\text{var}(z_j)}}{|E[z_j]|}$$

APPENDIX B

RELATION BETWEEN DEFLECTION AND ITS VARIATION

A linear, multi-degree of freedom system with the characteristic equation given by Equation 2.7 is considered. If there are p elastic moduli defined in the system, and all of them are random variables with mean values equal to e_i, i=1,...p, one may write

$$\mathbf{K_0} = \sum_{i=1}^{p} \mathbf{K}^{e_i} \tag{B.1}$$

in which $\mathbf{K}^{e_i}$ is the stiffness contribution of all the members having an elastic modulus equal to e_i to the total stiffness of the system, $\mathbf{K_0}$. Accordingly, the total displacement of the system, $\mathbf{u_0}$, can be decomposed to the contributions coming from the members having elastic modulus e_i, $\mathbf{u}^{e_i}$, as follows

$$\mathbf{u_0} = \sum_{i=1}^{p} \mathbf{u}^{e_i} \tag{B.2}$$

where

$$\mathbf{u}^{e_i} = \mathbf{K}_0^{-1}\mathbf{K}^{e_i}\mathbf{u}_0 \tag{B.3}$$

On the other hand, based on the definition of partial derivative of **K** with respect to e_i, it may be written

$$\mathbf{K}'^{e_i} = \frac{\mathbf{K}^{e_i}}{e_i} \tag{B.4}$$

Using Equations B.3 and B.4, the vector $\mathbf{a}_i$ defined in Equation 2.17 becomes

$$\mathbf{a}_i = \frac{\mathbf{u}^{e_i}}{e_i} \tag{B.5}$$

with its k^{th} element associated with the k^{th} degree of freedom given by

$$a_{ki} = \frac{u_k^{e_i}}{e_i} \tag{B.6}$$

in which $u_k^{e_i}$ is the k^{th} element of $\mathbf{u}^{e_i}$. Replacing the value of a_{kl} from Equation B.6 into Equation 2.28, approximating $E[u_k]$ by u_k, one may get

$$d_{ki} = \frac{u_k^{e_i}}{u_k} \tag{B.7}$$

With the new definition of d_{ki}, the variation in deflection at degree of freedom k due to variation in e_i, given by the notation $CV(u_k)|e_i$, may be expressed by

$$CV(u_k)|e_i = (\frac{u_k^{e_i}}{u_k})CV(e_i) \tag{B.8}$$

or

$$\frac{CV(u_k)|e_i}{CV(e_i)} = (\frac{u_k^{e_i}}{u_k}) \tag{B.9}$$

Equation B.9 means that, the ratio of $CV(u_k)$ due to variation in e_i to $CV(e_i)$ is equal to the share of displacement from members having elastic modulus e_i, to the total displacement of the system. It should be noted that, as Equation B.3 implicitly implies, the ratio of the displacements may be related to the ratio of the stiffnesses.

For a special case where elastic moduli are completely correlated in pairs (ρ_{ij}=1, for all i,j=1,...p), and have the same variation (CV(e_i)=CV(e), for all i=1,...p), Equation 2.26, with respect to Equation B.2, results in

$$CV(u_k) = CV(e) \tag{B.10}$$

Replacing Equation B.10 in B.9 yields

$$\frac{CV(u_k)|e_i}{CV(u_k)} = \frac{u_k^{e_i}}{u_k} \tag{B.11}$$

which means that, for the above mentioned conditions, the ratio of variations is equal to the ratio of displacements when comparing a set of elements with elastic modulus e_i to the total elements in the system. Equation B.11 may also be expressed as

$$\frac{CV(u_k)|e_i}{CV(u_k)|e} = \frac{u_k^{e_i}}{u_k^{e}} \tag{B.12}$$

where e is a subset of the p random variables. This relation may be utilized to find the deflection contribution ratio of one layer to a group of layers, knowing the associated variations in the deflections.

As was pointed out previously, the deflection ratio may be substituted by the stiffness ratio, therefore, allowing one to investigate the role of the stiffness of a layer in the total stiffness of a group of layers, or the whole system, using stochastic analysis.

APPENDIX C

DAMPING MATRIX

Damping in a pavement system comprises of two types; material damping, and radiation damping.

Material Damping

Material damping refers to the internal energy dissipation due to frictional losses occurring in materials. In this study, the material damping was assumed to be of a hysteretic nature, which seems to better explain the damping behavior of soils (Mamlouk and Davies 1984). As a result, the material damping matrix **C** was related to the stiffness matrix **K** through a frequency invariant hysteretic damping ratio ζ as follows (Wolf 1988)

$$\mathbf{C} = \frac{2\zeta}{w}\mathbf{K} \qquad \text{(C.1)}$$

Strictly speaking, this equation should be defined on the element level, and then the resulting element damping matrices assembled to form the global damping matrix. In this study a unique hysteretic damping ratio was assumed for all the material types, hence, the dynamic stiffness matrix of the system was simplified to the form

$$\tilde{\mathbf{K}}_n = (1+2\zeta\, i)\mathbf{K} - \mathbf{M}w_n^2 \qquad (C.2)$$

Simulations were completed using 5% damping which is quite common for soils; see, for example, Richart et al. (1970)

Radiation Damping

One important consideration in the steady state analysis of a pavement system is radiation damping. In a semi-infinite problem, the energy transferred to the pavement system radiates from the point of load application in all directions with no reflection of the energy back into the system. With the finite element discretization of the real problem, however, propagating waves are reflected at artificial boundaries, unless energy absorbing mechanisms are provided at such boundaries. These mechanisms, which are referred to as transmitting boundaries, absorb the energy and simulate the condition of radiation damping of an infinite media where in fact there is a limiting boundary.

There are different types of transmitting boundaries, e.g., infinite elements (Zeinkeiwicz et al. 1983), consistent boundaries (Wolf 1985), viscous dampers or dashpots (Wolf 1988), etc. For the purpose of this study, consistent viscous dampers were used owing to their simplicity and relatively good performance (Chow 1985). The transmitting boundary condition is formulated by Lysmer and Kuhlemeyer (1969) as

$$\sigma = \rho v_p \dot{u} \tag{C.3}$$

$$\tau = \rho v_s \dot{v} \tag{C.4}$$

in which, as indicated in Figure C.1, σ and τ are the normal and shear stresses, respectively, $\dot{u}$ and $\dot{v}$ are the normal and tangential velocities, respectively, ρ is the mass density, and v_p and v_s are the velocities of P-waves and S-waves, respectively.

The conditions given in Equations C.3 and C.4 are exact when body waves impinge at a right angle on the boundaries. For inclined angles, they are approximate and a small part of the total energy is reflected. Lysmer and Kuhlemeyer (1969) have shown that nearly perfect absorption is obtained, if the incident angle is greater that 30 degrees. In many cases, such as the case under study, the farther one places the artificial boundary from the source of excitation, the more the incident angle will approach 90 degrees, and thus, the better the viscous dampers will perform.

The frequency independent coefficients of viscous dampers in the normal direction, c_n, and tangential direction, c_s, may be defined by

$$c_n = \rho v_p \tag{C.5}$$

$$c_s = \rho v_s \tag{C.6}$$

Based on the approach of Bathe (1982), the element damping matrix of a viscous damper is given by

$$C_b^e = \int_{\Omega} N^t C_{xy} N \, d\Omega \tag{C.7}$$

$$C_{xy} = T^t \begin{bmatrix} c_n & 0 \\ 0 & c_s \end{bmatrix} T \tag{C.8}$$

where N is the matrix of the shape functions with N^t being its transpose, T is the transformation matrix from local (n-s) to global (x-y) coordinates, and Ω is the area of the element. Element damping matrices are then multiplied by the frequency and mapped into the imaginary part of the dynamic stiffness matrix.

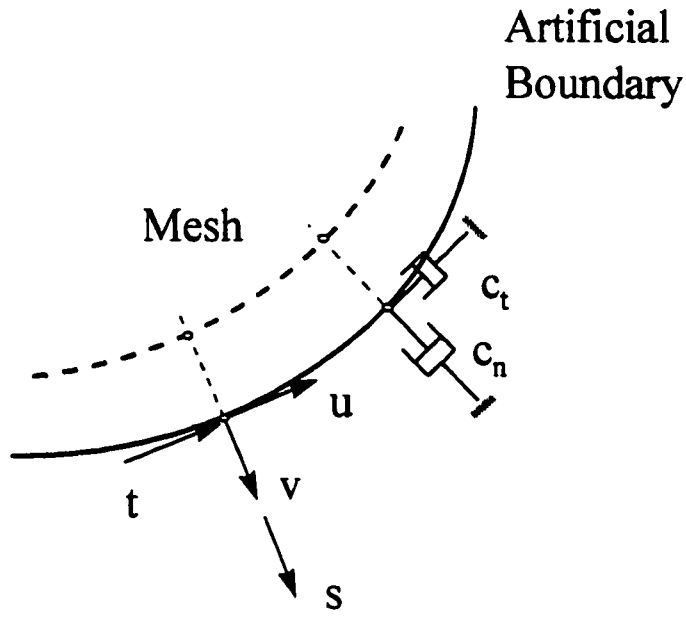

Figure C.1 Transmitting Boundary using Lumped viscous dampers (after Wolf 1988)

APPENDIX D

PARAMETRIC EVALUATION OF THE MODEL

A schematic of the finite element mesh of the model is given in Figure D.1, with the characteristics of the reference grid summarized in Table D.1. A series of simulations were carried out maintaining material properties constant but changing the discretization in order to confirm the suitability of the proposed finite element mesh for dynamic analysis.

Table D.1 Characteristics of the reference finite element mesh

Direction	**No. of Elements in each Size Category**				**Total No. of Elements**	**Size of the Model (m)**
	0.075 m	0.15 m	0.30 m	0.60 m		
X Direction	2	18	10	10	40	11.85
Y Direction	2	18	5	5	30	7.35

Size and Number of Elements

In order to examine the proposed finite element configuration with respect to the element size and number, two other configurations were considered. The arrangements of the elements for all three models are given in Table D.2. The following criteria were used for discretization:

- Element size right under the load should remain constant.

- Based on Lysmer and Kuhlemeyer (1969), to obtain accurate results, the maximum element size in the region of interest should not exceed one twelfth of the wavelength associated with the highest frequency component of the loading. For this problem, the recommendation dictates an element size not bigger than 0.15 m in the vicinity of the load.

- To provide reasonable size of the domain and because of the computer memory constraints with respect to the maximum number of elements, the element size farther away from the load should be increased.

Table D.2 Arrangement of the elements in the three models

Element	**Number of Elements**					
Size *	**Model 1**		**Model 2**		**Model 3**	
(m)	X Dir.	Y. Dir.	X Dir.	Y Dir.	X Dir.	Y Dir.
0.075	2	2	2	2	2	2
0.15	58	38	28	18	8	8
0.30	-	-	15	10	15	5
0.60	-	-	-	-	5	5
Total	60	40	45	30	30	20

* The overall size of all three models is 8.85 m x 5.85 m.

Simulations were completed for the highest frequency component (w=500 rad/s), which imposed the highest restriction from the element size perspective. The results are summarized in Figure D.2. The figure indicates that the difference in the deflection amplitude for the first two models is negligible with a small deviation noticeable when using the coarse grid. Similar observation was made when comparing the deflection phase angle of the three models.

Size of the Model

The distance of the transmitting boundary to the excited zone is an important factor in the accuracy of the results. This is generally due to the imperfect energy absorption of such boundaries. To find the minimum acceptable distance L of the transmitting boundary to the load, the results of analyses for two models with L=8.85 m, and L=13.35 m were compared and reported in Figure D.3. Since the optimum distance is usually defined in terms of the highest wavelength of the waves propagating in the media (Lysmer and Kuhlemeyer 1969), simulations were carried out for w=50 rad/s. According to the figure, the difference between the deflection amplitudes of the two models is very small.

Based on the above observations, it was concluded that, the proposed mesh specification would provide accurate results.

Effectiveness of the Transmitting Boundary

To examine the effectiveness of the transmitting boundary, deflection amplitudes were calculated at low and high frequencies with and without the viscous dampers. For each case, hysteretic damping was assumed either zero or 5%.

For the case of low frequency (w=50 rad/s), Figure D.4 shows that the presence of viscous dampers at the artificial boundary is not significant for both cases of zero and 5%

material damping. Moreover, the figure indicates that the value of material damping makes almost no difference on the results of the analysis for such low frequency.

When analysis was carried out at high frequency (w=500 rad/s), the results were different. By looking at the outcomes in Figure D.5, it is clear that, although for 5% material damping the existence of the dampers was not important, they had a noticeable effect when there was no material damping. The behavior of the system for the latter case was completely different with and without the dampers. The observation may be explained considering that, for a 5% material damping, the energy of the propagating wave almost dissipates before it reaches the boundary, which is located relatively far from the excitation source. The figure also shows that, unlike the previous case, at high frequency, the presence of material damping does change the results of the analysis.

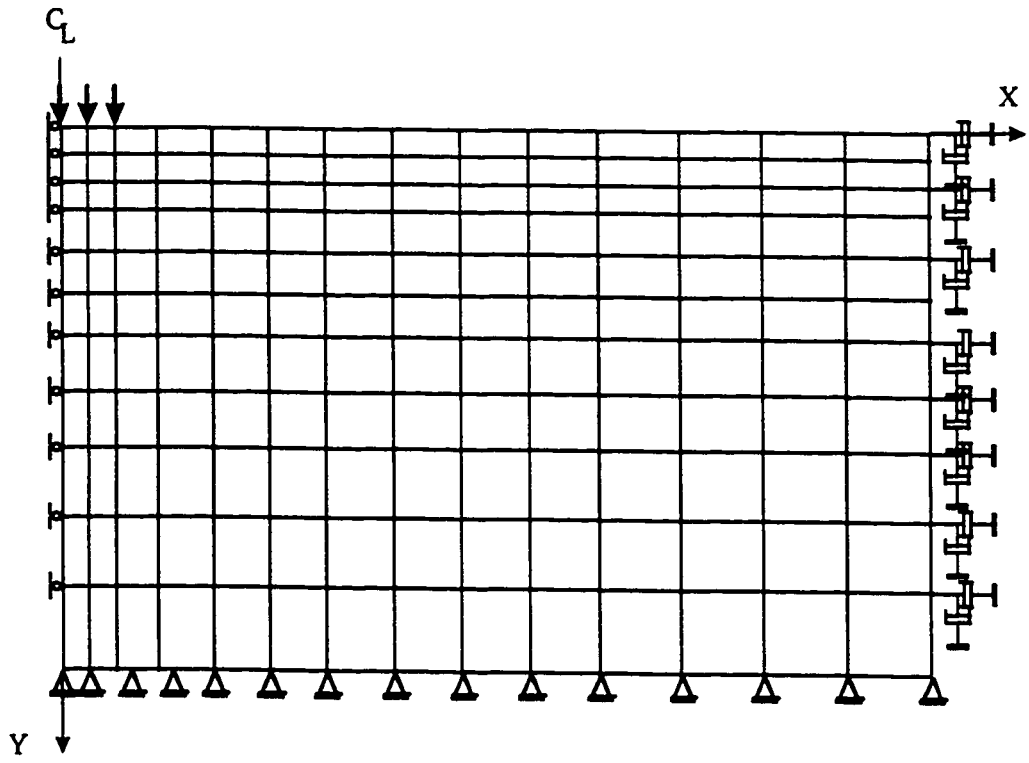

Figure D.1 Schematic of the finite element mesh for dynamic model

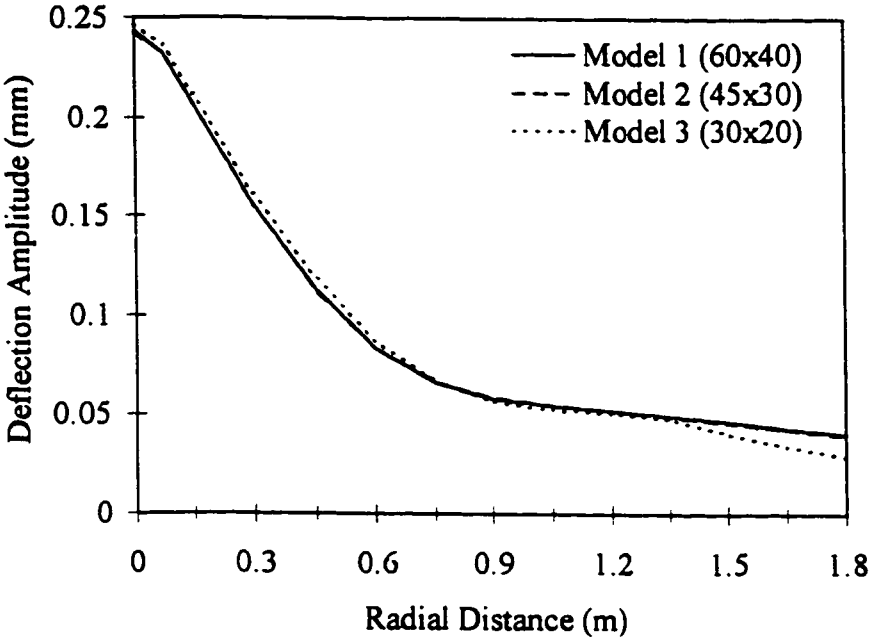

Figure D.2 Effect of size and number of elements in the model on the results

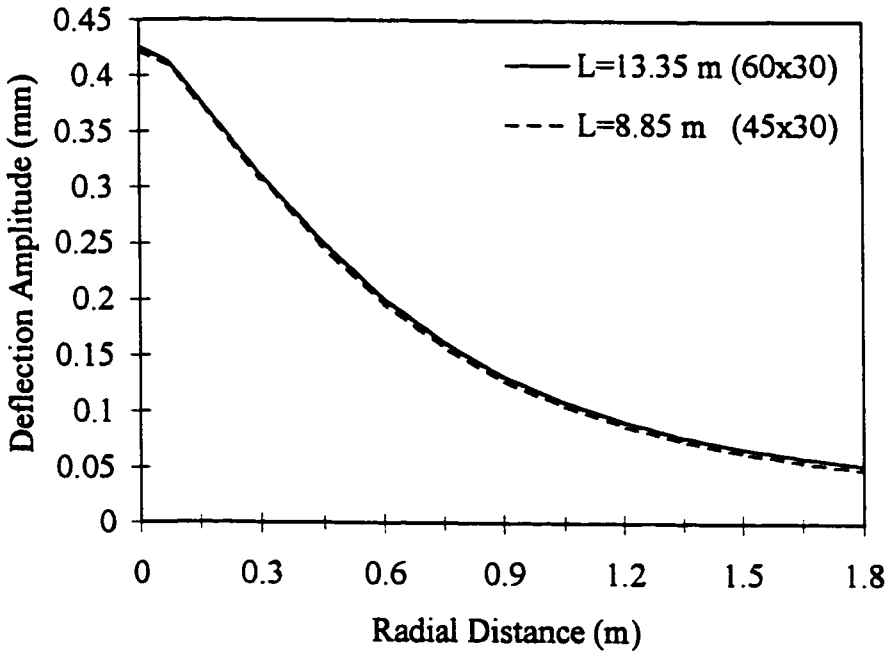

Figure D.3 Effect of size of the model on the results

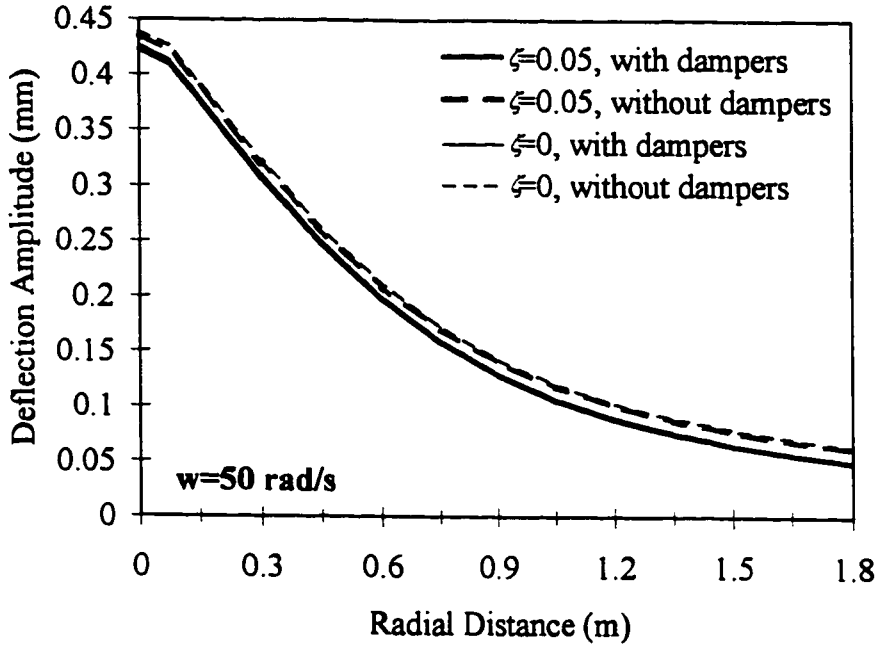

Figure D.4 Effect of transmitting boundary at low frequency

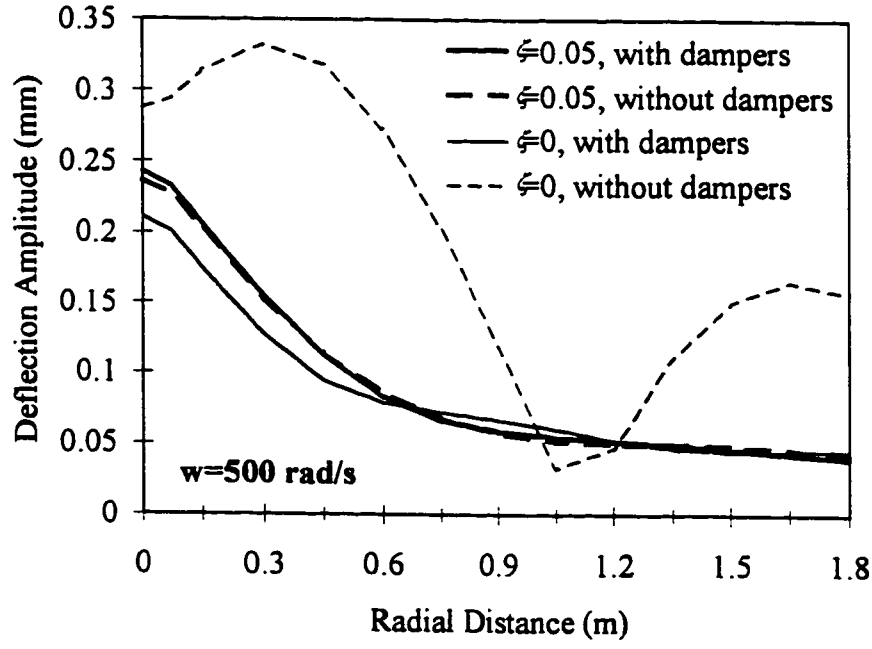

Figure D.5 Effect of transmitting boundary at high frequency

APPENDIX E

FOURIER SERIES EXPANSION OF AN FWD LOAD

In this section, the Fourier series analysis is used to express the FWD impact load in terms of its harmonic components. Theoretically, Fourier series analysis is only applicable to periodic loads. In practice, the approach may be applied to transient FWD impact loading, if it is assumed that the load history repeats itself after a long quiescent stage which follows the short impulse. For a periodic load where the response is zero at the end of each period, the steady-state response automatically includes the effect of zero initial conditions. Such a condition is encountered for systems with high damping subjected to a short impulse at the beginning of a relatively long period.

In order to simplify the resulting Fourier expansion, and consequently, the equations for the expected value and variance of the response, the forcing function is transformed to an even function, for which the Fourier expansion only includes cosine terms. This is done by shifting the function back in time by an amount equal to $t_0/2$, however, when calculating the response history and the other time-dependent quantities,

the appropriate change of variable $\bar{t} = t - \frac{t_0}{2}$ must be applied to account for the assumed shift in time.

The accuracy of the Fourier series approximation depends on the frequency range of the expansion, and the number of harmonic components included in the range. To find the proper range, one criteria is to look at the frequency extent over which most of the power is contained for the impact load. As a tool, power spectral density analysis may be used for this purpose. The spectra was found via Fourier transformation (Bendat and Piersol 1980) using the following approximate relation

$$S = \frac{F * \bar{F}}{N} \tag{E.1}$$

in which S is the spectral density, F is the Fourier transform of the loading function, f(t), and $\bar{F}$ is its complex conjugate. N is the length or the number of points in F. The Fourier transform of f(t) was calculated by the Fast Fourier Transform (FFT) algorithm using MATLAB Signal Processing Toolbox.

Figure E.1 illustrates the normalized power spectral density function. Based on the results, almost all of the power associated with the idealized FWD impact load is contained within the frequency range of 0 to 300 rad/s. This range was initially selected along with a tentative ten harmonic components (Sebaaly et al. 1986) to model the half-sine impulse load. It was found, however, that the range was not adequate to properly

approximate the shape of the half-sine impulse. Extending the frequency range up to 500 rad/s gave an acceptable approximation, as is depicted in Figure E.2.

Another set of calculations, which aimed to provide the optimum number of the components, revealed that when keeping the frequency range constant and decreasing the number of Fourier terms, by increasing the frequency interval, the shape did not change significantly. Nevertheless, to have enough frequency components in order to better approximate the actual response of the system by the superimposed harmonics, eleven components were selected. Based on the frequency increment of 50 rad/s (10 intervals in the range of 0 to 500 rad/s), the period was $T = \frac{2\pi}{w_1} = 0.13$ s, which is long enough compared to the FWD pulse duration of t_0 =0.03 s.

The normalized coefficients of the cosine terms in the expansion (a_n/f with f=566 kPa), which were calculated using MAPLEV computer arithmetic package, are given in Figure E.3. The Figure confirms that the coefficients associated with frequencies up to 500 rad/s are significant. Given the coefficients, the Fourier series expansion of the load is then expressed as

$$f(t) = \frac{a_0}{2} + \sum_{n=1}^{10} a_n \cos[50n(t - 0.015)] \qquad \text{(E.2)}$$

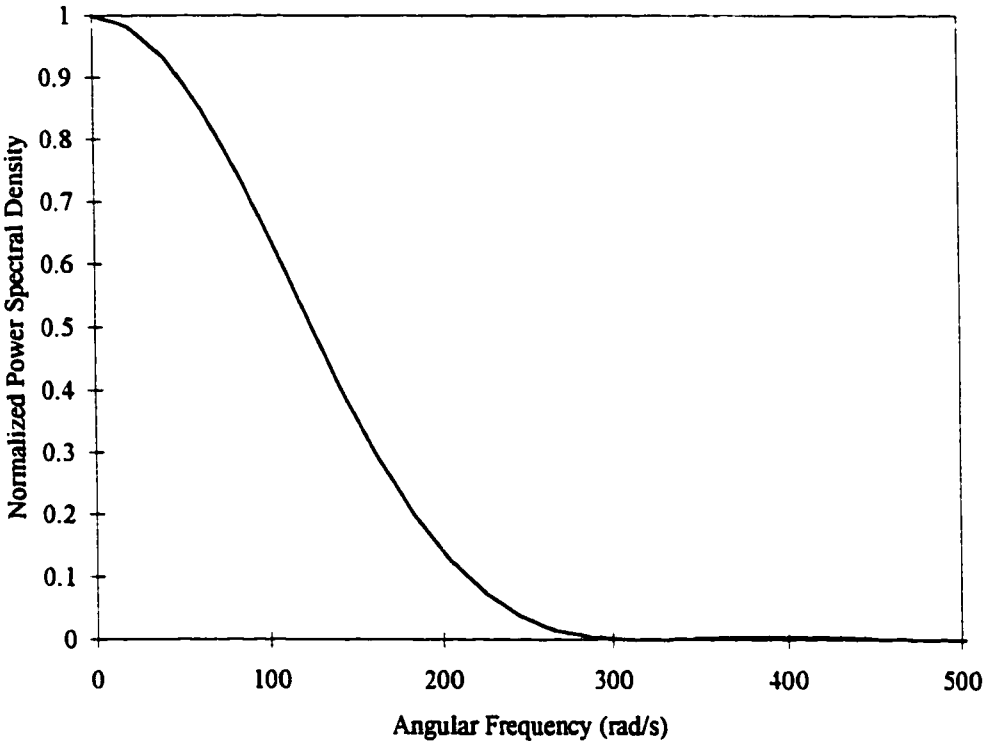

Figure E.1 Normalized power spectral density function of the idealized FWD impulse load

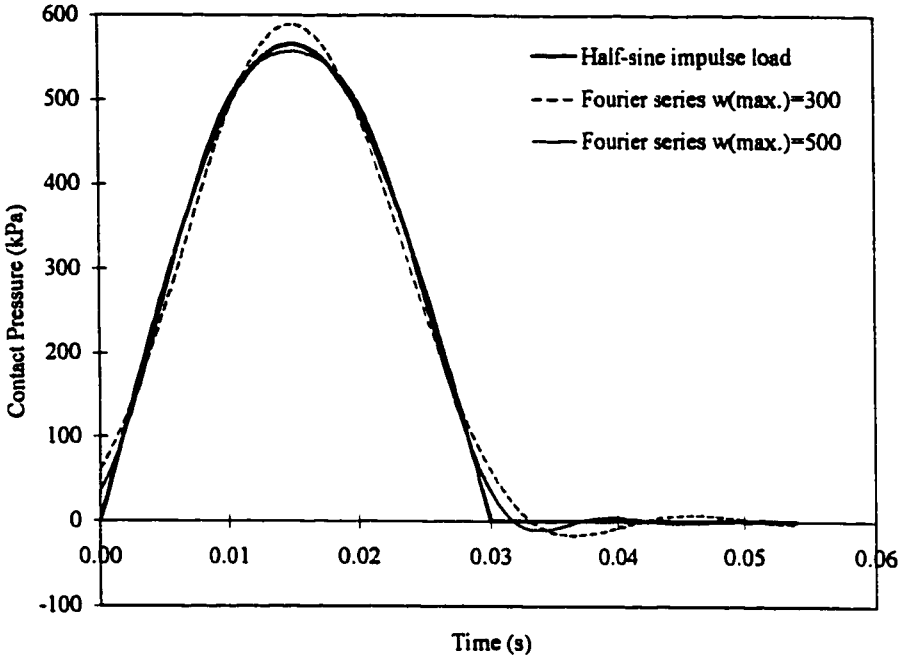

Figure E.2 Idealized impulse load and its Fourier series approximations

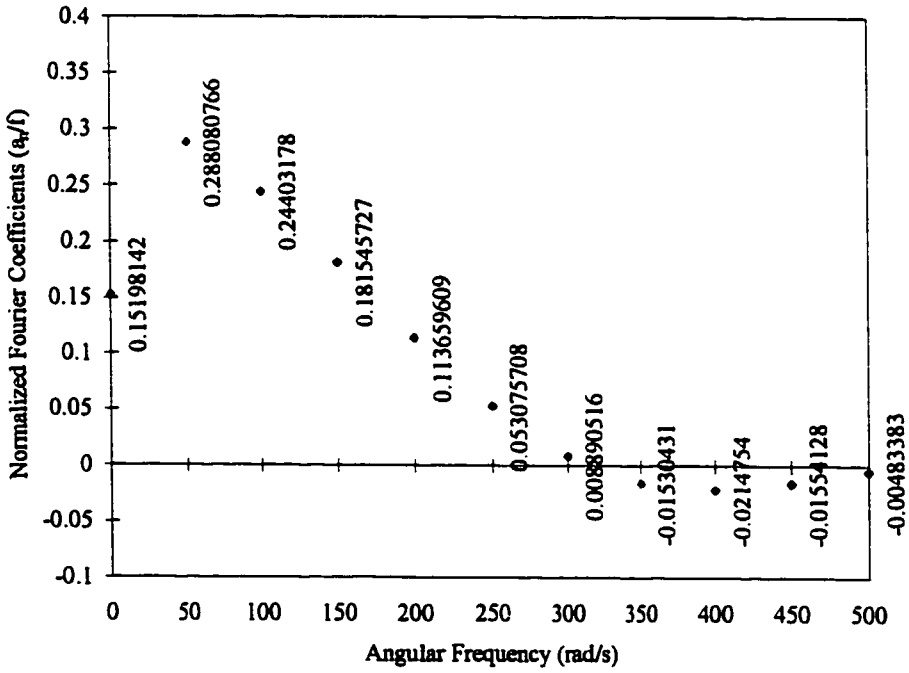

Figure E.3 Normalized coefficients of Fourier series expansion

APPENDIX F

DERIVATION OF THE VARIATION COEFFICIENT MATRIX

Static case

The Relation between the covariance matrix of deflections and that of p random elastic moduli is given by Equation 2.15 as

$$\mathbf{cov(u)} = \mathbf{A}\ \mathbf{cov(e)}\ \mathbf{A}^{t} \qquad \text{(F.1)}$$

If it is assumed that random moduli are independent in pair, i.e., $cov(e_i , e_j)=0$ for all i,j=1,..p and i≠j, **cov(e)** becomes diagonal and Equation F.1 may be transformed to

$$\mathbf{var(u)} = \mathbf{B}\ \mathbf{var(e)} \qquad \text{(F.2)}$$

in which **var(e)** and **var(u)** are the vectors containing the diagonal elements of **cov(e)** and **cov(u)**, respectively, and **B** is a matrix whose elements are the square of the corresponding

elements in **A**. If the elements of **B** are multiplied by the square of the pertinent mean modulus and divided by the square of the expected value of deflection associated with that element, Equation F.2 may be expressed in terms of CV as

$$\mathbf{CV2(u)} = \mathbf{D}\ \mathbf{CV2(e)} \tag{F.3}$$

in which **CV2(u)** and **CV2(e)** are vectors containing the square of CV(u) and CV(e), respectively, and **D** is the variation coefficient matrix. From a backcalculation point of view, it is desirable to invert Equation F.3 in order to relate variation in estimated moduli to variation in measured deflections, which is

$$\mathbf{CV2(e)} = \mathbf{G}\ \mathbf{CV2(u)} \tag{F.4}$$

where $\mathbf{G} = [\mathbf{D}^t\mathbf{D}]^{-1}\mathbf{D}^t$, and $\mathbf{D}^t$ is the transpose of **D**.

It should be noted that Equation F.3 may be adopted for a subset of deflections at degrees of freedom which are of interest, e.g., vertical surface deflections close to the load. However, to apply Equation F.4, variations of deflections for all degrees of freedom should be included in the relation.

Dynamic Case

As indicated in the main text, Equation 3.47 can be used to establish the relation between the covariance matrix of deflections **cov(u(t))**, and the covariance matrix of layer moduli **cov(e)**. It was demonstrated in Equation 3.48 that terms such as $\mathbf{cov}(x_j, y_l)$ are given by

$$\mathbf{cov}(x_j, y_l) = [A_x]_j \mathbf{cov(e)} [A_y]_l^t \qquad \text{(F.5)}$$

with **A** matrices defined in Equations 3.49 and 3.50.

Assuming that the off-diagonal terms of **cov(e)** are zero, which means that there is no correlation between the moduli of any two layers, Equation F.5 may be transformed to the following equation

$$\mathbf{var}(x_j, y_l) = [B_{xy}]_{j,l} \mathbf{var(e)} \qquad \text{(F.6)}$$

in which $\mathbf{var}(x_j, y_l)$ is the vector including the diagonal elements of $\mathbf{cov}(x_j, y_l)$. The elements of $[B_{xy}]_{j,l}$ are the product of the elements in A_x by the corresponding elements in transposed A_y. Replacing the variance vectors defined by Equation F.6 with the covariance matrices in Equation 3.47, and factoring out **var(e)** gives an equation identical to Equation F.2 in which **B** is defined by

$$\mathbf{B} = \frac{a_0^2}{4}[\mathbf{B_{xx}}]_{0,0} + \sum_{j=0}^{N}\sum_{l=1}^{N} a_j a_l \{[\mathbf{B_{xx}}]_{j,l}\cos(jwt)\cos(lwt) + [\mathbf{B_{yy}}]_{j,l}\sin(jwt)\sin(lwt) - [\mathbf{B_{xy}}]_{j,l}\cos(jwt)\sin(lwt) - [\mathbf{B_{yx}}]_{j,l}\sin(jwt)\cos(lwt)\} \quad \text{(F.7)}$$

where a_k is one of the N Fourier coefficients.

Using exactly the same procedure as that outlined for the static case, equations similar to Equations F.3 and F.4 can be derived for the dynamic case, except that, as Equation F.7 suggests, the resulting equations are time dependent.

REFERENCES

Adomian, G. 1983. Stochastic Systems. Academic press, NY.

Baecher, G.B., and Ingra, T.S. 1981. Stochastic FEM in Settlement Predictions. Journal of the Geotechnical Engineering Division, ASCE, 107(GT4), pp. 449-463.

Bathe, K.J. 1982. Finite Element Procedures in Engineering Analysis. Prentice Hall, Inc., Englewood Cliffs, NJ.

Bendat, J.S., and Piersol, A.G. 1980. Engineering Applications of Correlation and Spectral Analysis. John Wiley & Sons, Inc., NY.

Benjamin, J.R. and Cornell, C.A. 1970. Probability, Statistics and Decision for Civil Engineers. McGraw-Hill, NY.

Bharrucha-Reid, A.T. 1959. On Random Operator Equations in Banach Space. Bull. Acad. Polon. Sci., Ser. Sci. Math. Astr. Phys., Vol. 7, pp. 561-564.

Billingsley, P. 1995. Probability and Measure. John Wiley & Sons, NY.

Brzakala, W., and Pula, W. 1992. Neumann Expansion in the Stochastic Finite Element Method. Internal Report, Institute of Geotechnics and Hydrotechnics, Technical University of Wroctaw, Poland.

Brzakala, W., and Pula, W. 1992a. Stochastic Finite Element Method in a Settlement Analysis. Numerical Models in Geomechanics, Pande & Pietruszczk, Eds., Balkema, Rotterdam.

Burmister, D.M. 1943. The Theory of Stresses and Displacements in Layered Systems and Applications to the Design of Airport Runways. Highway Research Record, Vol. 23, Highway Research Board, Washington, D.C.

Bush, A.J., III. 1980. Nondestructive Testing for Light Aircraft Pavements, Phase II: Development of the Nondestructive Evaluation Methodology. Report No. FAA-RD-80-9-II, Federal Aviation Administration, Washington, D.C.

Bush, A.J. III, and Alexander, D.R. 1985. Pavement Evaluation Using Deflection Basin Measurements and Layered Elastic Theory. Transportation Research Board, Record 1022, National Research Council, Washington, D.C., pp.16-29.

Chang, D.W., Kang, Y.V., Roesset, J.M., and Stokoe II, K.H. 1992. Effect of Depth of Bedrock on Deflection Basins Obtained with Dynaflect and Falling Weight Deflectometer Tests. Transportation Research Board, Record 1355, National Research Council, Washington, D.C., pp. 8-16.

Chapra, S.C., and Canale, R.P. 1988. Numerical Methods for Engineers. McGraw-Hill, NY.

Chou, Y.J. 1993. Knowledge-Based System for Flexible Pavement Structural Evaluation. Journal of Transportation Engineering, ASCE, 119(3), pp. 450-466.

Chou, Y.J., and Lytton, R.L. 1991. Accuracy and Consistency of Backcalculated Pavement Layer Moduli. Transportation Research Board, Record 1293, National Research Council, Washington, D.C., pp. 72-85.

Chou, Y.J., Uzan, J., and Lytton, R.L. 1989. Backcalculation of Layer Moduli from Non-destructive Pavement Deflection Data Using the Expert System Approach. Nondestructive Testing of Pavements and Backcalculation of Moduli, ASTM STP 1026, A.J. Bush III and G.Y. Baladi, Eds., ASTM, Philadelphia, pp. 341-354.

Chow, Y.K. 1985. Accuracy of Consistent and Lumped Viscous Dampers in Wave Propagation Problems. International Journal for Numerical Methods in Engineering, Vol. 21, pp. 723-732.

Clough, R.W., and Penzien, J. 1975. Dynamics of Structures. McGraw-Hill, NY.

Contreras, H. 1980. The Stochastic Finite-Element Method. Comput. And Struct., 12, pp. 341-348.

Cornell, A. 1975. First-Order Uncertainty Analysis in the Finite Element Method in Linear Elasticity. Proc., 2nd Int. Conf. On Application of Statistics and Probability in Soil and Struct. Engrg., Aachen, Germany, pp. 67-88.

Dasgupta, G. 1985. Stochastic Finite Element Analysis of Soil-Structure System. Proc. Fourth Int. Conf. on Struct. Safety and Reliability, I. Konish, A. H.-S. Ang, and M. Shinozuka, Eds., 2, pp. 525-532.

Ghanem, R., and Brzakala, V. 1994. Stochastic Finite Element Analysis for Layered Geotechnical Media. Computer Methods and Advances in Geomechanics, Siriwardane & Zaman (Eds), Balkema, Rotterdam.

Ghanem, R.G., and Spanos, P.D. 1991. Stochastic Finite Element: A Spectral Approach. Springer-Verlag Inc., NY.

Glaser, S. 1995. System Identification and its Application to Estimating Soil Properties. Journal of Geotechnical Engineering, ASCE, Vol. 121(7), pp. 553-560.

Harr, M.E. 1977. Mechanics of Particular Media-A Probabilistic Approach. McGraw-Hill, NY.

Helstrom, C.W. 1984. Probability and Stochastic Processes for Engineers. Mcmillan Publishing Company, NY.

Heukelom, W., and Foster, C.R. 1960. Dynamic Testing of Pavements. Journal of the Structural Division, ASCE, pp. 1-28.

Hisada, T., and Nakagiri, S. 1985. Role of the Stochastic Finite Element Method in Structural Safety and Reliability. Proc. Fourth Int. Conf. on Struct. Safety and Reliability, I. Konish, A. H.-S. Ang, and M. Shinozuka, Eds., 1, pp. 385-394.

Hoffman, M.S., and Thompson, M.R. 1982. Comparative Study of Selected Nondestructive Testing Devices. Transportation Research Board, Record 852, National Research Council, Washington, D.C., pp. 32-41.

Houston, W.N., Mamlouk, M.S., and Perera, R.W.S. 1992. Laboratory Versus Nondestructive Testing for Pavement Design. Journal of Transportation Engineering. ASCE, 118(2), pp. 207-222.

Huang, Y.H. 1993. Pavement Analysis and Design. Prentice Hall, Inc., Englewood Cliffs, NJ.

Humar, J.L. 1990. Dynamics of Structures. Prentice Hall, Inc., Englewood Cliffs, NJ.

Irwin, L.H. 1983. Users Guide to MODCOMP 2. Report No. 83-8, Cornell University Local Roads Program, Cornell University, Ithaca, NY.

Ishii, K., and Suzuki, M. 1987. Stochastic Finite Element Method for Slope Stability Analysis. Struct. Safety, 4, pp. 111-129.

Karhunen, K. 1947. Uber Lineare Methoden in der Wahrschein-lichkeitsrechnung, Amer. Acad. Sci., Fennicade, Ser. A, I, Vol. 37, pp. 3-79.

Kausel, E., and Peek, R. 1982. Dynamic Loads in the Interior of a Layered Stratum: An Explicit Solution. Bulletin of the Seismological Society of America. Vol. 72, No. 5, pp. 1459-1481.

Kleiber, M., and Hien, T.D. 1992. The Stochastic Finite Element Method: Basic Perturbation Technique and Computer Implementation. John Wiley and Sons Inc., Chichester.

Loeve, M. 1948. Fonctions Aleatoires du Sercond Ordre, Supplement to P. Levy, Processus Stochastic et Mouvement Brownien, Paris, Gauthier Villars.

Lysmer, J., and Kuhlemeyer, R.L. 1969. Finite Element Model for Infinite Media. Journal of the Engineering Mechanic Division, ASCE, pp. 859-877.

Lytton, R.L. 1989. Backcalculation of Pavement Layer Properties. Nondestructive Testing of Pavements and Backcalculation of Moduli, ASTM STP 1026, A.J. Bush III and G.Y. Baladi, Eds., ASTM, Philadelphia, pp. 7-38.

Lytton, R.L, and Michalak, C.H. 1979. Flexible Pavement Deflection Equation Using Elastic Moduli and Field Measurements. Research Report 207-7F, Texas Transportation Institute, Texas A&M University, College Station, TX.

Mamlouk, M.S. 1985. Use of Dynamic Analysis in Predicting Field Multilayer Pavement Moduli. Transportation Research Board, Record 1043, National Research Council, Washington, D.C., pp. 113-121.

Mamlouk, M.S., and Davies, T.G. 1984. Elasto-Dynamic Analysis of Pavement Deflections. Journal of Transportation Engineering, ASCE, 110(6), pp. 536-550.

Meier, R.W., and Rix, G.J. 1995. Backcalculation of Flexible Pavement Moduli from Dynamic Deflection Basins Using Artificial Neural Networks. Transportation Research Board, Record 1473, National Research Council, Washington, D.C., pp. 72-81.

Miller, K.S. 1974. Complex Stochastic Processes. Addison-Wesley Publishing Company Inc., Massachusetts.

Miller, G.F., and Pursey, H. 1955. On the Partition of Energy Between Elastic Waves in a Semi-Infinite Solid. Proceedings, Royal Society of London, Series A, Vol. 233, pp. 55-59.

Nakagiri, S., and Hisada, T. 1982. Stochastic Finite Element Method Applied to Structural Analysis with Uncertain Parameters. Proc. Int. Conference on the Finite Element Method, pp. 206-211.

Nazarian, S., and Bush, A.J., III. 1989. Determination of Deflection of Pavement Systems Using Velocity Transducers. Transportation Research Board, Record 1227, National Research Council, Washington, D.C., pp. 147-158.

Nazarian, S., and Stokoe, K.H., II. 1984. Nondestructive Testing of Pavements using Surface Waves. Transportation Research Board, Record 993, National Research Council, Washington, D.C., pp. 67-79.

Nazarian, S., and Stokoe, K.H. II. 1989. Nondestructive Evaluation of Pavements by Surface Wave Method. Nondestructive Testing of Pavements and Backcalculation of Moduli, ASTM STP 1026, A.J. Bush III and G.Y. Baladi, Eds., ASTM, Philadelphia, pp. 119-137.

Odemark, N. 1949. Investigations as to the Elastic Properties of Soils Design of Pavements According to the Theory of Elasticity. Staten Vaeginstitut, Stockholm, Sweden.

Ong, C.L., Newcomb, D.E., and Siddharthan, R. 1991. Comparison of Dynamic and Static Backcalculation Moduli for Three-Layer Pavements. Transportation Research Board, Record 1293, National Research Council, Washington, D.C., pp. 86-92.

Parvini, M. 1997. Stochastic Finite Element Program. Internal Report, Civil Engineering Department, McMaster University, Canada.

Parvini, M., and Stolle, D.F.E. 1996. Application of Stochastic Finite Element Method to Deflection Analysis of Pavement Structures. Transportation Research Board, Record 1540, National Research Council, Washington, D.C., pp. 64-70.

Peiravian, F. 1994. Interpretation of In-situ Pavement Properties Using FWD Testing Technique. A Thesis Submitted to the School of Graduate Studies in Partial Fulfillment of the Requirements for the Degree of Master of Engineering, McMaster University, Canada, pp. 33-36.

Ramirez, R.W. 1985. The FFT, Fundamentals and Concepts. Prentice Hall, Inc., Englewood Cliffs, NJ.

Richart, F.E., Jr., Hall, J.R., Jr., and Woods, R.D. 1970. Vibrations of Soils and Foundations. Prentice Hall, Inc. Englewood Cliffs, NJ.

Righetti, G., and Harrop-Williams, K. 1988. Finite Element Analysis of Random Soil Media. Journal of Geotechnical Engineering., ASCE, 114(1), pp. 59-75.

Rosenblueth, E. 1975. Point Estimates for Probability Moments. Proc. Natn. Acad. Sci. USA 72, No. 10, pp. 3812-3814.

Scrivner, F.H., Michalak, C.H., and Moore, W.M. 1973. Calculation of the Elastic Moduli of a Two-Layer Pavement System from Measured Surface Deflection. Highway Research Record No. 431, Highway Research Board, Washington, D.C.

Scullion, T., and Michalak, C. 1991. Modulus 4.0 User's Manual. Research Report 1123-4. Texas Transportation Institute, and Texas State Department of Highway and Public, Texas.

Sebaaly, B., Davis, T.G., and Mamlouk, M.S. 1985. Dynamics of Falling Weight Deflectometer. Journal of Transportation Engineering, ASCE, 111(6), pp. 618-632.

Sebaaly, B.E., Mamlouk, M.S., and Davies, T.G. 1986. Dynamic Analysis of Falling Weight Deflectometer Data. Transportation Research Board, Record 1070, National Research Council, Washington, D.C., pp. 63-68.

Shinozuka, M. 1985. Response Variability due to Spatial Randomness. Methods of Stochastic Structural Mechanics, F. Casciati and L. Faravelli, Eds., SEAG, Pavia, Italy.

Shinozuka, M., and Yamazaki, F. 1988. Stochastic Finite Element Analysis: an Introduction. Stochastic Structural Dynamics, Progress in Theory and Application, S.T. Ariaratnam, G.I. Schueller, and I. Elishakoff, Elsevier Applied Science, London.

Siddharthan, R., Norris, G.M., and Epps, J.A. 1991. Use of FWD Data for Pavement Material Characterization and Performance. Journal of Transportation Engineering, ASCE, 117(6), pp. 660-678.

Siddharthan, R., Sebaaly, P.E., and Javaregowda, M. 1992. Influence of Statistical Variation in Falling Weight Deflectometers on Pavement Analysis. Transportation Research Board, Record 1377, National Research Council, Washington, D.C., pp. 57-66.

Spanos, P., and Ghanem, R. 1989. Stochastic Finite Element Expansion for Random Media. Journal of Engineering Mechanic, ASCE, 115(5), pp. 1035-1053.

Stolle, D.F.E. 1992. Analysis and Interpretation of Falling Weight Deflectometer Data. Ontario Ministry of Transportation. Project No. 21230, Canada.

Stolle, D., and Hein, D. 1989. Parameter Estimates of Pavement Structure Layers and Uniqueness of the Solution. Nondestructive Testing of Pavements and Backcalculation of Moduli, ASTM STP 1026, A. J. Bush III and G. Y. Baladi, Eds., American Society for Testing and Materials, Philadelphia, pp. 313-322.

Stolle, D., Hein D., and Wang, Y. 1988. Elastostatic Analysis and Backcalculation Estimates of Pavement Layer Moduli. Proceeding of 1988 Annual Conference, Roads and Transportation Association of Canada, Vol. 1, pp. C39-C59.

Stolle, D.F.E., and Jung, F.W. 1992. Simplified, Rational Approach to Falling Weight Deflectometer Data Interpretation. Transportation Research Board, Record 1355, National Research Council, Washington, D.C., pp. 82-89.

Stolle, D.F.E., and Peiravian, F. 1996. Falling Weight Deflectometer Data Interpretation Using Dynamic Impedance. Canadian Journal of Civil Engineering. **23**: pp. 1-8.

Stolle, D.F.E., and Sedran, G. 1995. Influence of Inertia on Falling Weight Deflectometer (FWD) Test Response. Canadian Geotechnical Journal, National Research Council of Canada, 32(6), pp. 1044-1048.

Swift, G. 1972. An Empirical Equation for Calculating on the Surface of a Two-Layer Elastic System. Texas Transportation Institute Research Report 136-4, Texas A&M University, College Station, TX.

Swift, G. 1973. Graphical Technique for Determining the Elastic Moduli of a Two-Layer Structure from Measured Surface Deflections. Highway Research Record No. 432, Highway Research Board, Washington, D.C.

Taylor, J. R. 1982. An Introduction to Error Analysis, Oxford University Press, CA.

Thomas, J.B. 1971. An Introduction to Applied Probability and Random Processes, Wiley, NY.

Ullidtz, P. 1987. Pavement Analysis. Elsevier, Amesterdam.

Uzan, J. 1994. Dynamic Linear Backcalculation of Pavement Material Parameters. Journal of Transportation Engineering, ASCE, 120(1), pp. 109-126.

Uzan, J, and Lytton, R.L 1989. Experiment Design Approach to Nondestructive Testing of Pavements. Journal of Transportation Engineering, ASCE, 115(5), pp. 505-520.

Uzan, J., Lytton, R.L., and Germann, F.P. 1988. General Procedure for Backcalculating Layer Moduli. First International Symposium on Nondestructive Testing of Pavement s and Backcalculation of Moduli, ASTM, Baltimore, MD.

Vanmarcke, E.H., and Grigoriu, M. 1983. Stochastic Finite Element Analysis of Simple Beams. Journal of the Engineering Mechanic Division, ASCE, 109(5), pp. 1203-1214.

Wolf, J.P. 1985. Dynamic Soil-Structure Interaction. Prentice-Hall, Inc., Englewood Cliffs, NJ.

Wolf, J.P. 1988. Soil-Structure-Interaction Analysis in Time Domain. Prentice-Hall, Inc., Englewood Cliffs, NJ.

Yamazaki, F., Shinozuka, M., and Dasgupta, G. 1988. Neumann Expansion for Stochastic Finite Element Analysis. Journal of Engineering Mechanic, 114(8), pp. 1335-1354.

Yin Hou, T. 1977. Evaluation of Layered Material Properties from Measured Surface Deflections. Ph.D. dissertation, University of Utah.

Yoder, E.J., and Witczak, M.W. 1975. Principles of Pavement Design. John Wiley & Sons, NY.

Zaghloul, S.M., White, T.D., Drnevich, V.P., and Coree, B. 1994. Dynamic Analysis of FWD Loading and Pavement Response Using a Three-Dimensional Dynamic Finite-Element Program. Nondestructive Testing of Pavements and Backcalculation of Moduli (Second Volume), ASTM STP 1198, H.L. Von Quintas, A.J. Bush III, and G.Y. Baladi, Eds., ASTM, Philadelphia, pp. 125-142.

Zeinkeiwicz, O.C., Emson, C., and Bettess, P. 1983. A Novel Boundary Infinite Element. International Journal for Numerical Methods in Engineering. Vol. 19, pp. 393-404.